



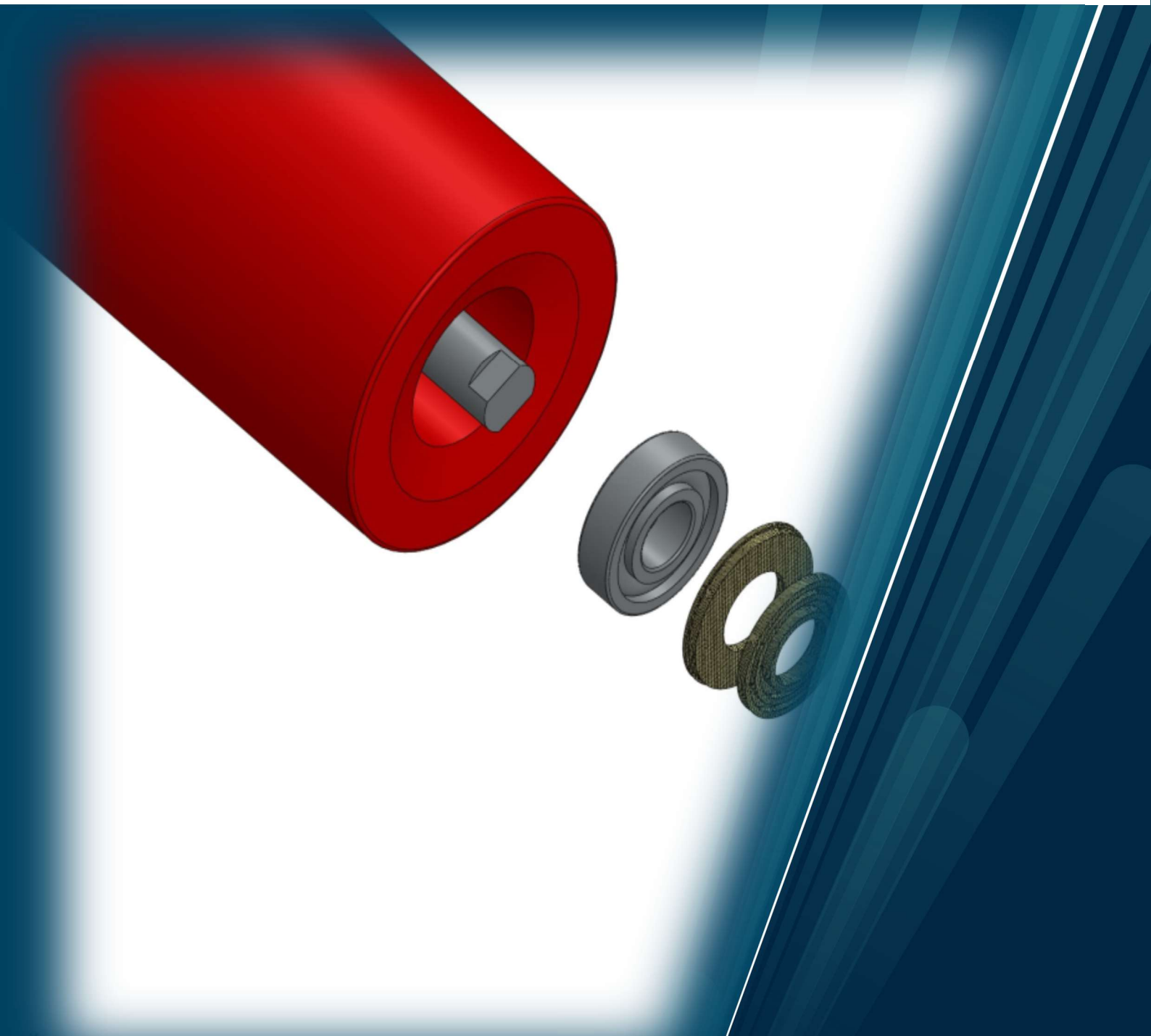
**UiT** The Arctic University of Norway

Faculty of Engineering Science and Technology

## **Optimization Conveyor Roller, LKAB**

Ghulam Mahyyudin

Master's thesis in Engineering Design, May 2024



## **Acknowledgements**

I would like to express my sincere gratitude to my thesis supervisors, Dr. Guy Beerli Mauseth and Dr. Andrei Karzhou, for their invaluable guidance, unwavering support, and insightful feedback throughout the course of this master's thesis. Their expertise, encouragement, and mentorship have been instrumental in shaping the direction and quality of this research. I am grateful to Daniel Valen Nilsen (Maintenance Engineer at LKAB) for the assistance and provision of vital information related to the thesis topic, as well as to the entire team at LKAB for the opportunity to visit their facility in Narvik and gain firsthand insights to the conveyor and idler roller condition. Lastly, I am deeply grateful to my family and friends for their unwavering support, encouragement, and understanding throughout this academic endeavor. Thank you to everyone who has contributed to the completion of this thesis. Your support and assistance have been deeply appreciated.

---

## **Abstract**

This master thesis presents a study on the structural optimization of conveyor idlers, focusing on the idler shell and shaft. The research aims to enhance the performance and efficiency of conveyor systems by reducing weight and improving stability of idler roller, beginning with a thorough load analysis to determine the static and dynamic forces exerted on idler. The study employs a combination of numerical simulations and analytical methods to analyze the idler's structural integrity and performance, using SOLIDWORKS and ANSYS, and provide insights into stress distribution, deformation characteristics, and mode shapes inherent in idler roller system, forming the basis for further optimization.

Alternative materials such as Resin Epoxy, PVC, and HDPE are evaluated against traditional structural steel for roller shell. Comparative analysis of mechanical properties, weight reduction potential, and cost-effectiveness identifies these materials as a viable alternative to steel, offering opportunities for improved performance and environmental stability. Moreover, the optimization of hollow shaft results in weight reduction while maintaining structural integrity, as evidenced by finite element analysis results. Modal analysis of the idler system reflects its dynamic behavior and vibration characteristics, enabling the development of damping strategies to ensure smooth operation under varying load conditions. In conclusion, this master thesis focuses on structural analysis for optimizing conveyor idler, addressing key challenges in materials handling systems and paving the way for further innovation in the field.

---

# Table of Contents

1.	Introduction .....	8
1.1	Problem Identification .....	8
1.2	Thesis Objective and Aims.....	8
2.	Literature review .....	9
2.1	Theoretical background .....	9
2.1.1	Role of idler in conveyor operation.....	10
2.1.2	Components of Idler roller.....	11
2.2	Types of Idler .....	12
2.3	Literature from Scientific Articles .....	15
2.3.1	Failure modes of Idler system .....	16
2.4	Idler roller technologies.....	17
2.4.1	Remarks .....	19
2.5	Regulation and Standards.....	19
3.	Design Methodology .....	21
3.1	Introduction.....	21
3.2	Identifying Opportunities and Clarifying Objectives .....	22
3.3	Setting requirements.....	24
3.4	Force Analysis of Idler roller:.....	26
3.4.1	Distribution of forces .....	26
3.4.2	Load Calculations .....	32
3.5	Prototype .....	34
4	Structural Analysis of Conveyor Idler.....	35
4.1	Numerical Analysis.....	35
4.1.1	Shell Analysis.....	35
4.1.2	Shaft Analysis .....	37
4.2	Theoretical Analysis.....	40
4.2.1	Shell Analysis.....	40
4.2.2	Shaft Analysis .....	41
4.3	Comparison Between Numerical and Theoretical Analysis.....	42
5	Modal Analysis .....	44
5.1	FEM Equations for Modal Analysis of Idler.....	44
5.2	FEM Model Analysis in ANSYS .....	45
6	Generative Alternatives .....	49
6.1	Shell Optimization .....	49

---

6.1.1	Weighted Decision Matrix .....	51
6.1.2	Analysis of Alternative Materials .....	52
6.1.3	Discussion .....	52
6.2	Shaft Optimization.....	53
6.2.1	Discussion .....	56
7	Conclusion .....	58
8	Further Work.....	59
8.1	Experimental Validation.....	59
8.2	Idler Components Analysis.....	60
8.3	Dust and Water Tightness .....	61
9	References .....	64
	Appendix A.....	66
	Idler roller technologies .....	66
	RKM Roller Company PTY LTD .....	66
	Rulmeca .....	67
	ASGCO.....	68
	Conveyor Innovations International Pty Ltd.....	69
	Conveyor Products and Solutions-CPS.....	70
	Appendix B .....	71
	Idler 2D drawing.....	71
	Appendix C .....	75
	ANSYS Analysis Setup .....	75
	SHELL analysis for Alternative defined materials.....	76
	HDPE.....	76
	Resign Epoxy.....	77
	PVC .....	78
	Appendix D .....	81
	Material selection .....	81

## List of Tables

Table 1	Comparison of Idler products manufactured by leading companies. ....	18
Table 2:	Performance Specifications for Roller shell.....	24
Table 3:	Performance Specifications for Shaft.....	25
Table 4:	Roller dimensions .....	26
Table 5:	Principal factors for Force analysis .....	28
Table 6:	Belt width and corresponding pitch for upper and lower idler sets [21].....	28
Table 7:	-Belt weight with respect to different belt widths [22].....	29

---

Table 8: Service factor $F_s$ [21].....	30
Table 9 Environmental Factor $F_m$ [21].....	30
Table 10: Impact factor $F_d$ [21].....	31
Table 11: Calculated load on carrying and return set.....	33
Table 12: Comparison between numerical and analytical results for idler shell and shaft.....	43
Table 13: Three primary modes of vibration.....	45
Table 14: Mode shape number with corresponding frequencies.....	48
Table 15: Comparison of steel with alternative materials (Resin Epoxy, PVC and HDPE).....	50
Table 16: Weighted Chart.....	51
Table 17: Weighted score matrix.....	52
Table 18: Comparison of mechanical properties (stress and deformation) for Resin Epoxy, PVC, HDPE, and Steel.....	52
Table 19: Comparison of physical and mechanical properties of solid and hollow shaft.....	56
Table 20: Variation of shaft thickness vs shaft deflection.....	57

## List of Figures

Figure 1: A Conventional belt conveyor system [2].....	10
Figure 2: Trough idler carrying and return frame [2].....	11
Figure 3: Components of RULMECA Idler roller.....	12
Figure 4: Components of a trough idler assembly.....	13
Figure 5: Cutway Section of an Impact idler.....	14
Figure 6: A Suspended Return Idler.....	15
Figure 7: A trough shape idler system.....	15
Figure 8: A Systematic rational design methodology [18].....	21
Figure 9: 2D drawing of idler roller at LKAB.....	26
Figure 10: Force distribution on idler [20].....	27
Figure 11: Participation factor with respect to angle of troughing [21].....	30
Figure 12: a) 3D CAD model of Idler b) Exploded view CAD model of idler.....	34
Figure 13: Section view of idler CAD model.....	34
Figure 14: Section view of idler roller, showing neglected components.....	35
Figure 15: Boundary conditions for idler shell: A standard earth gravity of $9806.6\text{mm/s}^2$ , A distributed force of $6500\text{N}$ , fixed cylindrical supports at both ends.....	36
Figure 16: Total Deformation at idler shell with a maximum value of $0.007415\text{mm}$ .....	36
Figure 17: Equivalent Stress distribution with a maximum stress of $5.678\text{Mpa}$ .....	37
Figure 18: End Support.....	38
Figure 19: Boundary conditions at shaft: A load of $3000\text{N}$ on both bearing seats, standard earth gravity of $9806.6\text{mm/s}^2$ , remote displacements at ends.....	38
Figure 20: Total deformation at shaft.....	39
Figure 21: Stress distribution of shaft.....	39
Figure 22: Schematic of an idler under loads and reaction forces [21].....	40
Figure 23: Schematic cutaway of an idler shaft considering the bearings do not transmit any moment [23].....	42
Figure 24: First six mode shapes of idler roller.....	47

---

Figure 25: Mode shape at $f=1407$ Hz .....	48
Figure 26: Comparison of abrasive resistance of steel with other materials (15) .....	49
Figure 27: Deflection vs Thickness Graph .....	57
Figure 28: Three-point bending test [25].....	59
Figure 29: Free body diagram for vibrational analysis of idler roller .....	61
Figure 30: Heat flow directions [26] .....	62
Figure 31: RKM standard steel idler[13] .....	66
Figure 32: RKM Composite roller [13] .....	67
Figure 33: C2000 Idler with specifications [15] .....	68
Figure 34: Shaftless oneFits Idler CII [16] .....	69
Figure 35: Yellow roller composite roller CPS [17].....	70
Figure 36: 2D Drawing of Rulmeca Idler with dimensions .....	71
Figure 37: Idler shaft .....	72
Figure 38: Idler components with specifications .....	73
Figure 39: Typical idler troughing system .....	73
Figure 40: LKAB TR010 conveyor Assembly.....	74
Figure 41: Front view TR010 conveyor LKAB.....	74
Figure 42: ANSYS workflow for structural optimization.....	75
Figure 43: meshing properties.....	75
Figure 44: properties of idler shell, nodes and elements for meshing .....	75
Figure 45: Shell analysis project flow and meshing configuration.....	76
Figure 46: Equivalent Stress HDPE shell .....	76
Figure 47: Total Deformation HPDE Shell .....	77
Figure 48: Equivalent Stress Resin Epoxy SHell .....	77
Figure 49: Total Deformation Resign Epoxy shell .....	78
Figure 50: Equivalent stress PCV shell .....	78
Figure 51: Total Deformation PVC shell.....	79
Figure 52: Material Selection Chart .....	82
Figure 53: Ranked Material based on material index stage 1 .....	83
Figure 54: Strength vs Density chart .....	83
Figure 55: Materials ranked for stage 2 .....	84

---

# 1. Introduction

## 1.1 Problem Identification

The challenge at LKAB's facility in Narvik lies in the frequent replacement of conveyor rollers, a critical component in the iron ore transportation process. As Europe's largest iron ore producer, LKAB relies on the efficient operations of the Ofotbanen railway to transport mined ore from Kiruna to the port of Narvik. However, the current issue arises from the high frequency of manual replacements of conveyor rollers, predominantly due to bearing damage and instances of rollers seizing up. The lifespan of these rollers is significantly influenced by their location, environmental conditions, and the loads they bear. To address this problem, the task is to find a solution that not only enhances the current situation but also contributes to increased lifespan, easier maintenance, cost effectiveness, and improved overall performance. The chosen solution must consider factors such as weight, environment and cost, as manual replacement is the existing practice, and there are accessibility challenges in certain areas of the facility. Therefore, the overarching goal is to devise an effective strategy or mechanism that mitigates the frequent failures of conveyor rollers, offering a sustainable and efficient solution for LKAB's iron ore transportation system in Narvik.

## 1.2 Thesis Objective and Aims

The primary objective of this master thesis is to develop and propose a solution to enhance the performance and lifespan of conveyor rollers at LKAB's facility in Narvik, ultimately optimizing the iron ore transportation process. The proposed solution should consider the weight of the components and tackle the challenges posed by the varied and sometimes difficult-to-access locations within the facility. For weight reduction, structural optimization of idler conveyor roller will be done to enhance the performance and lifespan which will ultimately results in optimizing the iron ore transportation process. The thesis work is further into following objectives:

- **Load Analysis:** Conduct a comprehensive force analysis of idler in the conveyor system, as the material transport on the conveyor. This analysis will help to determine static and dynamic forces on the center and wing idlers, considering factors such as belt load, belt speed, carrying and return troughing set pitch, belt weight per linear meter, participating factor, shock factor, service factor, ambient factor, and speed factor.



- **Structural Optimization:** Structural optimization is divided into shell and shaft optimization and focuses on the static analysis of idler system to determine the stress, deformation and deflection characteristics of idler and compare the numerical and theoretical results. Based on the results, the thesis aims to identify and select an optimal material for the roller shell that surpasses the performance of traditional stainless steel and optimized the solid shaft in terms of weight reduction. This new material should offer a superior combination of mechanical properties, including higher strength-to-weight ratio, better abrasive resistance, less wear, improved corrosion resistance, lower rotational resistance, and enhanced stiffness.
- **Contamination Prevention:** Design and evaluate a solution capable of effectively preventing the ingress of dust and water into the roller bearings. This solution should be robust enough to withstand the specific conditions at the loading points of the conveyor system, where rollers are most susceptible to contamination from the surrounding environment.

By achieving these objectives, this thesis aims to provide LKAB with a practical and effective solution to mitigate the frequent failures of conveyor rollers, offering a sustainable and efficient approach to enhance the iron ore transportation system in Narvik.

## 2. Literature review

### 2.1 Theoretical background

Belt Conveyor system is used to transport bulk material from one place to another via shortest possible distance, providing a continuous flow of material between different operations. It has been used in the industry since 1892, when Thomas Robbins designed a belt conveyor system to transport coal for Thomas Edison's Ore-Milling Company [1]. Most of the industry sector like mining, power, cement production and food industry depend upon the performance of belt conveyor system. These conveyors can operate continuously without having any time delays for loading or unloading or empty return trips and can be utilized for operations independent of traveling path. In terms of environmental impact, belt conveyors are a promising climate friendly mode of transport bulk material as they operate quietly, often within enclosure, neither cause air pollution nor deafen the ears. A conventional belt conveyor system, shown in Figure 1, consists of following important components:

- Frame
- Belt
- Tail and Head pulley
- Loading chute
- Carrying and return Idlers
- Electric motor
- Gear system

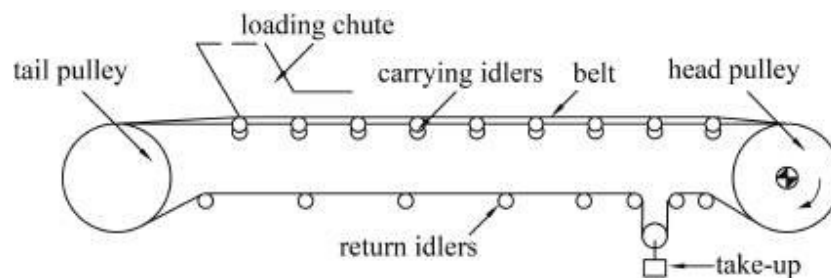


Figure 1: A Conventional belt conveyor system [2]

The belt is driven in the desired material flow direction through a friction force exerted in the form of tension by one or more drive pulleys operated by electric motors. A typical belt conveyor system, as shown in Figure 1, consists of a belt which moves around the head and tail pulley, the former is connected with an electric motor. Bulk material is spanned on the moving belt via loading chute, supported by spatially distributed carrying idlers, conveyed forward to the desired unloading place. After unloading, the belt reversed its direction, supported by tail pulley, and guided by return idlers, results in continuous operation [2].

### 2.1.1 Role of idler in conveyor operation

A typical idler provides support to the load while material transportation with minimum resistance to motion. The principal requirement of idler design is to support radial load from the belt and material over a particular idler spacing (pitch of idler). Different idler assemblies are created to control the profile of belt which provide consistency and flexibility to material transportation. For example, the trough shape idler assembly have center and wing rollers at different troughing angles, as shown in Figure 2, which supports both radial and axial load and provide tracking forces

and guiding. The center roll supports major portion of radial loads because of the material being transported while the wing rolls supports both axial loads as they are at an angle to the vertical axis.

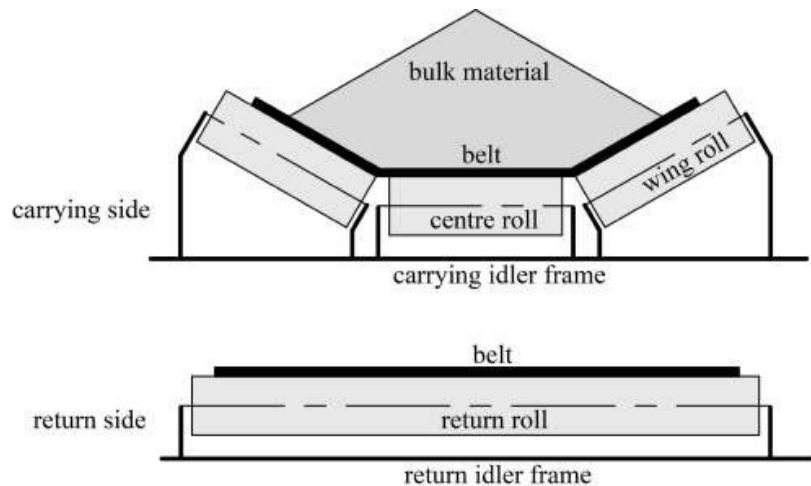


Figure 2: Trough idler carrying and return frame [2]

Idlers are one of the fundamental components of a belt conveyor and their function is to provide belt support, with low resistance to movement, while the material is conveyed along the full length, avoid spillage, absorb sudden impact while material loading and prevent the belt from stretching, swagging and failure.

To keep the material transport process continuous, reliability and safety of belt conveyor system is very important. Failure or malfunctioning of any component of the system may lead to a complete shutdown which results in large downtime and add maintenance cost. For example, a major portion of iron ore cost is transportation and around 30% of this cost consists of replace idlers in conveyor belts [3]. This study focuses on optimizing conveyor belt idlers to increase the reliability of conveyor belt system with a focus on mining industry.

### 2.1.2 Components of Idler roller

Idler roller consists of several integral components that contribute to its functionality and durability. A standard idler assembly consists of a roller shell, a cylindrical tube made up of steel material, having specific thickness and diameter. Inside the shell, bearing housing is positioned by either welding or deep swaged. The bearing housing is designed with a specific thickness to reduce the angle of deflection between the bearing and spindle when the spindle is subjected to

deformation while the material is being transported. The bearings are used to transmit the load from the roller shell to the shaft and resist radial forces from the roller shell. Spindle or shaft is the major load carrying component of the roller, made of stainless-steel material with a specified length and thickness. A standard idler roller manufactured by RULMECA along with its components is shown in Figure 3.

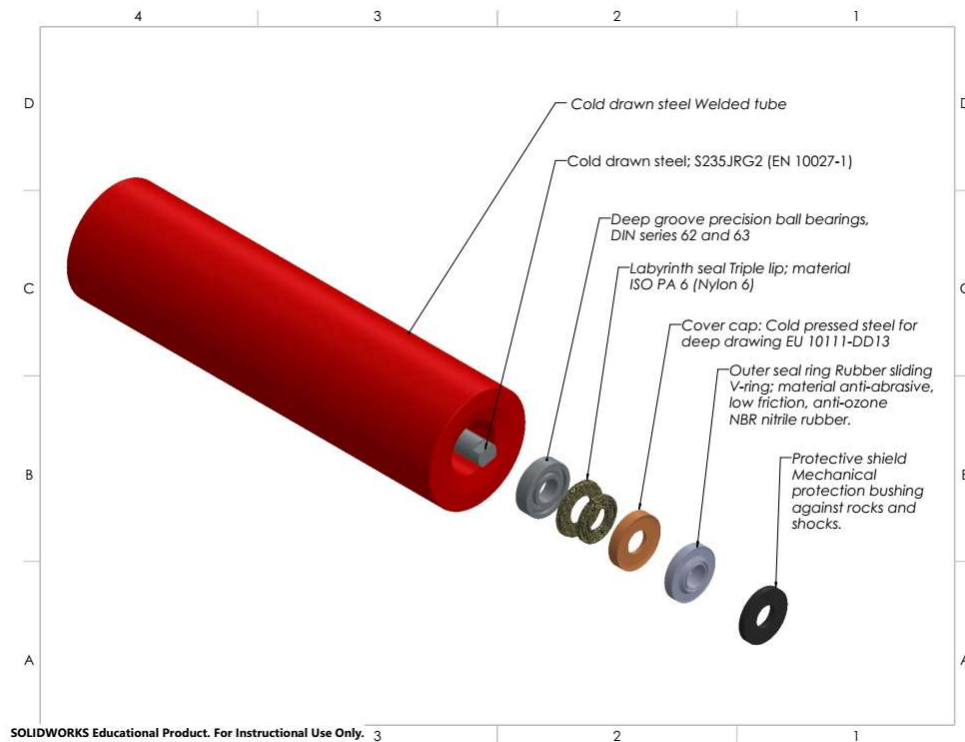


Figure 3: Components of RULMECA Idler roller

The spindle is designed to resist the load from roller shell which might cause excessive deflection and exerts irregular pressure on the bearings which reduces the roller life. To isolate the bearings from external environments, sealing solutions are used. Sealing solutions are essential for protecting the idler roller from environmental factors. These seals act as barriers against dust, moisture, and debris, reducing the risk of contamination and corrosion. Additional seals behind the bearings further enhance protection and reliability.

## 2.2 Types of Idler

According to ISO standards of 1537-1975 [4], idlers are classified into two categories:

- a) Carrying idlers, taking the material on belt conveyor, in line, of equal length

b) Return idlers, single or a set of two return idler of equal length, usually horizontal

According to the use, idlers can be divided into following types:

- Troughing carrying idlers
- Impact idlers
- Return Idlers

### **Trough carrying idlers**

Trough belts can carry more tonnage of material as compared to the flat belts, with same speed and width, because of increase cross sectional fill depth. Trough carrying idlers, shown in Figure 4, are the most common type of belt conveyor idlers used in handling bulk materials, consisting of three or five rollers with a center idler roll and wing rollers on either side at different angles. Idlers may have been in same plane, or they have an offset center roll depending upon the requirement. Angle of wing rollers determine the depth of trough created by the belt conveyor as it moves. Main function of trough idlers is to ensure consistency in the belt shape throughout its journey, improving stability and material carrying capacity, and to avoid material spillage.

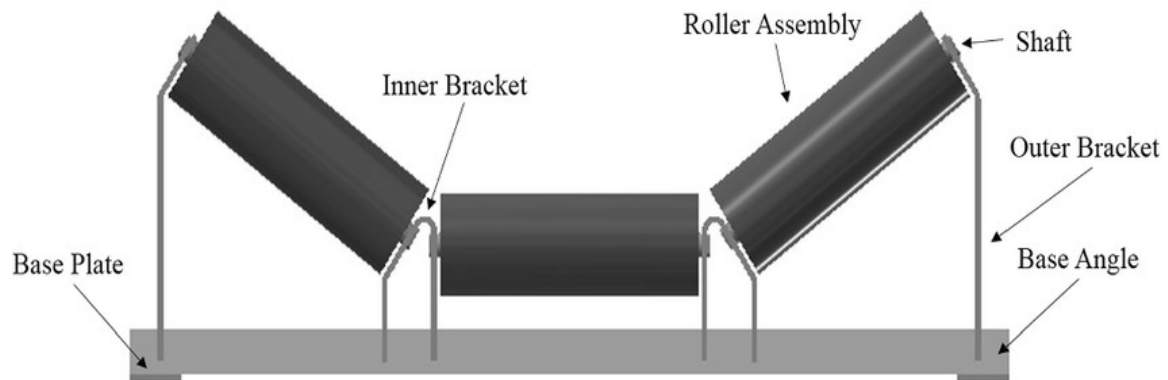


*Figure 4: Components of a trough idler assembly*

### **Impact idlers**

Impact idlers, also referred to as cushion idlers, are used to absorb sudden impact to prevent any damage to belt. Often installed at loading points on the conveyor belt where impact resulting from material density, lump size or height of material free fall may cause belt damage, if it is rigidly supported at that point. Equally spaced discs of rubber material, shown in Figure 5, vulcanized to

steel rolls, pneumatic tires or narrowly space discs are pressed on the steel tube to make it able to absorb the cushioning effect.

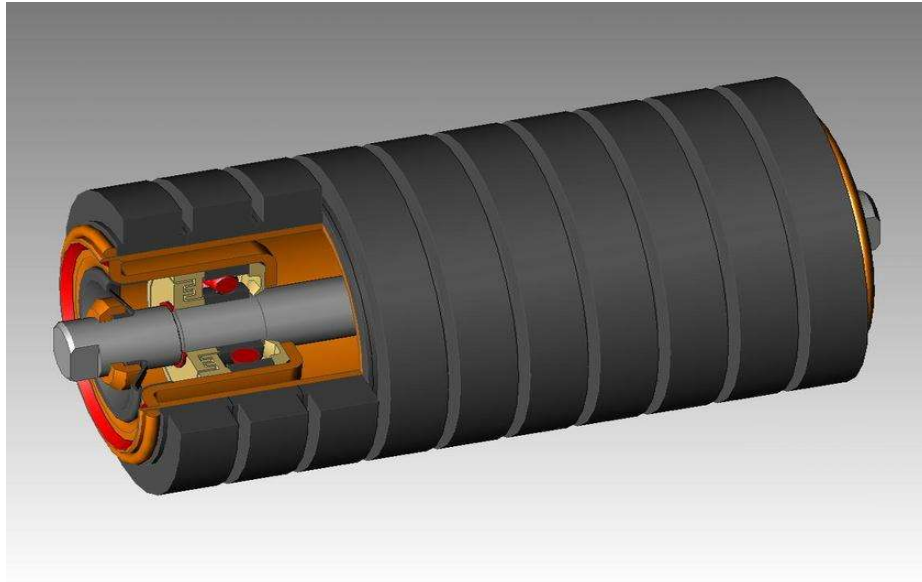


*Figure 5: Cutway Section of an Impact idler*

In case of disc, the material could be natural rubber with narrow space which allows the rubber to move under impact, help idler to absorb energy from impact loads and gives better support to belt as compared to pneumatic / semi-pneumatic types.

### **Return idlers**

A long single roll connected to mounting bracket and suspended below the lower flange of stringers supporting carrying idler is used as a return idler to support the return run of belt. Thicker material like mud, adhere to the belt carrying surface needs to be clean before the return motion of belt to prevent a large buildup which can seize the idlers or damage the belt. Hence, different styles of return idlers, a suspended return idler is shown in Figure 6, are available to overcome those challenges. For example, helical shaped self-cleaning return idlers made up of rubber or urethane disc can be used if the material is sticky. A rubber disc return idler can be used if additional abrasive resistance is required which extends the wear life of the roll.

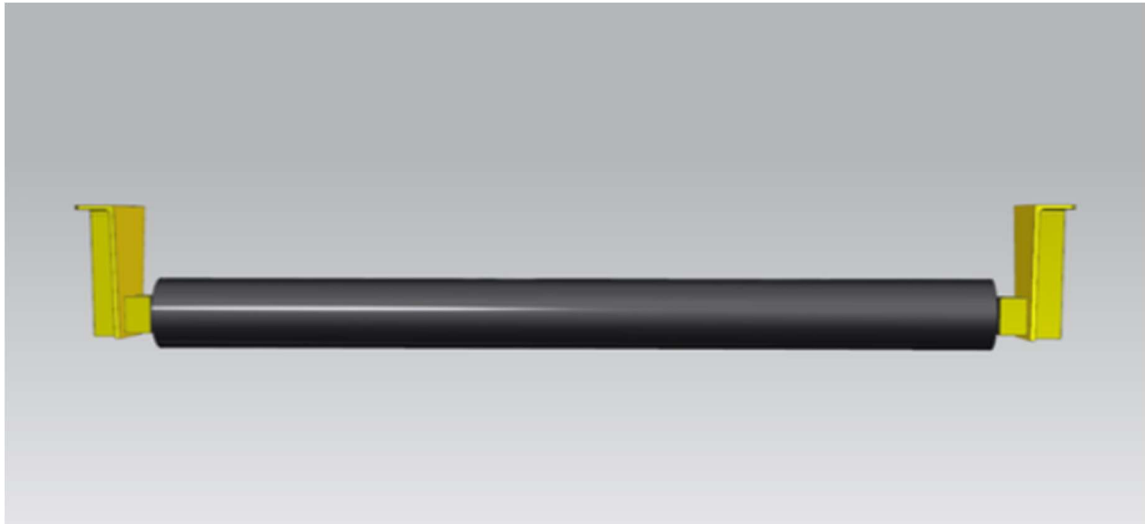


Figure 6: A Suspended Return Idler

### 2.3 Literature from Scientific Articles

The most economical and reliable system to transport bulk material from loading point to target place with higher capacity, minimal cost and less human effort is belt conveyor system. Any breakdown or malfunctioning of conveyor system components hinder the bulk material transportation resulting in delays, production loss, maintenance problems and finally the financial loss. In mining plants, as LKAB mining facility, 60% of plant downtime is contributed by conveyor system [5].

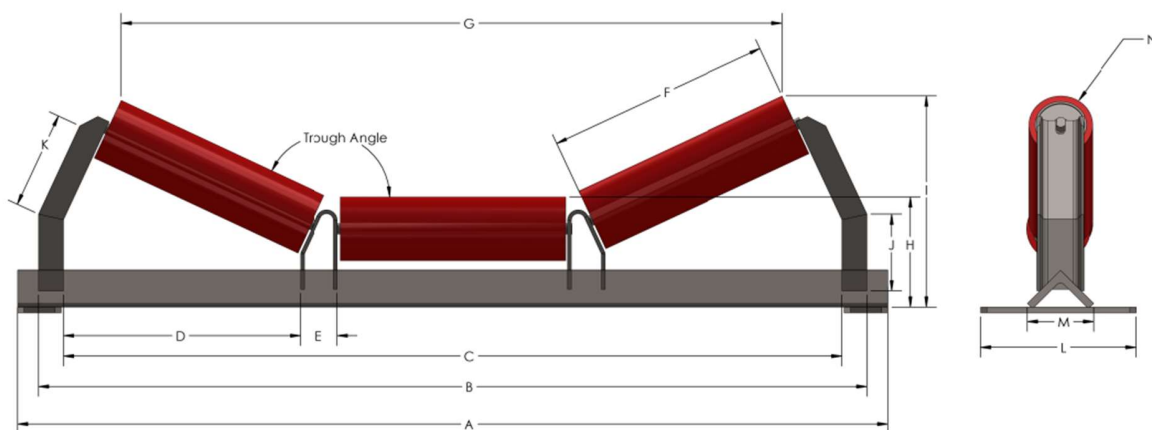


Figure 7: A trough shape idler system

The reliability of belt conveyor system depends upon the reliability of its rotating and stationary components. A conventional idler system in a mining industry consists of consists of two wing rollers and one center horizontal roller underneath the belt, as shown in Figure 7. The wing rollers are inclined at an angle of 20,35, or 45 degrees, making a trough shape. Rotating components of a conveyor such as pulley, idlers, and drive unit, contribute significantly to unplanned downtime, damage the belt seriously, causing major financial problems. Hence, optimization of idler rollers in a conveyor system could play an important role in reducing the maintenance time and cost which ultimately results in higher material handling efficiency. Condition monitoring system is considered as an effective technology to increase the reliability of belt conveyor components like belt, pulley, and drive units [6]. With current developments and latest sensors technology available in the market, belt conveyor components, except idlers, can be monitored online as well. Roughly around 20,000 rollers are installed in a 10 km long belt conveyor system, hence it is difficult to monitor them in automated ways [6].

### **2.3.1 Failure modes of Idler system**

To design and optimize an idler system, it is important to understand the possible reasons and mode of their failure. In a study examining the failure rates of twenty belt conveyors over a six-month period, Gurjar (2012) discovered that a significant portion, specifically 74.1 percent, of the mechanical failures in a belt conveyor system were attributed to issues with idler rolls [7]. The impact of idler roll failures goes beyond just mechanical concerns. Belt conveyors with idler rolls getting stuck can result in significantly higher energy consumption. For instance, if 10 % of rolls become seized, the conveyor system could require an additional 100% of power, highlighting the substantial energy implications associated with idler roll problems [7].

The most common cause of idler failure is shell wear and bearing failure. According to Flexco, a conveyor belt manufacturing company, an idler roller can be failed due to abrasion, corrosion, ineffectiveness of seal or end design failure. Abrasion or shell wear from the roller is due to friction between the roller shell and belt as the belt moves. Replacing traditional steel roll with engineering polymers (Nylon and HDPE) can be seen as a promising way to combat this type of failure [8].

Bearing seizure also caused increase rate of shell wear. Bearing malfunctioning is the most common idler roller failure mode and 43% of bearing failure are caused by moisture and dirt [8]. Bearing damage can arise from various factors, with poor sealing, impurities, moisture, and water infiltration, degrading grease and increasing rolling resistance. Contaminated grease can also



compromise bearing integrity. Problems like improper longitudinal leveling, lateral inclination, and uneven spacing between conveyor sections can lead to wear and tear, impacting the overall health of the bearings [9]. Idler roller bearings have lubrications that are supposed to work till the bearing rating life, but some bearings lack lubrication when they are approaching failure. Grease provides good dirt protection, but it is temperature dependent and have a limited-service life. Lithium based grease with labyrinth seals are providing better protection to bearings from external source [9].

According to Amarnath and Kankar, wear rates become more significant when a metal-to-metal contact takes place when metal particles from bearing elements come in between the contact surfaces preventing the formation of hydrodynamic lubrication regime [10]. Brittle particles produce less wear as compared to ductile which is more abrasive in nature. According to SKF, a leading bearing manufacturer, and ISO 15243: 2017 standards, bearing damage can be classified into five possible division: Operating conditions (excessive loading, induced vibrations), lubrication (insufficient lubrication and dirt), production defects (insufficient surface hardness, strength or material imperfections), Belt conveyor assembly (improper beading load, larger gaps between moving bodies) and environmental factors (dirt, water penetration) [11], [12].

## **2.4 Idler roller technologies**

This section explains the potential idler manufacturers: RKM Roller Company PTY LTD [13], RULMECA [14], ASGCO [15], Conveyor Innovations International PTY LTD [16] and Conveyor Products and Solutions-CPS [17] and compare their innovative technologies, manufacturing processes with reference to ferrous and non-ferrous idler system with a focus on weight, material properties like strength, hardness, abrasive resistance, and cost consideration. Detailed information about traditional and innovative idler products produced by each company is given in Appendix A.

At first, ferrous idlers particularly made from steel, aluminum are discussed followed by composite material idlers produced and manufactured by different companies. A brief comparison between the products produced by these companies as shown in Table 1.

Table 1 Comparison of Idler products manufactured by leading companies.

<b>Company</b>	<b>RKM Roller Company PTY LTD</b>	<b>Rulmeca</b>	<b>ASGCO</b>	<b>Conveyor Innovations International Pty Ltd (CII)</b>	<b>Conveyor Products and Solutions-CPS</b>
<b>Roller Type</b>	Standard Steel Roller	Various Types (PSV, TOP Series)	Composite Rolls (C2000 Series)	OneFits Idler Roller	Yeloroll Rollers
<b>Material</b>	Steel	Steel, Thermoplastic Polymer	Glass Reinforced Polyurethane	Steel, Vitresteel, Carbon Fiber	Steel, Aluminum, Composite
<b>Sealing Technology</b>	Triple-Layered Seals	Hermetic Seals	Zinc-Plated Sealing Solution	CNC Machined Sealed End Caps	Multi-Labyrinth Watertight Sealing
<b>Additional Features</b>	Upgraded Versions Available	High-Performance Options Available	Lighter Alternative to Steel	GEN 7 Roller with Condition Monitoring Features	M-PVC Shell Material
<b>Application</b>	Coal, Grain, Iron Ore	Various Industries	Corrosive Environments	Various Mining Applications	Light, Medium, Heavy-Duty Uses
<b>Temperature Range</b>	-20°C to +100°C	Varies by Series	-40°F to +200°F	Not Specified	Not Specified
<b>Weight Reduction (Composite Rolls)</b>	N/A	Approximately 50% Lighter	30%	N/A	40% Lighter than Steel
<b>Strength</b>	Very high (300-400 Mpa)	Comparable to Steel	N/A	Twice as Strong as Black Steel	N/A
<b>Resistance to Impact/Cracks</b>	Very high	High Impact Resistance	Medium	Medium	Medium
<b>Noise Levels</b>	Higher	Reduced Noise Levels	Low	High	Substantial Noise Reduction
<b>Environmental Suitability</b>	Corrosion and rusting	Corrosive Environments	Excellent suitability	Ergonomic Benefits for Underground Mining	Excellent suitability

### 2.4.1 Remarks

For ferrous idler, the roller shell body is generally made up of mild steel with exception from CII to use Vitresteel in their shaftless idler design [16]. The roller shell is rounded from both ends to prevent any sharp edges to cut or damage the belt. Mostly, the end caps are welded using MIG welding into the shell on a groove position to the plate while some manufacturers press fit end caps into the shell body. Rulmeca utilize a single circular tube to fabricate shell, end plates and bearing seats by cold rolling and heated press [14]. CCI roller have bearing end cap, made up of hardened alloy and CNC manufactured, is mass swagged under 35 tones force into the tube ends eliminating traditional welding and reduce corrosion rates. Single row deep groove ball bearings with C3 internal clearance is used by all companies except CCI's double row deep groove ball bearing for supporting both radial and axial loads [16]. Bearings are factory sealed for life with permanent lubrication for low to medium material handling applications. For heavy duty applications, rollers with re-greaseable bearings are used which have the advantage of the older lubrication to get flushed along with any dirt particles and clean grease replaces the old, soiled grease. Solid or hollow mild steel shafts or spindles are used for roller supports with standard double or triple labyrinth sealing for bearings.

Non-ferrous/composite rollers have a greater diversity in construction and material use as compared to steel idlers. Depending on the costs and different material grades, a vast variety of non-ferrous idlers are available in the market with different constraints and limitations. Various shell construction in composite idlers is made up of aluminum, UHMWPE, PU, PVC and most commonly HDPE material. The end caps and bearing housing are produced using PU, polymeric inserts, homopolymer acetal resin or glass filled nylon with antistatic copper pin [17]. Single deep groove ball bearing with C3 internal clearing is used with four different types of sealings: four-rake press fit seals and a lip and labyrinth arrangement, labyrinth, and reverse labyrinth [16], [17], [18].

## 2.5 Regulation and Standards

Different companies and many international organizations have set some standards which can be used as reference material by engineers to design and analyze a belt conveyor and its components. Following is a brief overview of standards from CEMA, BS, JIS, AFNOR, FEM, DIN, and ISO:

- **CEMA (Conveyor Equipment Manufacturers Association):** CEMA 502-2016 – “*Bulk Material Belt Conveyor Troughing and Return Idlers - Selection and Dimensions*”: This

standard provides guidelines for the selection and dimensions of troughing and return idlers used in belt conveyors.

- **BS (British Standards):** BS 2890:1989 – “*Specifications for Troughed belt conveyors*”: This British Standard provides recommendations for the general design and construction features of troughed belt conveyors and includes specifications for idlers.
- **JIS (Japanese Industrial Standards):** JIS B 8803:2013 – “*Conveyor belts - Idlers - Specifications*”: This JIS standard specifies the technical requirements and test methods for conveyor belt idlers and is used in Japan.
- **AFNOR (Association Française de Normalisation):** NF EN 1037:2008 – “*Conveyor belts - Determination of the elastic and permanent elongation and calculation of the elastic modulus*”: While not specific to idlers, this AFNOR standard is relevant to conveyor belt performance, which can impact idler design considerations.
- **FEM (Fédération Européenne de la Manutention):** FEM 3012 – “*Selection and dimensions of idlers for belt conveyors*”: This standard provides guidelines for the selection and dimensions of idlers for belt conveyors.
- **DIN (Deutsches Institut für Normung):** DIN 22112-1:2015 – “*Belt conveyors with carrying idlers - Calculation of operating power and tensile forces*”: This DIN standard outlines methods for calculating the operating power and tensile forces in belt conveyors with carrying idlers.
- **ISO (International Organization for Standardization):** ISO 1537:2015 – “*Belt conveyors - Idlers - Guide for the use and application of idlers (Second edition)*”: As mentioned earlier, this ISO standard provides guidance on the selection and application of conveyor idlers.
- **ISO 5048:** “*Continuous mechanical handling equipment - Belt conveyors with carrying idlers - Calculation of operating power and tensile forces*”: Provides the basis for the calculation of conveyor belt tensions and requires certain specific data about the design of the conveyor.
- **Rulmeca:** Rulmeca have shared an open-source comprehensive document “*Rollers and components for bulk handling*” in 2003, which provides a complete design guideline for conveyor idlers and conveyor components. This document shared information about types of belt conveyor, material transportation, and their load distribution in terms of analytical functions, how to determine belt speed, belt width, loading calculations for associated forces

on rollers and standards tables and dimensions for choice of roller with respect to belt and material being transported.

The Idlers used in LKAB facility in Narvik are manufactured by Rulmeca hence, the document from Rulmeca is chosen as a reference along with CEMA standards to analyze the loading, boundary conditions, load distribution, choice of roller diameter and mathematical modeling and analysis required for optimizing rollers at LKAB facility.

### 3. Design Methodology

#### 3.1 Introduction

A systematic rational design method developed by Nigel cross, shown in Figure 8, will be followed to design and optimize the conveyor idler. The design model, consists of seven stages, is a systematic solution driven process following a symmetrical relationship between problems/sub-problems with solutions/sub-solutions respectively [18].

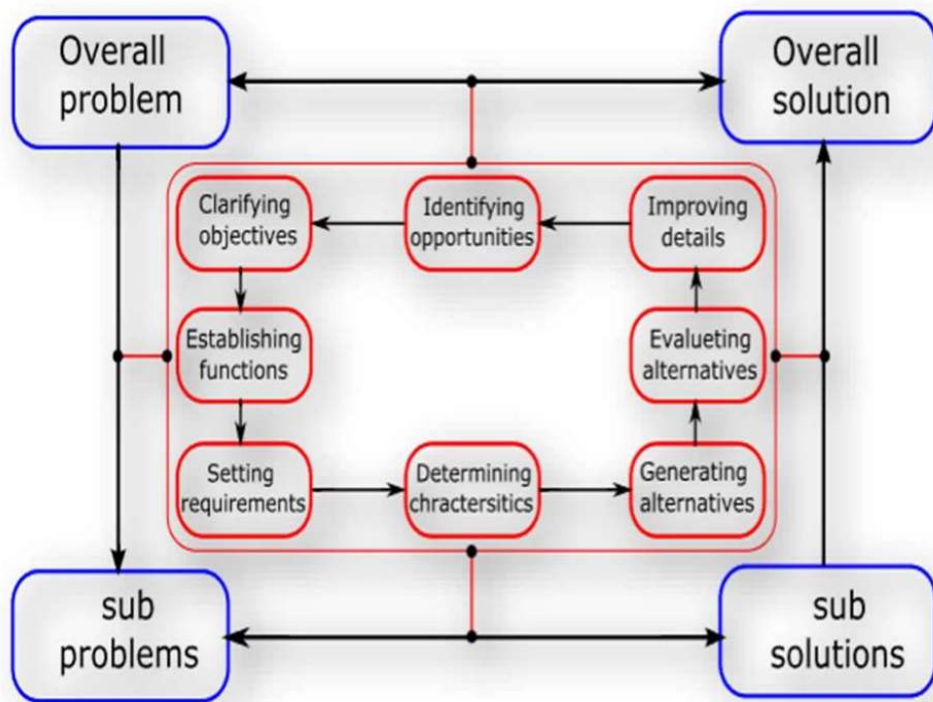


Figure 8: A Systematic rational design methodology [18]

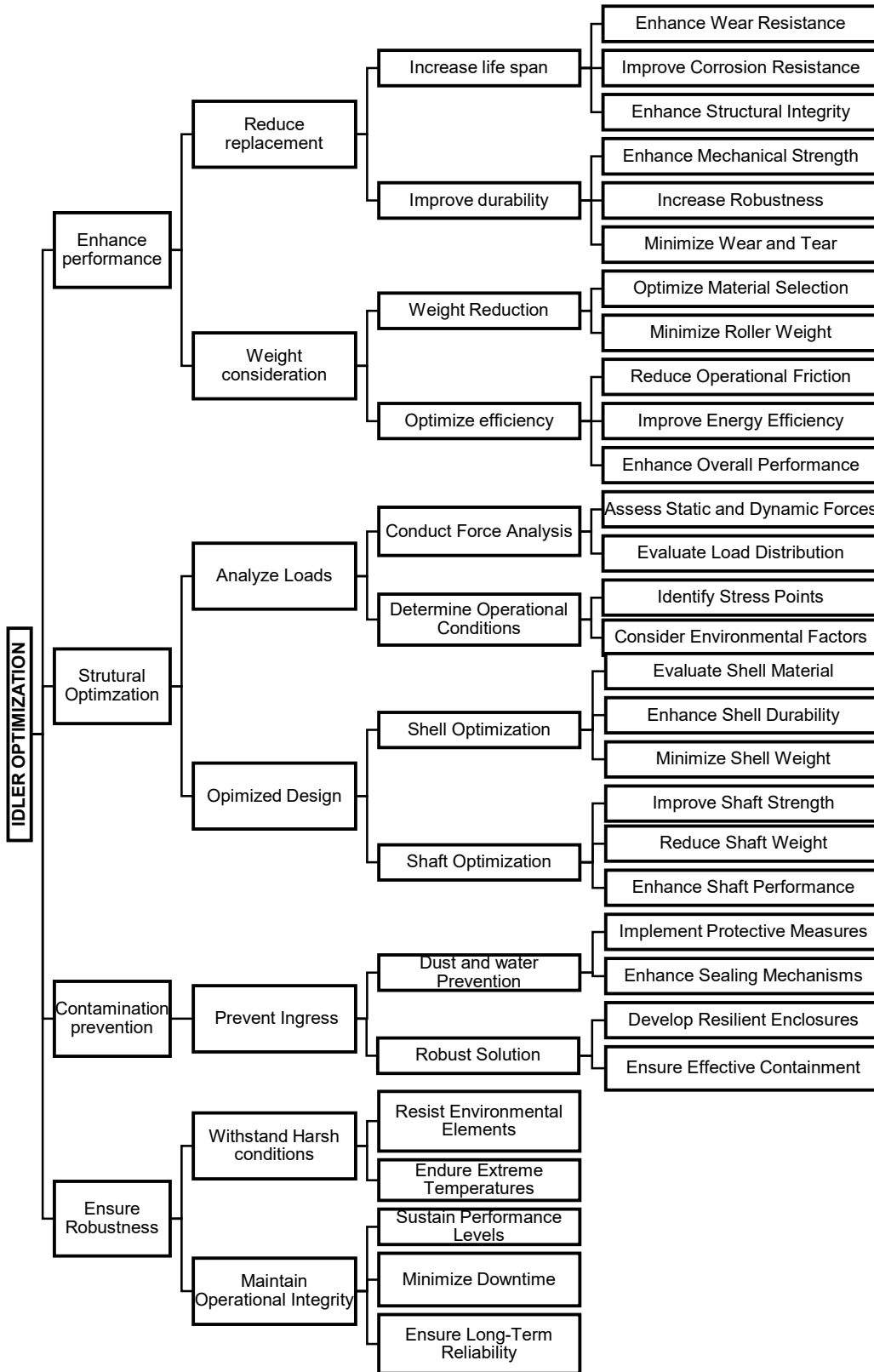
The designer explores both the problem and solutions together having an expected pattern of progression from a given problem to a proposed solution, following an anticlockwise movement direction from top left to top right along with substantial interactions going to-and-fro on both sides. In optimizing the idler roller, some components of this method are considered as an effective strategy to breakdown the problem and finding the solution for this master thesis.

### **3.2 Identifying Opportunities and Clarifying Objectives**

Among design stages, identifying opportunities and clarifying objectives involves determining the goals, constraints and objectives of the design which have been shortly discussed in Chapter 1, problem identification and thesis objective.

The objective tree, as shown below, divides the thesis main objective of “Idler optimization” into sub-components which provides a roadmap for addressing design challenges systematically and how to achieve the desired outcomes with a rational approach. For example, the sub-objective of structural optimization in objective tree diagram is further divided into force analysis and optimizing the idler shell and shaft design, to enhance durability, minimize wear, and improve overall performance. This step is essential in ensuring that the idlers can withstand the operational demands and environmental conditions they are subjected to, thereby prolonging their lifespan and reducing the frequency of replacements.

Contamination prevention strategies aim to prevent the ingress of dust and water into roller bearings, ensuring robustness and operational integrity under harsh environmental conditions. Ensuring that the idlers can withstand harsh conditions and maintain operational integrity is vital for minimizing downtime and maximizing productivity. Overall, the objective tree provides a systematic framework to address key challenges and achieve the goal of enhancing the performance and lifespan of conveyor rollers, ultimately optimizing the iron ore transportation process at LKAB's facility.



### 3.3 Setting requirements

Setting requirements includes establishing the criteria and performance attributes or characteristics that must be met by the idler roller optimized solution. These requirements, shown in Table 2 and 3 for roller shell and roller shaft respectively, serve as a benchmark for guiding the design process and evaluating potential solutions, ensuring that the resulting idler roller and its components meet the specified criteria and perform optimally in its intended application.

Table 2: Performance Specifications for Roller shell

<b>Performance Characteristic</b>	<b>Description</b>	<b>Range</b>	<b>Units</b>	<b>Priority</b>
<b>Load Capacity (D)</b>	Maximum weight the idler can support without failure	10,000 - 50,000	N	High
<b>Wear Resistance (D)</b>	Ability to withstand abrasion and maintain shape over time	High resistance to wear and tear	-	High
<b>Corrosion Resistance (D)</b>	Resistance to rust and degradation due to exposure to moisture and chemicals	Highly resistant to corrosion	-	High
<b>Weight (W)</b>	Overall weight of the idler system	10kg to 20kg	kg	Medium
<b>Noise Level (W)</b>	Level of noise generated during operation	40-60	dB	Medium
<b>Rotational Resistance (W)</b>	Smooth rotation of the idler with minimal resistance	Low friction for efficient operation	N	Medium
<b>Sealing Efficiency (D)</b>	Effectiveness of seals in preventing dust and water ingress	Highly effective sealing to protect internal components	-	High
<b>Structural Strength (D)</b>	Ability to withstand applied forces and maintain structural integrity	1-500	MPa	High
<b>Temperature Stability (W)</b>	Ability to withstand fluctuations in temperature without compromising performance	-20°C to 80°C	°C	Low
<b>Cost (W)</b>	Total cost of procurement and maintenance	Cost-effective solution without compromising quality	NOK	Low
<b>Material Compatibility (D)</b>	Compatibility with conveyed materials (e.g., coal, ore)	Compatible with a wide range of materials	-	High



<b>Bearing Lifespan (D)</b>	Lifespan of the idler bearings before replacement or maintenance	50,000 - 100,000	hours	High
<b>Environmental Impact (W)</b>	Environmental footprint of the idler material and manufacturing process	Low environmental impact and sustainability considerations	-	Low
<b>Alignment Accuracy (D)</b>	Precision of alignment with the conveyor belt to minimize wear and tracking issues	± 1	mm	High
<b>Maintenance Requirements (W)</b>	Frequency and complexity of maintenance tasks required	Low maintenance requirements for prolonged uptime	-	Medium
<b>Durability (D)</b>	Longevity and resistance to premature wear or failure	Extended service life with minimal degradation	-	High
<b>Energy Efficiency (W)</b>	Efficiency in power consumption during operation	Energy-efficient design for reduced operating costs	kW	Medium

*Table 3: Performance Specifications for Shaft*

<b>Performance Characteristic</b>	<b>Description</b>	<b>Target Value</b>	<b>Units</b>	<b>Priority</b>
<b>Strength</b>	Ability to withstand applied forces without deformation or failure	> 400	MPa	High
<b>Stiffness</b>	Resistance to bending or deflection under load	> 2000	MPa	High
<b>Shaft Deflection (D)</b>	Bending of shaft downward	≤ 12	degree	High
<b>Toughness (D)</b>	Resistance to indentation	>1.5	MPa M <sup>1/2</sup>	High
<b>Shaft Diameter</b>	Maximum diameter of shaft	15-35	mm	High
<b>Weight</b>	Overall weight of the shaft	< 10	kg	Medium
<b>Bearings</b>	Types of roller bearings	6302 to 6310	N/A	High
<b>Corrosion Resistance</b>	Resistance to rust and degradation in harsh environments	8+	Rating (e.g., ASTM G85)	Medium
<b>Surface Finish</b>	Smoothness and quality of the surface	>0.8	Ra (µm)	High
<b>Machinability</b>	Ease of machining and fabrication	4+	Rating (e.g., ASTM B108)	High
<b>Cost</b>	Total cost of procurement and manufacturing	<1000	NOK	Medium
<b>Environmental Impact</b>	Environmental footprint of the material and manufacturing process	Low	Rating (e.g., Life Cycle Assessment)	Medium

### 3.4 Force Analysis of Idler roller:

Based on the dimensions provided by LKAB for conveyor belt and roller, loading conditions, dimension constraints and boundary conditions on the idler are calculated with reference to Rulmeca document “Roller and components for bulk handling” and CEMA 502-2016 – “Bulk Material Belt Conveyor Troughing and Return Idlers - Selection and Dimensions” [19].

From the information given by LKAB, center idler dimensions are shown in Figure 9 and Table 4.

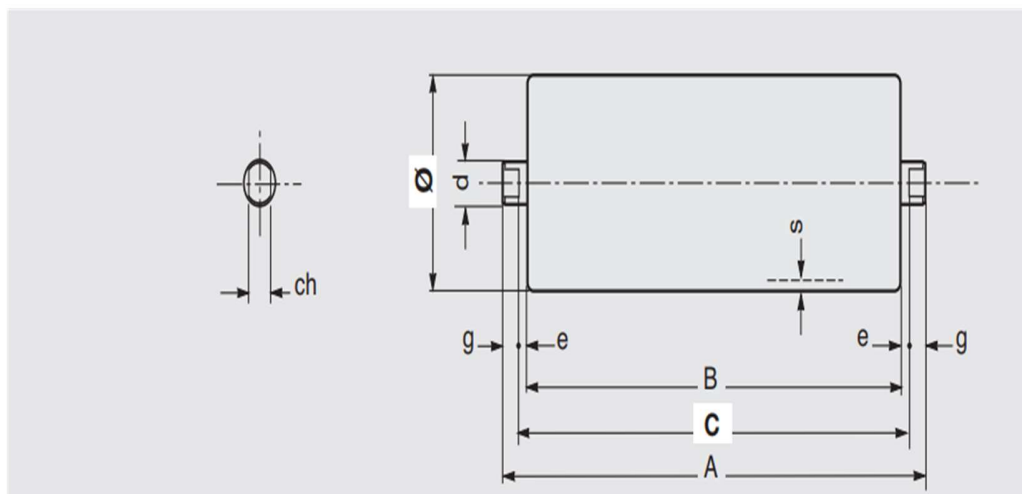


Figure 9: 2D drawing of idler roller at LKAB

Table 4: Roller dimensions

Variables	$\phi$	A	B	C	d	Ch	s	e	g
Dimension(mm)	159	632	600	608	30	22	4.5	4	12

#### 3.4.1 Distribution of forces

The force analysis of this idler in a conveyor system involves considering both vertical and horizontal forces exerted on the idler as the conveyor belt operates. When the pulley moves the conveyor, the conveyor belt bypass the idler which is supporting the belt at the moment and is stationary. The conveyor belt motion exhibits force in the form of tension to stationary idler which slowly overcome its rotational resistance under the influence of this force and ultimately start rotating with an angular velocity.

The force occur on idler in the vertical direction includes the total weight of the material and conveyor belt (G) while the horizontal direction force consists of tension of the conveyor belt on

the idler ( $F$ ), both are primary forces contributing to load as compared to idler resistance [20]. Horizontal forces, such as the resistance of the bracket to the idler roller ( $F_2$ ) and the rotational resistance of the bracket to the idler ( $M$ ), as shown in Figure 10.

**Assumption:**

- Only vertical forces are considered in this analysis because the idler rotational resistance becomes smaller as compared to vertical load when the belt is running smoothly.
- The analysis accounts for belt deflection, with consideration of two theoretical possibilities: (1) the material remains at the center of the conveyor belt as it runs or (2) the material completely follows the belt. Under extreme conditions, when the material stays at the center of the conveyor, the carrying idler experiences ideal loading. When materials completely follow the belt, conveyor belt deflection is not more than 10% of belt width [20]. Consequently, the impact of conveyor belt deflection on idler analysis can be disregarded.

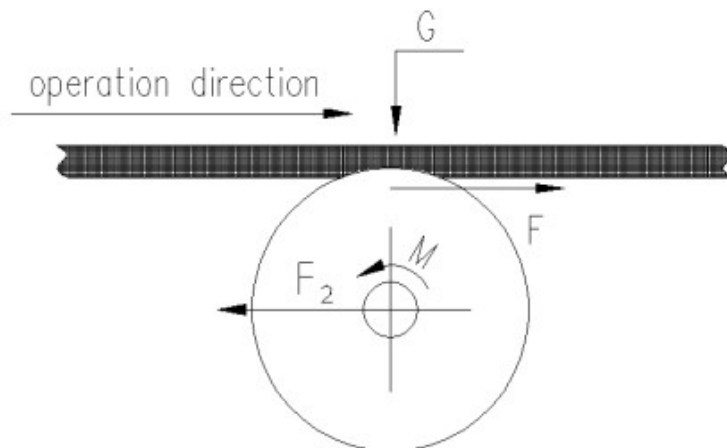


Figure 10: Force distribution on idler [20]

In order to determine the static and dynamic forces on the center and wing idlers, *Rulmecca Rollers and components for bulk handling* [21], Chapter 2 -Rollers (p. 75-79) is used.

Following principal factors, shown in Table 5 are important to consider while determining the load on idler.

Table 5: Principal factors for Force analysis

Symbol	Principle Variable	Unit
$I_v$	Belt load	t/h
$v$	Belt speed	m/s
$a_0$	Carrying trough set pitch	m
$a_u$	Return set pitch	m
$q_b$	Belt weight per linear meter	Kg/m
$F_p$	Participating factor of higher stressed roller	-
$F_d$	Shock factor	-
$F_s$	Service factor	-
$F_m$	Ambient factor	-
$F_v$	Speed factor	-

Table 6: Belt width and corresponding pitch for upper and lower idler sets [21]

Belt Width	Pitch of Upper Troughing set			Lower
	<i>Specific weight of conveyed material t/m<sup>3</sup></i>			
m	<1.2 m	1.2 ÷ 2.0 m	> 2.0 m	> 3.0 m
<b>300</b>				
<b>400</b>				
<b>500</b>	1.65	1.50	1.40	3.0
<b>650</b>				
<b>800</b>	1.50	1.35	1.25	3.0
<b>1000</b>	1.35	1.20	1.10	3.0
<b>1200</b>				
<b>1400</b>				
<b>1600</b>	1.20	1.00	0.80	3.0
<b>1800</b>				
<b>2000</b>				
<b>2200</b>	1.00	0.80	0.70	3.0

The belt load or belt capacity is 9000 t/h, the belt speed is 3m/s and the carrying and return troughing set pitch (distance between two consecutive troughing sets) is selected from Rulmecca document as shown in the Table 6. The belt weight per linear meter for a conveyor depends on various factors, including the width and thickness of the belt, as well as the material it's made of. Typically, the weight of the belt is specified in kilograms per meter (kg/m) and can be approximated from Dunlop Conveyor Design manual, see Table 7 [22].

*Table 7: -Belt weight with respect to different belt widths [22]*

	<b>Operating condition</b>			
	<b>Duty</b>	<b>Light</b>	<b>Medium</b>	<b>Heavy</b>
<b>Width</b>	<b>Duty</b>	<b>Duty</b>	<b>Duty</b>	<b>Duty</b>
<b>(mm)</b>	<b>(kg/m)</b>	<b>(Kg/m)</b>	<b>(kg/m)</b>	<b>(kg/m)</b>
<b>500</b>	4,1	6,2	10,3	
<b>600</b>	5,0	7,4	12,3	
<b>750</b>	6,2	9,3	15,5	
<b>900</b>	7,4	11,1	18,5	
<b>1050</b>	8,6	13,0	21,6	
<b>1200</b>	9,8	14,8	24,7	
<b>1350</b>	11.0	16,7	27,8	
<b>1500</b>	12,3	18,6	30,9	
<b>1650</b>	13.5	20,5	33,9	
<b>1800</b>	14,7	22,3	37,0	
<b>2100</b>	17,2	26,0	43,3	
<b>2200</b>	18,0	27,3	45,3	

For different operating factors, RULMECCA document is used to determine their operational values based on working hours, impact factor due to lump size and environment, see Figure 11 and Table 8, 9 and 10 below. These factors account for the operating conditions in which the idler roller is working. Participation factor accounts for the troughing angle which the center idler is making with wing rollers. A higher troughing angle generally leads to a more concentrated load distribution

towards the center of the belt as shown in by the participation factor value in Figure 11. Service factor accounts for the number of hours the conveyor is operating while environmental factor considered the surrounding environment.

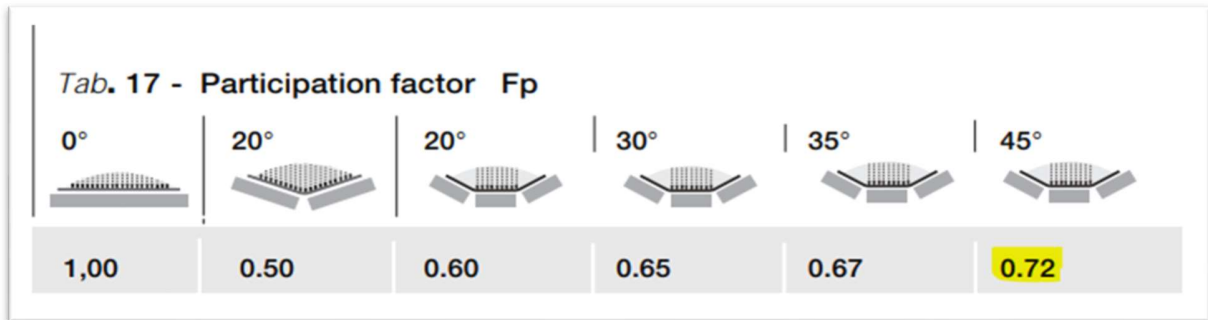


Figure 11: Participation factor with respect to angle of troughing [21]

Table 8: Service factor  $F_s$  [21]

Service Factor	
Life	$F_s$
Less than 6 hours per day	0.8
From 6 to 9 hours per day	1.0
From 10 to 16 hours per day	1.1
Over 16 hours per day	1.2

Table 9 Environmental Factor  $F_m$  [21]

Environmental factor	
Conditions	$F_m$
Clean and fine material presence	0.9
Abrasion or corrosion material presence	1.0
Very Abrasion or corrosion material presence	1.1

Table 10: Impact factor  $F_d$  [21]

Material Lump size	Belt speed m/s						
	2	2.5	3	3.5	4	5	6
0 ÷ 100 mm	1	1	1	1	1	1	1
100 ÷ 150 mm	1.02	1.03	1.05	1.07	1.09	1.13	1.18
150 ÷ 300 mm	1.04	1.06	1.09	1.12	1.16	1.24	1.33
In layers of fine material							
150 ÷ 300 mm	1.06	1.09	1.12	1.16	1.21	1.35	1.5
without layers of fine material							
300 ÷ 4500 mm	1.2	1.32	1.5	1.7	1.9	2.3	2.8

Hence, based on the above tables from the reference document of Rulmeca, the principal factors with their values are as follows:

Symbol	Value	Unit
$I_v$	9000	t/h
$v$	3	m/s
$a_0$	0.8	m
$a_u$	3	m
$q_b$	32	Kg/m
$F_p$	0.72	-
$F_d$	1.09	-
$F_s$	1.1	-
$F_m$	1.1	-
$F_v$	0.92	-

### 3.4.2 Load Calculations

With reference to RULMECA “Rollers and components for bulk handling, Page 52”, the static load  $C_a$  acting on the carrying troughing set can be determined using *Equation (3.1)*

$$C_a = a_0 \times \left( q_b + \frac{I_v}{3.6 \times v} \right) \times 9.81 \quad (3.1)$$

Where  $q_b$  = Belt weight per meter,  $I_v$  = Belt load per meter,  $a_0$  = Pitch of carrying idler of troughing set.

$$C_a = 6791.136 \text{ N}$$

For Dynamic Load, *Equation (3.1)* is multiplied with the operating factors to find the dynamic load  $C_{a1}$  acting on the idler set as shown in *Equation (3.2)*

$$C_{a1} = C_a \times F_d \times F_s \times F_m \quad (3.2)$$

Where  $F_d$  = Shock factor,  $F_s$  = Service factor and  $F_m$  = Environmental factor. Hence, the dynamic load is

$$C_{a1} = 8956.82 \text{ N}$$

For our assumption, all the rollers are equal in dimensions in the troughing set, the maximum load is supported by the center idler  $c_a$ , can be calculated by multiplying the participation factor  $F_p$  with the dynamic load. Hence, by using the *Equation (3.3)*, the maximum load on center idler can be calculated.

$$c_a = C_{a1} \times F_p \quad (3.3)$$

$$c_a = 6448.91 \text{ N}$$

Since, the return idler does not take any material load, the static load on return set can be calculated using *Equation 3.4*.

$$C_r = a_u \times q_b \times 9.81 \quad (3.4)$$

Where  $a_u$  = Return idler set pitch,  $q_b$  = Mass of belt per meter length

$$C_r = 941.76 \text{ N}$$

The dynamic load  $C_{r1}$  on return idler set is independent of shock factor as there is no material transported on return idler, hence it is calculated by following equation

$$C_{r1} = C_r \times F_s \times F_m \times F_v \quad (3.5)$$

$$C_{r1} = 1048.36 \text{ N}$$



Equation 3.6 is used to determine the load on single return roller  $c_r$  by multiplying the dynamic load  $C_{r1}$  for return idler with participation factor  $F_p$ .

$$c_r = C_{r1} \times F_p \quad (3.6)$$

$$c_r = 754.81N$$

These values are determined based on the given equations and assumptions, considering factors such as belt weight, velocity, and dynamic load factors. The loads provide insight into the forces experienced by the idler sets and individual idlers in the conveyor system, aiding in design and optimization efforts. Values presented in Table 11 shows that the dynamic loads on both the carrying and return idler sets surpass their respective static loads, reflecting the additional forces induced by the movement of the conveyor belt and the conveyed material. Conversely, the static load on the center idler slightly exceeds that on the carrying idler set, indicating potentially higher forces experienced by the center idler.

Table 11: Calculated load on carrying and return set

<i>Variable</i>	<i>Value</i>
<i>Static load on Carrying idler set</i>	6791.136N
<i>Dynamic load on Carrying idler set</i>	8956.82N
<i>Static load on center idler</i>	6448.91N
<i>Static load on return idler set</i>	941.76N
<i>Dynamic load on return idler set</i>	1048.36N
<i>Load on single return idler</i>	754.81N

### 3.5 Prototype

Based on provided dimensions, the 3D model of the idler roller is drawn using SOLIDWORKS for analysis. Figure 12 (a, b) shows the 3D model of center idler along with its components in exploded view. Figure 13 presents a section view of the CAD model, offering insights into the internal structure and design features of the idler. The detailed 2D drawings of the idler and its components provided in Appendix B, complements these visual representations and shows precise specifications and dimensions for reference. Together, these representations form a prototype that accurately reflects the physical geometry and specifications of the idler.

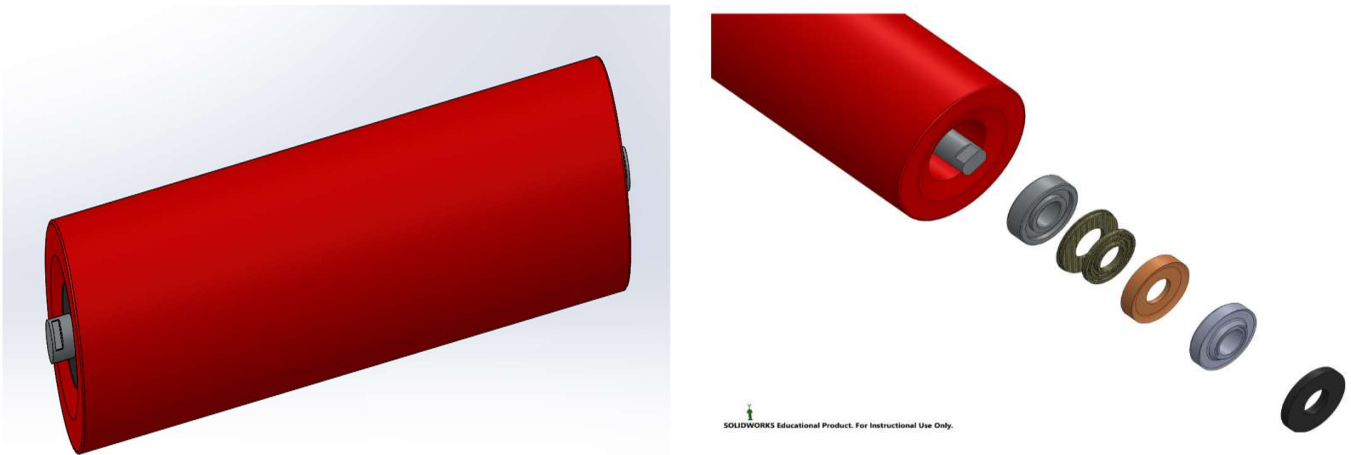


Figure 12: a) 3D CAD model of Idler b) Exploded view CAD model of idler

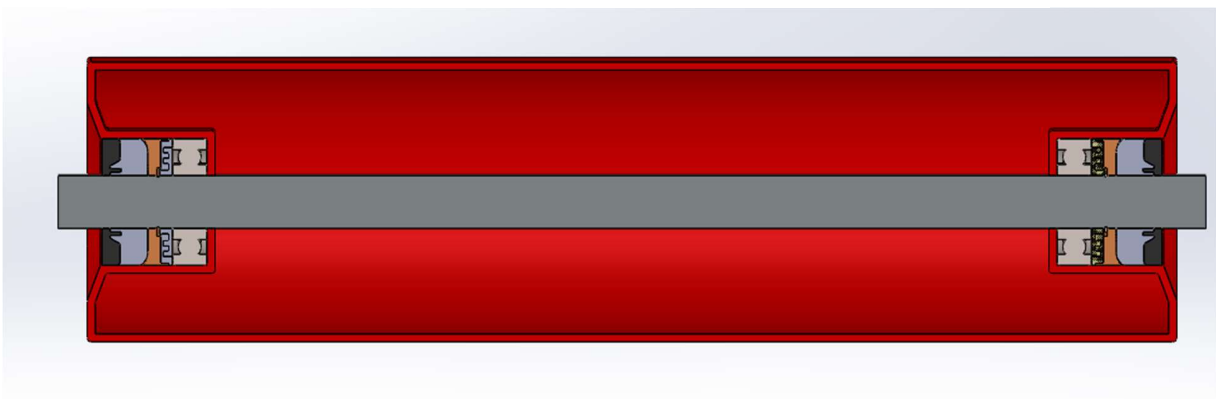


Figure 13: Section view of idler CAD model

## 4 Structural Analysis of Conveyor Idler

### 4.1 Numerical Analysis

The analysis phase is utilizing ANSYS Static Structural to evaluate the structural integrity and performance of the conveyor idler through Finite Element Analysis (FEA). By applying boundary conditions and material properties to the SolidWorks prototype, parameters such as stress distribution, deformation, and factor of safety are calculated. This analysis provides information about potential areas of weakness or excessive loading, allowing for iterative design improvements and optimization.

#### 4.1.1 Shell Analysis

For Idler shell analysis, the 3D CAD model is converted into STEP file format and imported into ANSYS static structural. Following assumptions are considered in this analysis:

##### Assumptions:

- For simplicity and efficiency, the analysis focuses solely on the idler shell with cylindrical supports at the ends, neglecting other shell components like end cap, labyrinth seals, bearing housing and bearings shown in Figure 14.
- Static load on center idler is 6448.91N which is approximated to 6500N (uniformly distributed) and weight of other all other components are ignored.
- The bearing housing is welded with the roller shell which does not allow any motion in all three cylindrical co-ordinates; hence a fixed cylindrical end support is used for the analysis.

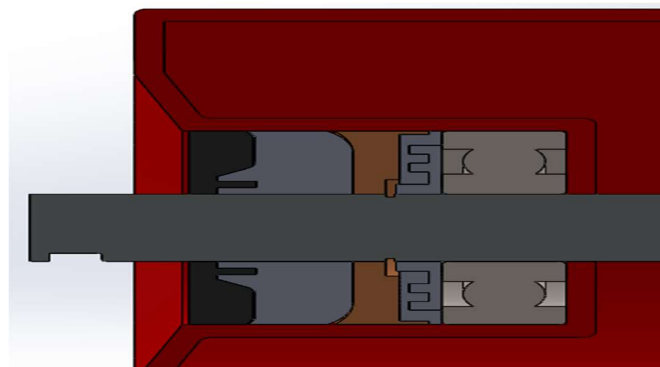


Figure 14: Section view of idler roller, showing neglected components

For material assignment, structural steel is selected, and the meshing is done using program controlled meshing settings with element size of 5mm, having 20566 mesh elements. The detailed analysis steps for both shell and shaft are given in Appendix C. A uniformly distributed static load of 6500N is applied to the idler shell and the end points are given a fixed cylindrical support as shown in Figure 15.

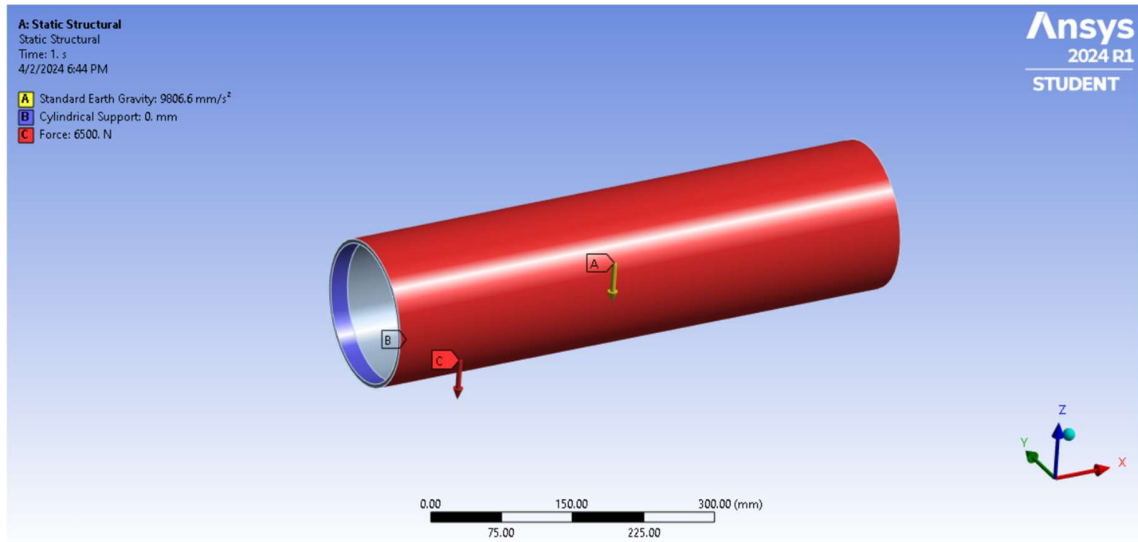


Figure 15: Boundary conditions for idler shell: A standard earth gravity of  $9806.6 \text{ mm/s}^2$ , A distributed force of 6500N, fixed cylindrical supports at both ends

The system is solved, and following results are obtained for displacement and equivalent von misses stress shown in Figure 16 and 17 respectively.

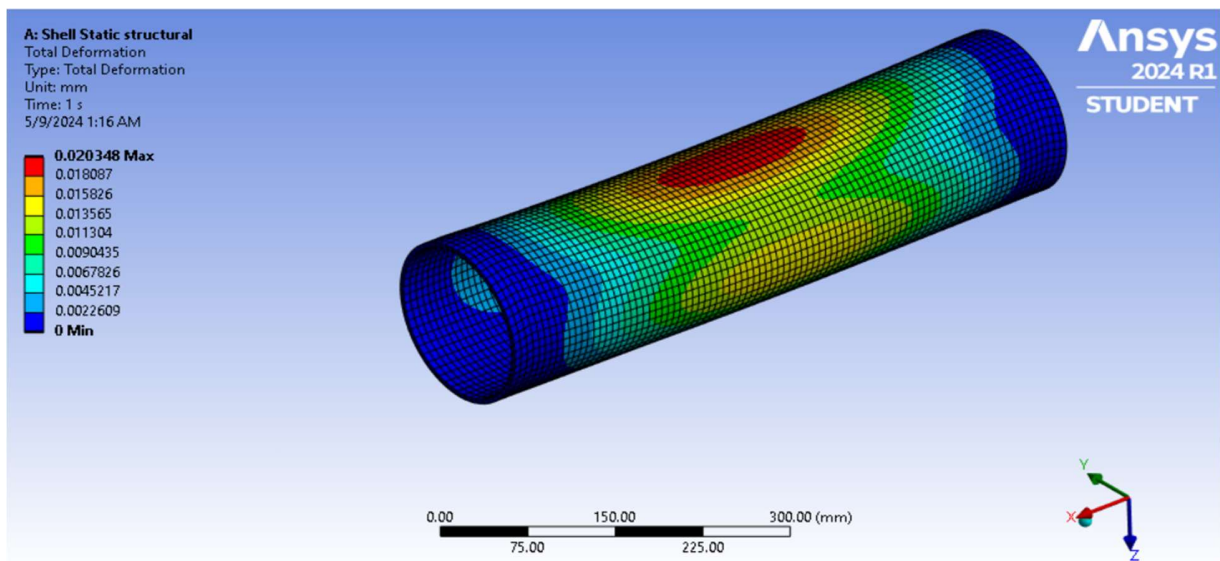


Figure 16: Total Deformation at idler shell with a maximum value of 0.007415mm

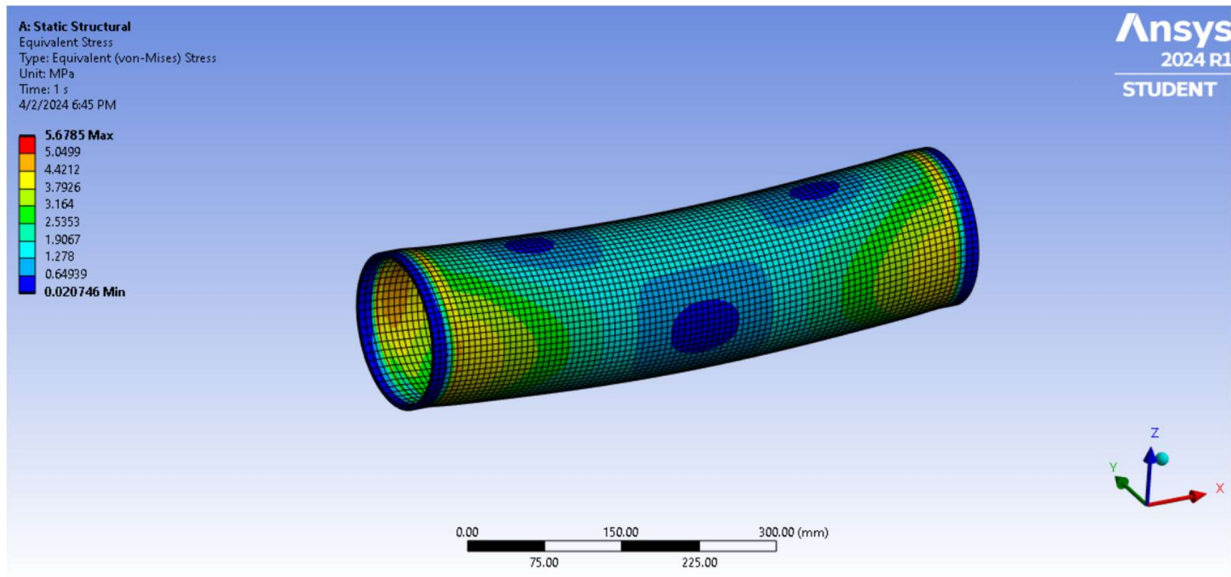


Figure 17: Equivalent Stress distribution with a maximum stress of 5.678Mpa

The maximum deflection and maximum stress obtained in this analysis are 0.0213 mm and 5.68 MPa respectively. It can be seen that both the total deformation and equivalent von-mises stress are uniformly distributed along the length of idler shell which shows absence of any discontinuity or abnormal stress variation when the material is transported.

#### 4.1.2 Shaft Analysis

The force transmission to the shaft of an idler in a conveyor system involves multiple factors. Firstly, the primary force is exerted by the conveyor belt itself which applies downward pressure onto the idler roller as it moves along the conveyor. This force is transferred through the roller shell to the shaft, which serves as the central support for the roller's rotation.

Additionally, lateral forces resulting from material loading or changes in direction can also affect the idler shaft. These forces are distributed along the length of the shaft and must be accommodated by the bearing and housing assembly to ensure smooth and reliable operation of the conveyor system. Therefore, the design and material selection of the idler shaft are critical to withstand these forces and maintain the overall functionality of the conveyor.

#### Assumptions

- For simplicity, only vertical loads are considered and the resultant load acting by the bearings on the shaft.

- Lateral forces, lateral forces resulting from material loading or changes in direction are neglected.
- Shaft end is supported by a slot in idler frame structure which is assumed to have pinned support at both ends for the analysis, see figure 18.

On left end, displacement in xyz axis is zero, but it is allowed to rotate in z direction. On right end, displacement in y, z is zero, but the shaft is allowed to move in x-axis direction and rotate around z axis as shown in Figure 19. This approach is used to make the end points as simply supported to match with real life situation. A force of 3000 N is acting on the bearing position on both sides with a standard earth gravity acting in the negative y-direction.



Figure 18: End Support

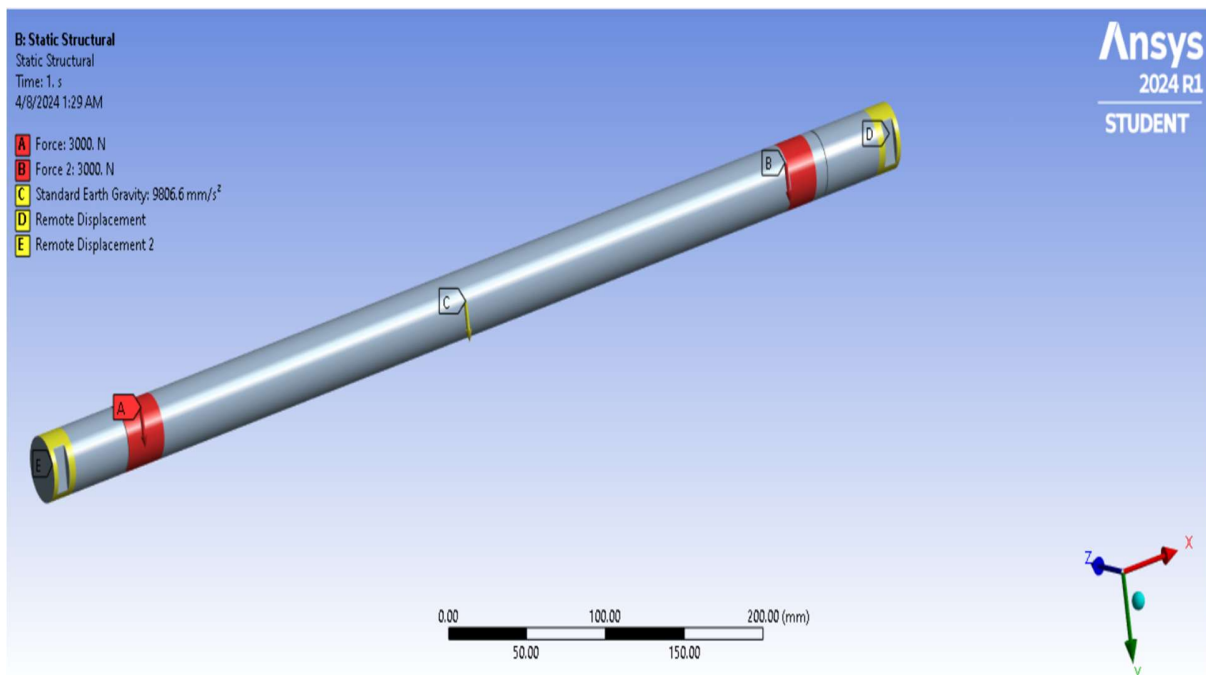


Figure 19: Boundary conditions at shaft: A load of 3000N on both bearing seats, standard earth gravity of 9806.6mm/s<sup>2</sup>, remote displacements at ends

With these inputs, the structural analysis is carried out, resulting in the determination of total deformation and equivalent Von Mises stress distribution across the system, see Figure 20 and 21.

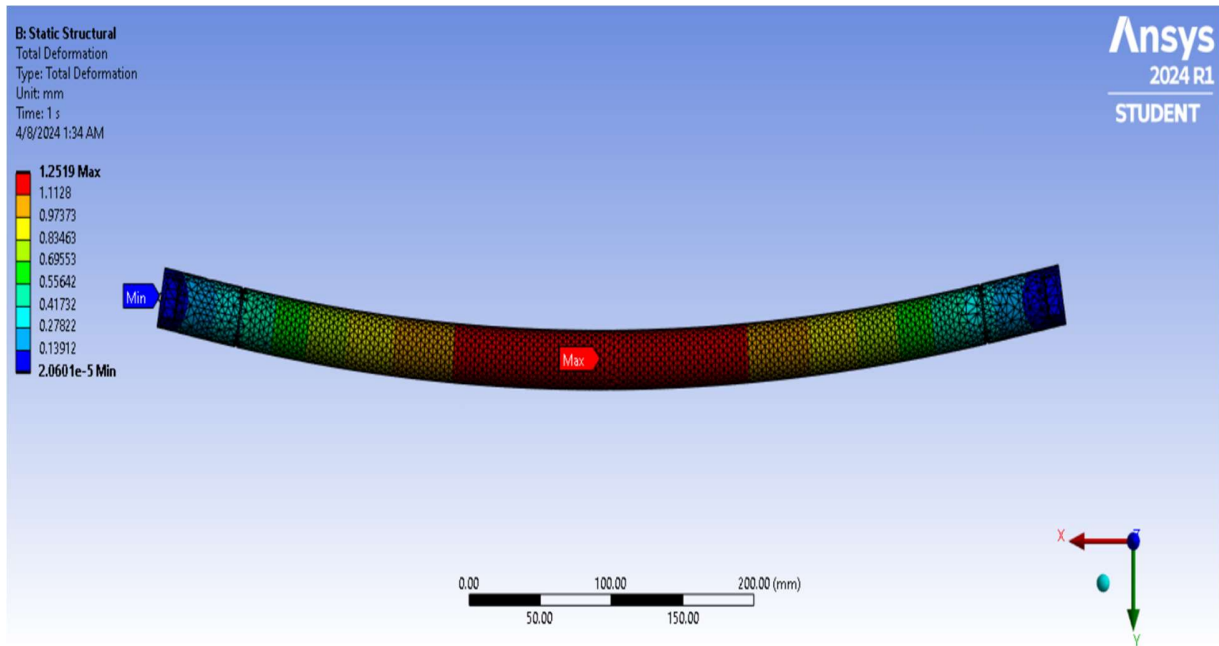


Figure 20: Total deformation at shaft

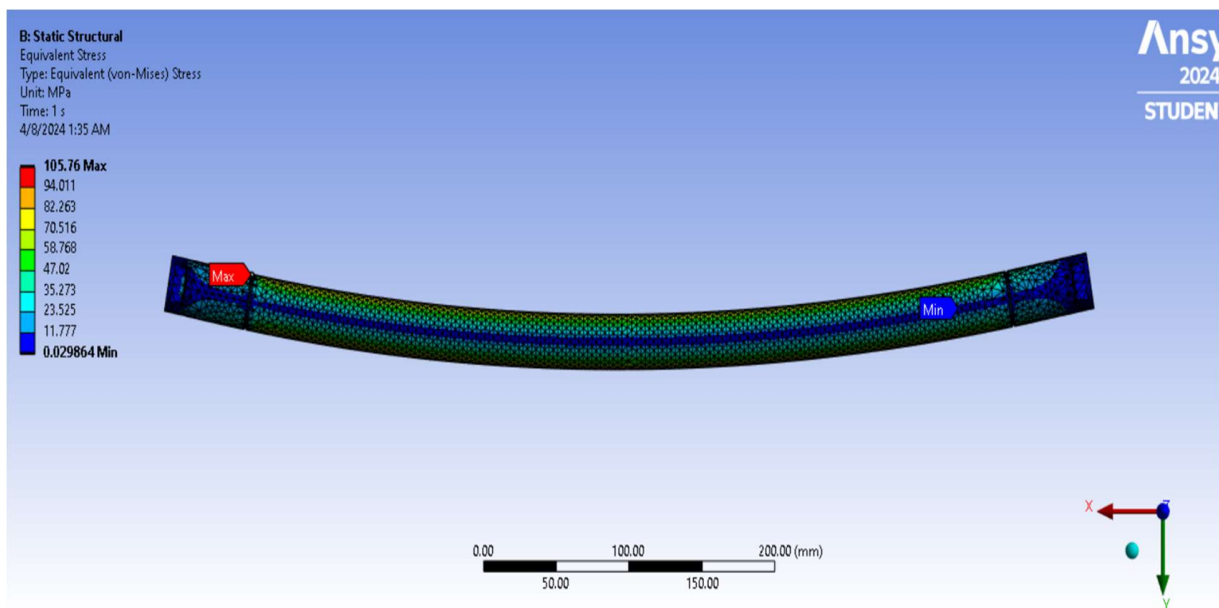


Figure 21: Stress distribution of shaft

The analysis shows that the maximum deformation of 1.2519 mm is at the center of the shaft and the maximum stress value of 105MPa is acting at the end points. Both the stress and deformation have uniform distribution and the shaft is deformed exactly as per the real condition with pinned supported behavior which shows the applied boundary conditions are correct. The observed behavior validates the correctness of the applied boundary conditions, confirming their ability to

accurately simulate the structural response of the system. This analysis provides insights into the structural integrity and performance of the shaft under the specified loading and support conditions, facilitating informed decision-making in the design and optimization process. In order to validate these results for both idler shell and shaft, theoretical calculations are performed to compare both and figure out the differences between the numerical simulations and analytical results.

## 4.2 Theoretical Analysis

### 4.2.1 Shell Analysis

The Idler shell needs to withstand the combined load from the conveyor belt and the bulk material being transported. Additionally, it must maintain minimal eccentricity and unbalance to ensure smooth and quiet operation of the roller. When dimensioning the shell, thickness is a critical parameter. For theoretical analysis, following assumptions are made:

#### Assumption

- For idler rolls positioned in a straight trajectory, it can be assumed that the load on the center roll is evenly distributed along the entire length of the shell as shown in Figure 22.

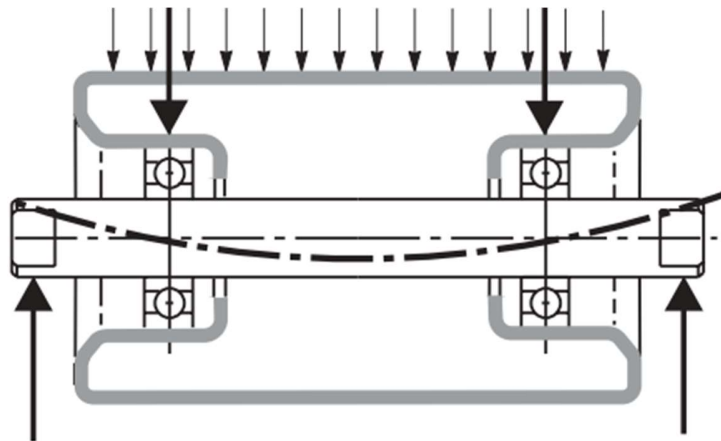


Figure 22: Schematic of an idler under loads and reaction forces [21]

Assuming a uniform load distribution acting on the roller shell, the maximum stress can be calculated using the following Equation (4.1),

$$\sigma = \frac{My}{I} \quad (4.1)$$



Where  $M$  = Maximum moment,  $y$  = Distance from neutral axis to one edge,  $I$  = Moment of inertia for a thin tubular wall which can be determined by following formula

$$I = \frac{\pi}{4} (r_{out}^4 - r_{in}^4) \quad (4.2)$$

Where  $r_{out} = 0.0795$  is outer radius and  $r_{in} = 0.075$  is the inner radius of tube. Hence, using Equation (4.2), moment of inertia is

$$I = 6.522 \times 10^{-6} \text{ m}^4$$

Assuming shell as a simply supported beam, with a uniformly distributed load, the maximum bending moment  $M$  occurs at the centre of the beam and is equal to  $\frac{wl^2}{8}$ , where  $w=10000\text{N/m}$  is the magnitude of the distributed load per unit length and  $L=0.6\text{m}$  is the length of the beam, and  $y=0.0795\text{m}$ . Hence, Equation 4.1 takes the following form.

$$\sigma = \frac{\left(\frac{wL^2}{8}\right)(y)}{\frac{\pi}{4}(r_{out}^4 - r_{in}^4)} = 5.485 \text{ MPa}$$

For the shell deflection, following equation applied to calculate the angular deflection  $y(\text{shell})$  of the shell of center roll.

$$y_{shell} = \frac{wl^4}{24 EI} \quad (4.3)$$

Whereas  $w$  = Load on shell per unit length,  $l$  = Length of idler shell,  $E = 2 \times 10^{11}\text{Pa}$  young modulus of material,  $I$  = Moment of inertia. Hence, by putting values in Equation (4.3) the deflection is

$$y_{shell} = 0.0192 \text{ mm}$$

## 4.2.2 Shaft Analysis

The deflection of roll shafts plays a critical role in bearing performance, directly impacting their fatigue life. Excessive deflection, beyond a certain threshold, can induce additional stress on bearing contacts, leading to premature fatigue failure. The schematic cutaway of a roll shaft, as depicted in Figure 23, provides insight into the structural considerations involved. In calculating shaft deflection, radial forces acting on the bearings are the primary influencing factors.

Assumption:

- The radial forces acting on two bearings are equal for a center roller

- Weight of bearing housing, end cap and sealings are neglected
- Only bearings are experiencing the material and belt load
- Bearings do not transmit any moment load

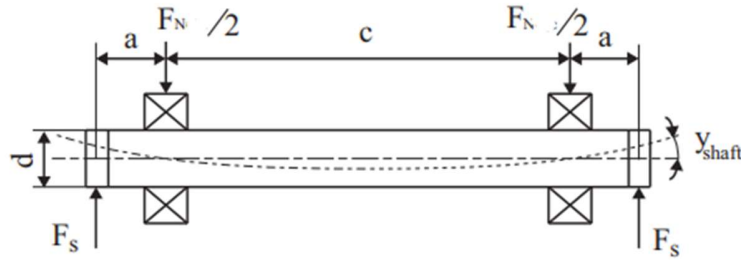


Figure 23: Schematic cutaway of an idler shaft considering the bearings do not transmit any moment [23]

The shaft deflection equation is given as:

$$\delta_{shaft} = \frac{F_N a^2 (3L - a)}{6EI} \quad (4.4)$$

Whereas  $F_N=6000$  is the total radial force in N,  $a=0.075$ m and  $c=0.450$ m are dimensions shown in figure 22 and  $d=0.030$ m is the diameter of shaft in m. Hence by putting values in SI units, the shaft deflection from Equation (4.4) is calculated as

$$\delta_{shaft} = 1.22 \text{ mm}$$

The maximum bending stress for the shaft is calculated by using Equation (4.1).

$$\sigma = \frac{My}{I} = 84.8 \text{ MPa}$$

### 4.3 Comparison Between Numerical and Theoretical Analysis

Table 12 shows the comparison of analytical results with numerical calculations. The idler shell experiences relatively low stress and deformation. The differences between numerical and analytical results are relatively small, indicating that the analytical model used is reasonably accurate for this component. For the idler shell, the equivalent stress values obtained through numerical analysis (5.67 MPa) closely align with the analytical results (5.485 MPa), exhibiting a relatively small error percentage of 3.26%.

For comparison of idler shell deformation, it can be seen that both the numerical and analytical results gave same results, with numerical analysis yielding a value of 0.02034 mm compared to the analytical result of 0.0192 mm, representing an error percentage of 5.92%. This suggest that the analytical model for the idler shell is reasonably accurate, with some minor differences due to simplifications or assumptions made in the analytical calculations.

Table 12: Comparison between numerical and analytical results for idler shell and shaft

	Numerical results		Analytical Results		Error	
	Equivalent stress (MPa)	Directional deformation(mm)	Equivalent stress (MPa)	Maximum deflection(mm)	Error % Stress	Error % Deformation
<b>Idler shell</b>	5.67	0.02034	5.485	0.0192	3.26	5.92
<b>Shaft</b>	105.76	1.2519	84.5	1.22	24	2.54

In contrast, comparison of shaft analysis for both deflection and equivalent stress reveals more deviations between numerical and analytical results. The equivalent stress obtained through numerical analysis (105.76 MPa) significantly exceeds the analytical result (84.5 MPa), indicating a significant error of 24%. For total deformation, the numerical analysis yields a maximum deflection value of 1.2519 mm compared to the analytical result of 1.22 mm, giving an error of only 2.54%. These differences suggest that the analytical model for the shaft may be less accurate, potentially due to oversimplifications or idealizations made in the analytical calculations.

**Possible reason for difference in results:**

- The shaft, subjected to diverse loads and boundary conditions, exhibits expected behavior under loading circumstances. When applying loads at concentrated points, such as through bearings onto a shaft, it's vital to acknowledge the distribution of force. Bearings, acting as interfaces, disperse loads across a contact area rather than concentrating them as idealized point loads assumed in analytical calculations. Consequently, the actual load distribution onto the shaft may deviate from the assumed point of application.

- End supports, boundary conditions, extend over a material area beyond theoretical points considered in analytical models. This expanded contact area alters how loads are transmitted, introducing discrepancies between analytical predictions and actual behavior.
- Additionally, factors like stress concentration effects, non-linear material behavior, and geometric irregularities further contribute to differences between analytical and numerical results for shaft components.

## 5 Modal Analysis

Modal analysis of the idler roller 3D model is done in ANSYS to understand the dynamic behavior and vibrational characteristics exhibited by the idler under varying loading conditions. Through the utilization of finite element analysis (FEA) methods, modal analysis determines the mode shapes and corresponding natural frequencies inherent within the idler system (24).

### 5.1 FEM Equations for Modal Analysis of Idler

The modal analysis of a structure is governed by equations describing free and forced vibrations [24]. In the case of free vibration, the governing equation is expressed as

$$[K]\{U\} + [M]\{A\}\omega^2\{U\} = \{0\} \quad (5.1)$$

Where  $[K]$  = Stiffness matrix,  $[M]$ = Mass matrix,  $\{U\}$ = Displacement vector,  $\{A\}$ = Damping matrix, and  $\omega$ = Angular frequency. When subjected to dynamic loads, the free vibration *Equation (5.1)* becomes

$$[K]\{U\} + [M]\{A\}\omega^2\{U\} = \{F(t)\} \quad (5.2)$$

Where  $\{F(t)\}$  =Time-dependent external force vector.

The motion of a system, such as an idler roller, can be described using the equation

$$mx'' + cx' + kx = F(t) \quad (5.3)$$

Where  $m$ = Mass matrix,  $c$  = Damping matrix,  $k$  = Stiffness matrix, and  $x$ = Vector of nodal displacements. To determine the natural frequencies and mode shapes of the structure, the eigenvalue equation:

$$(K - \omega^2 M) \varphi = -C\omega\varphi \quad (5.4)$$

where  $\varphi$  = Eigenvector or mode shape of the structure. The eigenvalues calculated from *Equation (5.4)* correspond to the natural frequencies squared, while the eigenvectors represent the mode shapes.

## 5.2 FEM Model Analysis in ANSYS

FEM modal analysis generate mode shapes and natural frequencies which give information about the idler's vibrational characteristics. The lowest energy modes, typically ranging from mode one to six, are analyzed to assess the predominant vibrational patterns generated by the idler roller. Mode shapes represent idler displacement pattern under dynamic loading conditions, while natural frequencies indicate the oscillation frequency associated with each mode. Through finite element analysis (FEM), modal analysis identifies three primary mode shapes: flexural (bending), transverse, and torsion [24]. These mode shapes show how the idler deforms and oscillates in response to external forces or vibrations. By examining modal analysis results, one can determine critical resonant frequencies and potential modes of vibration that may affect the idler's performance and structural integrity. This analysis aids in optimizing the idler design to remove undesirable vibrational effects and ensure reliable operation in conveyor systems.

Table 13 gives a general overview about three mode shapes and their primary causes. Each mode type is characterized by distinct motion patterns and causes, which impact the structure differently. The flexural mode is caused by self-weight of the component or the loads acting in vertical direction which is more significant in our case as the majority of the load is due to self-weight of the idler, belt weight and the weight of iron ore transported on the conveyor. Transverse load cause lateral instability in structures and can be avoided by introducing damping mechanisms. The torsional mode involves twisting in structures due to unequal load distribution and the torsional stiffness can be increased by achieving symmetry in structures [24].

*Table 13: Three primary modes of vibration*

<b>Mode Type</b>	<b>Nature of Motion</b>	<b>Primary Causes</b>	<b>Impact on Structure</b>	<b>Frequency</b>	<b>Design Considerations</b>
<b>Flexural</b>	Up and down	Self-weight and load	Deflection, cracking	Lowest	Material selection, geometry
<b>Transverse</b>	Side to side	Self-weight and load	Lateral instability	Higher than flexural	Wind barriers, damping
<b>Torsional</b>	Twisting	Uneven weight distribution	Twisting, warping	Higher than flexural and transverse	Symmetry, torsional stiffness

In Figure 24, the first six mode shapes of conveyor roller using modal analysis in ANSYS are shown. The first mode of vibration in the idler roller corresponds to the flexural mode, which is also referred to as the first fundamental mode. The flexural mode being a predominant vibrational mode in structures, requires minimal energy for excitation when mass is uniformly distributed.

Consequently, the entire structure exhibits cohesive vibration in the flexural mode. This observation aligns with the fundamental principle dictating that the natural frequency of a structure is inversely proportional to the square root of its mass. This relationship shows the significance of mass distribution and structural geometry in influencing the vibrational behavior of the idler roller system during modal analysis.

In Figure 24(a), the first flexural mode exhibits the highest wavelength, corresponding to a resonant frequency magnitude of 412.86 Hz. This mode represents the fundamental vibrational pattern with minimal variation in modal displacements across the structure. In Figure 24 (b), the second mode illustrates the transverse bending mode at 430.53 Hz. These initial two modes emphasize deflection in the idler shaft, highlighting its critical role as a susceptible component to vibrations, especially in the context of the first two lowest energy states.

In second and third mode, deflection of shell seems to be significant. For the third and fourth mode, flexure mode and transverse bending mode occurred at a frequency of 627.99Hz and 631.99 Hz respectively, shown in figure 24(c) and 24(d). Moreover, Figure 24 (e) and (d) show significant torsional mode shape (first twist mode) and second flexure respectively at the frequency of 632.05 Hz and 652.02Hz respectively.

The investigation shows that as the mode shape frequencies increase, the corresponding wavelengths decrease. This deduction implies a multiplication of displacement variation, leading to more pronounced oscillations with increasing frequency, as shown below in Figure 25, a mode shape at 1407 Hz. Particularly, the observation shows that at higher frequencies, the mode shapes exhibit a combination of flexural, transverse, and torsional modes, indicating a complex interplay of structural dynamics. A sudden variation in natural frequency, see Table 14, of the system shows a significant mode of vibration which can be avoided by introducing a damper in the system to prevent the structure to vibrate at this frequency.

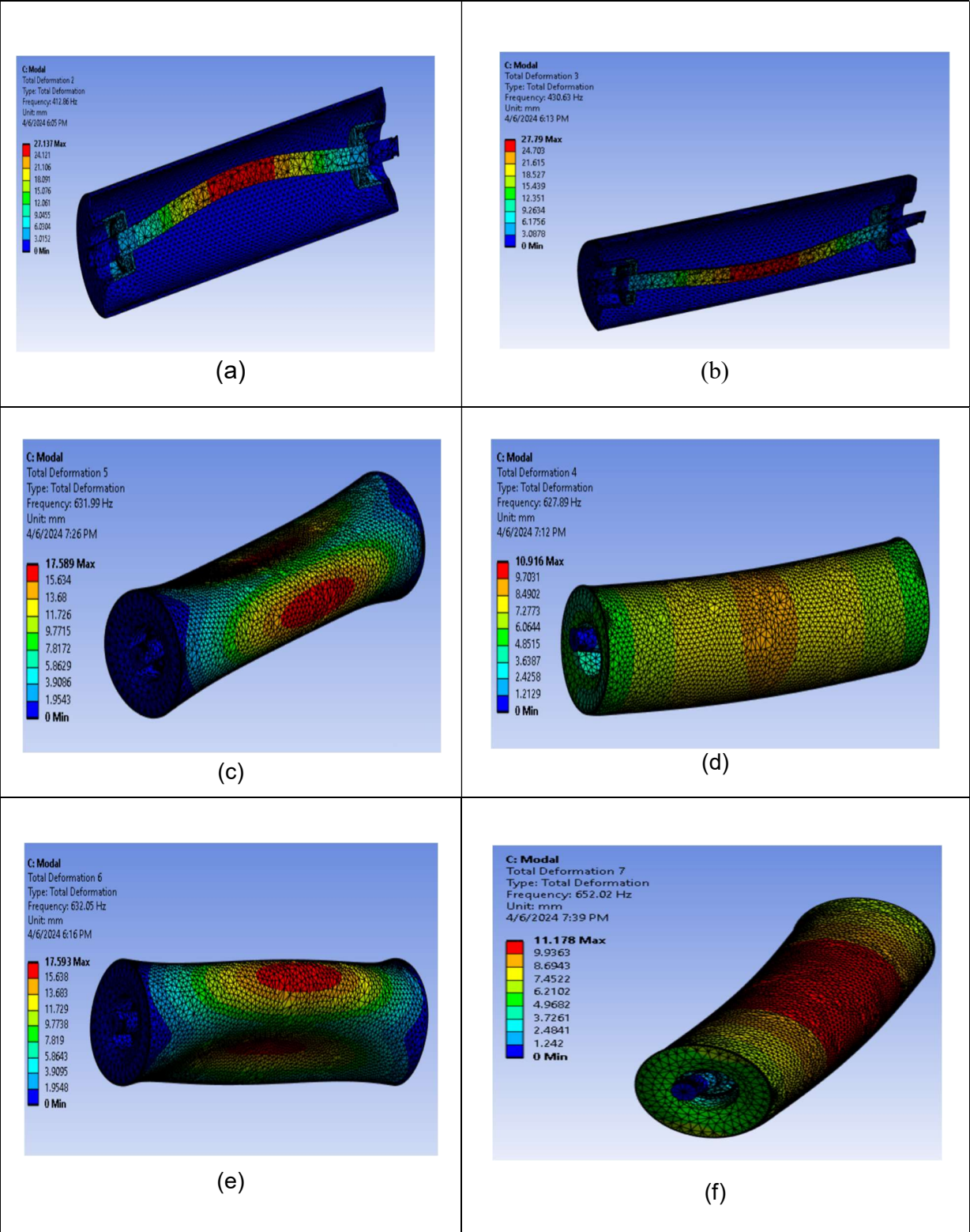


Figure 24: First six mode shapes of idler roller

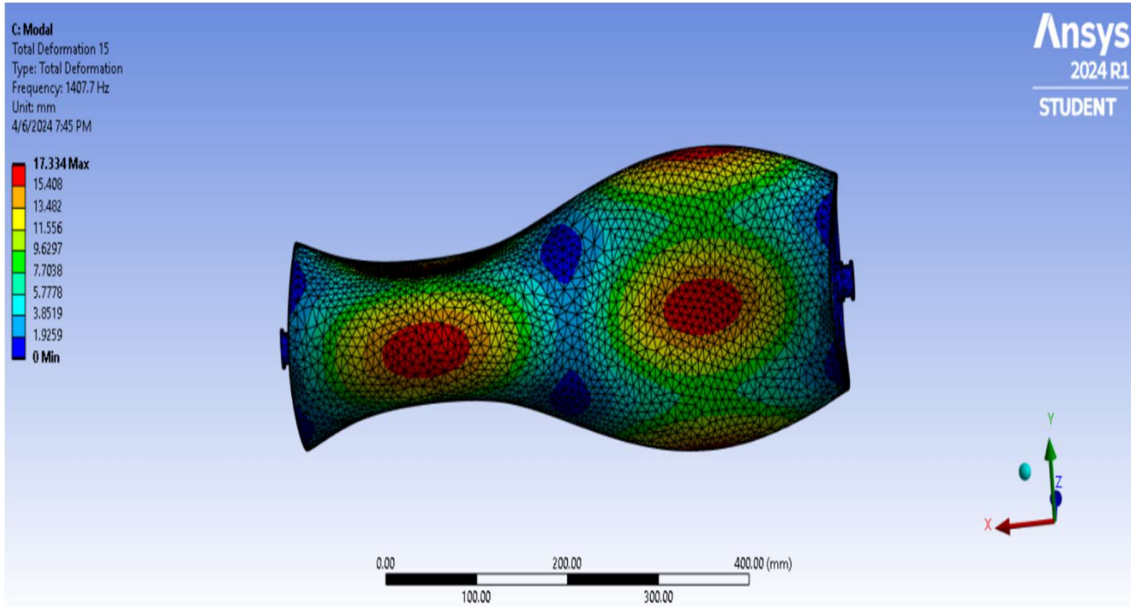


Figure 25: Mode shape at  $f=1407$  Hz

The most significant frequencies are the one which can be achieved (lowest energy modes of vibration) easily, where the amplitude will become maximum, and resonance occur. The resonance frequencies for the first twenty mode shapes are shown in Table 14.

Table 14: Mode shape number with corresponding frequencies

Mode shape and Frequencies					
<b>Mode</b>	1	2	3	4	5
<b>Frequency (Hz)</b>	412.86	430.63	627.89	631.95	632.05
<b>Mode</b>	6	7	8	9	10
<b>Frequency (Hz)</b>	652.02	656.05	927.79	1021	1059.2
<b>Mode</b>	11	12	13	14	15
<b>Frequency (Hz)</b>	1063.7	1407.7	1407.7	1427.1	1427.1
<b>Mode</b>	16	17	18	19	20
<b>Frequency (Hz)</b>	1591.2	1642.6	1642.7	1681.6	1681.7



## 6 Generative Alternatives

In order to optimize the roller shell, different materials can be investigated which can replace traditional steel and have better mechanical and physical properties than steel. Moreover, a solid idler shaft is installed in Rulmeca roller which can be made a hollow tube of specific thickness to achieve mass minimization. A hollow shaft, with the same stiffness and modulus, results in higher resistance to deflection and torsion as the material is distributed farther for neutral axis [25].

### 6.1 Shell Optimization

Material selection based on the literature review and market analysis is used to generate alternatives for idler rollers, as it involves identifying and evaluating various materials to optimize the performance of the roller while meeting specific design requirements. With a focus on properties such as strength, stiffness, abrasion resistance, and corrosion resistance, advanced materials like high-strength alloys or fiber-reinforced composites may emerge as optimal choices.. The general material selection procedure is shown in Appendix D, for stiffness and strength-based design. However, based on the literature review and current market analysis of idler shell available in industry, Resin Epoxy, Polyvinylchloride (PVC) and High-Density Polyethylene (HPDE) are selected for analysis to replace traditional stainless-steel material [25]. These materials are significantly lighter than steel which might results in weight reduction of the roller assembly, lower energy consumption during operation and may lead to cost savings and environmental benefits.

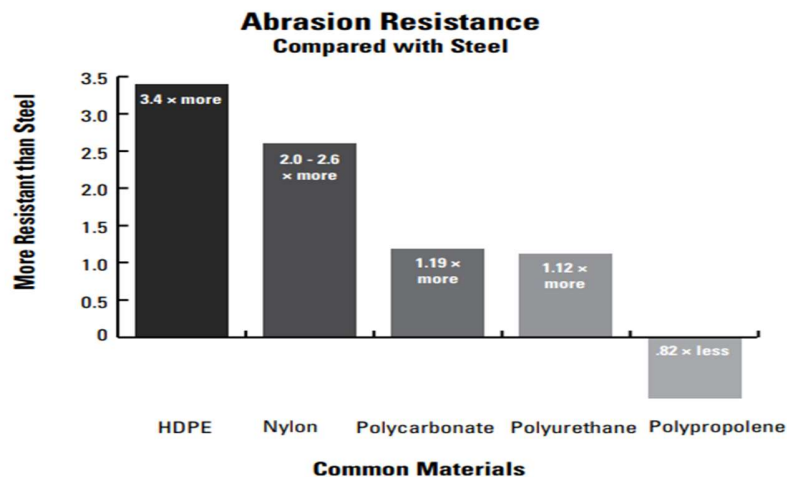


Figure 26: Comparison of abrasive resistance of steel with other materials (15)

HDPE and PVC exhibit high corrosion resistance, making them suitable for use in harsh environments where traditional steel rollers may corrode over time. Moreover, these alternative materials are less prone to wear and abrasion, leading to longer service life and reduced maintenance requirements, see Figure 25. Overall, the choice of alternative materials like HDPE, resin epoxy and PVC presents a practical solution for achieving lightweight, durable, and cost-effective roller shells without compromising on performance.

The comparison in Table 15 shows that resin epoxy, characterized by moderate to high abrasion and impact resistance along with high chemical resistance and electrical insulation, emerges as a promising option for roller shell bodies, particularly in environments requiring robustness and protection against wear. PVC, although offering low abrasion and impact resistance, presents advantages in terms of moderate cost and machinability, making it a viable choice for less demanding applications where cost-effectiveness is paramount. On the other hand, HDPE showcases high abrasion and moderate impact resistance, coupled with low environmental impact and moisture absorption, positioning it as a suitable option for roller shell bodies subjected to varying operating conditions.

Table 15: Comparison of steel with alternative materials (Resin Epoxy, PVC and HDPE)

Property	Resin Epoxy	PVC	HDPE	Steel
<b>Strength (MPa)</b>	70-120	20-60	250-500	250-500
<b>Stiffness (GPa)</b>	3-4	2.0-3.0	200-210	200-210
<b>Density (kg/m<sup>3</sup>)</b>	1130-1190	1300-1450	950-970	7850-8050
<b>Abrasion Resistance</b>	Moderate to High	Low	High	High
<b>Impact Resistance</b>	Moderate to High	Low	Moderate to High	Moderate to High
<b>Chemical Resistance</b>	High	High	Low to Moderate	High
<b>Environmental Impact</b>	Moderate	Moderate	Low	High
<b>Cost</b>	Moderate to High	Moderate	Moderate to High	Moderate to High
<b>Machinability</b>	Moderate	Low	Moderate to High	Low
<b>Thermal Conductivity</b>	Low	Low	Moderate	High
<b>Moisture Absorption (%)</b>	<1	<0.1	<0.1	Negligible
<b>Electrical Insulation</b>	High	High	Low	Low

### 6.1.1 Weighted Decision Matrix

A weighted decision matrix, shown in Table 16, is defined based on the material properties to investigate Resin Epoxy, PVC, HDPE, and Steel as potential materials for roller shell bodies. Weights are assigned to each criterion to reflect its relative importance in the decision-making process. After normalizing the values of each property across all materials, each normalized value is multiplied by its corresponding weight for each material to calculate the weighted scores. These scores were then summed up to provide an overall assessment of each material's suitability, shown in Table 17.

The scores indicate that Resin Epoxy emerges as the top-performing material for structural optimization of roller shell bodies, with a score of 25.4. Following closely behind is HDPE with a score of 19.7, suggesting its strong suitability as well. PVC scores 20.1, demonstrating its competitiveness. Despite Steel's longstanding dominance, these findings highlight the viability of exploring newer materials like Resin Epoxy, PVC, and HDPE for enhanced performance in roller shell body applications.

Table 16: Weighted Chart

Criteria	Weight	Steel	PVC	Resin Epoxy	HDPE
Strength	0.9	4	2	3	1
Stiffness	0.8	4	2	3	1
Density	0.6	1	5	2	3
Abrasion Resistance	0.7	4	1	3	3
Impact Resistance	0.7	4	1	3	2
Chemical Resistance	0.8	4	4	5	1
Environmental Impact	0.5	1	2	3	5
Cost	0.8	2	3	3	3
Machinability	0.5	1	2	3	1
Thermal Conductivity	0.4	1	1	1	2
Moisture Absorption	0.6	1	1	2	5
Electrical Insulation	0.7	1	1	5	1

Table 17: Weighted score matrix

Material	Score
Steel	18.4
PVC	20.1
Resin Epoxy	25.4
HDPE	19.7

### 6.1.2 Analysis of Alternative Materials

Geometric parameters such as shell thickness, length, internal and outer diameters are kept constant for analysis to obtain static structural analysis results, which are compared with steel idler shell using ANSYS. The obtained values, shown in Table 18, provide insights into stress and deformation, aiding in material comparison and selection. The ANSYS results for each material roller shell is shown in Appendix C.

Table 18: Comparison of mechanical properties (stress and deformation) for Resin Epoxy, PVC, HDPE, and Steel

Property	Resin Epoxy	PVC	HDPE	Steel
Strength (MPa)	54.6	45.3	29.1	460
Stiffness (GPa)	3.78	2.861	1.08	200
Density (kg/m <sup>3</sup> )	1160	1392	958.5	7850
Equivalent Von Mises stress (Mpa)	5.111	5.02	4.989	4.948
Total Deformation(mm)	0.3654	0.49422	1.32	0.021
Mass	2.7	2.95	1.96	3.6
Percentage mass reduction	25%	18%	46%	-

### 6.1.3 Discussion

Steel has the highest density at 7850 kg/m<sup>3</sup>, while Resin Epoxy, PVC, and HDPE offer significantly lower densities at 1160 kg/m<sup>3</sup>, 1392 kg/m<sup>3</sup>, and 958.5 kg/m<sup>3</sup>, respectively. This indicates that the

alternative materials are much lighter than steel and offers potential benefits in terms of weight reduction and energy efficiency in conveyor applications. In terms of stress distribution, the equivalent Von Mises stress values for Resin Epoxy, PVC, and HDPE are slightly higher than steel, with values ranging from 4.989 MPa to 5.111 MPa compared to 4.948 MPa for steel. This indicates that the proposed alternative materials may experience slightly higher stress levels under the same loading conditions. However, these stress levels remain within acceptable limits for all materials, suggesting that they can effectively withstand applied loads without risk of failure.

The comparison of deformation characteristics reveals more significant differences between the materials. While steel exhibits a total deformation of only 0.021 mm, Resin Epoxy, PVC, and HDPE demonstrate much higher deformation values of 0.3654 mm, 0.49422 mm, and 1.32 mm, respectively. These results indicate that the proposed alternative materials are more prone to deformation under applied loads compared to steel.

Steel roller shells have a mass of approximately 3.6 kg while Resin Epoxy, PVC, and HDPE shells weigh only 2.7 kg, 2.95 kg, and 1.95 kg, respectively. This substantial reduction in mass for the alternative materials further highlights the advantages in terms of weight optimization and operational efficiency. While steel idler roller shells have a mass of 3.6 kg, Resin Epoxy, PVC, and HDPE shells weigh only 75%, 82%, and 54% of the steel mass, respectively. The comparison of these materials in Table 14 suggests that these alternative materials offer acceptable mechanical performance in terms of stress distribution and deformation under applied loads. Generally, they have lower environmental impact and cost compared to steel. These non-metallic materials offer cost-effective and environmentally friendly alternatives, particularly if weight reduction and corrosion resistance are critical factors in the roller design.

In conclusion, Resin Epoxy, PVC, and HDPE present viable alternatives with their own set of advantages as compared to steel. Resin Epoxy offers comparable mechanical properties and corrosion resistance, making it suitable for applications where weight reduction is a priority. PVC and HDPE provide lightweight and cost-effective options, making them attractive for applications where weight optimization and affordability are key considerations.

## **6.2 Shaft Optimization**

A solid shaft, with the same strength and modulus, can be made more stronger and stiffer when loading in bending by shaping it into a hollow tube. From Table 5, it can be seen that the von

misses stress and maximum deformation on the shaft subjected to the loading is 105.7 MPa and 1.24 mm respectively while the yield strength of steel is 240 MPa. This indicates that the shaft can be optimized into a hollow circular tube with a specific thickness to handle the same stress and deformation.

The shaft deflection is given using *Equation 4.4* as:

$$\delta_{shaft} = \frac{F_N a^2 (3L - a)}{6EI}$$

The shaft factor for elastic bending of shaft is given as

$$\phi_B^e = \frac{3r}{\pi t} = \frac{I_{hollow}}{I_{solid}} \quad (6.1)$$

Where  $I_{hollow}$  = Moment of area of hollow shaft (shaped),  $I_{solid}$  = Moment of area of solid shaft,  $r$  = Radius of shaft,  $t$  = Thickness of hollow shaft,  $\phi_B^e$  = Elastic bending shape factor.

Using *Equation 6.1*, moment of inertia for hollow section is calculated and inserted in *Equation 4.1* as shown below:

$$I_{hol} = \frac{3r}{\pi t} (I_{solid}) = \frac{3r}{\pi t} \times \frac{\pi}{4} r^4$$

$$I_{hollow} = \frac{3r^5}{4t} \quad (6.2)$$

$$\delta_{shaft} = \frac{F_N a^2 (3L - a)}{6E \left( \frac{3}{4t} r^5 \right)} \quad (6.3)$$

Rearranging *Equation 6.3*, the shaft thickness can be taken on one side and rest of the expression on other side of the equation.

$$t = \frac{\delta_{shaft} \times 18E(r^5)}{F_N a^2 (3L - a) 4} \quad (6.4)$$

Where  $F=6000N$ ,  $a=0.075m$  is distance from one end to the applied force,  $E=210Gpa$ ,  $r=0.015m$  is radius of shaft.

By reduction the shaft deflection ( $\delta_{shaft} = 1.22mm$ ), to half of its original value 0.61mm, the thickness of hollow shaft is calculated using *Equation (6.4)* as:

$$t = 0.00716m \text{ or } 7.16 \text{ mm}$$

and the bending stress is determine using *Equation (4.1)*:

$$\sigma = \frac{My}{I} = 116.67 \text{ MPa}$$

For reducing the deflection by 1/3<sup>rd</sup>, the calculated thickness is:

$$t = 0.00477\text{m or } 4.77 \text{ mm}$$

The bending stress at the shaft deflection of  $\delta = \frac{1.22}{3} = 0.4 \text{ mm}$  and a thickness of 4.77 mm is given as

$$\sigma = \frac{My}{I} = 108 \text{ MPa}$$

Since the bending stress still is less than the yield strength of stainless steel 316, the hollow shaft with outside and internal diameter of 30mm and 20 mm respectively is not subject to elastic bending failure. For yielding failure:

$$S > \frac{F}{A_{\text{hollow}}} \quad (6.5)$$

Where  $F$ = Applied load,  $S$ = Yield strength of stainless-steel shaft and  $A_{\text{hollow}} = \pi(r_{\text{out}}^2 - r_{\text{in}}^2)$  is the cross-sectional area of hollow shaft.

$$S > \frac{6000}{\pi((0.015)^2 - (0.010)^2)} = 15.2 \text{ Mpa}$$

Hence,  $S = 250 \text{ MPa}$  while the yield stress is only 15.2 MPa which indicates the hollow shaft is not allowed to have yielding as failure mode.

Table 19 shows the comparison between the solid shaft and hollow shaft with two different wall thickness values of 7.16 and 4.77mm respectively. The hollow shafts, while composed of the same material as the solid shaft, demonstrate significantly reduced deflection compared to the solid shaft, with reductions of approximately 50% and 67% for Hollow Shafts 1 and 2, respectively.

One of the most significant advantages of the hollow shafts is the substantial reduction in mass. Hollow Shaft 1 achieves a mass reduction of approximately 25%, while Hollow Shaft 2 achieves an even more significant reduction of approximately 46% compared to the solid shaft. This reduction in mass not only contributes to overall weight savings but also offers potential benefits in terms of reduced inertia and improved efficiency.

Table 19: Comparison of physical and mechanical properties of solid and hollow shaft

Property	Solid shaft	Hollow shaft	
		1	2
Material	Stainless steel 316	Stainless steel 316	Stainless steel 316
Yield Strength (MPa)	250	250	250
Stiffness (GPa)	210	210	210
Deflection(mm)	1.22	0.61	0.4066
Von Mises stress (Mpa)	84.8	116.67	108
Wall Thickness(mm)	-	7.16	4.77
Internal Diameter	-	15.68	20.46
External Diameter	-	30	30
Mass(kg)= $\rho AV$	3.6	2.7	1.95
Percentage mass deduction (%)	-	25	45.83

This reduction in deflection indicates enhanced rigidity and stability under load, crucial for applications requiring precise rotational motion. Moreover, the equivalent Von Mises stress in the hollow shafts remains within acceptable limits despite the thinner wall thickness, highlighting their structural integrity and reliability. Although the stress levels are slightly higher in the hollow shafts compared to the solid shaft, they are well within the material's yield strength, ensuring safe operation under load conditions.

### 6.2.1 Discussion

Table 20 show the results obtained by solving Equation 6.3 for varying shaft thickness from the solid shaft of 15mm radius to a hollow shaft of 2 mm thickness. The deflection values are plotted against the corresponding shaft thickness and a graph is obtained. Figure 27, shows that the deflection decreases gradually as the shaft thickness decreases, suggesting that thinner shafts experience less deflection. This aligns with the principle of optimizing an idler shaft for strength and stiffness by shaping it into a hollow tube. In Table 20, as the thickness decreases from 15mm to 2mm, the corresponding deflection values decrease accordingly. It must be noted that beyond a



certain threshold, there's a trade-off between deflection reduction and the risk of encountering failure modes. While reducing shaft thickness may improve stiffness and reduce deflection, it may also increase the risk of encountering other failure modes, such as buckling or fatigue failure. As the thickness decreases beyond a certain limit, the shaft's ability to withstand lateral loads and resist buckling diminishes, which can potentially compromise its structural integrity. Moreover, thinner shafts may be more susceptible to fatigue failure due to increased stress concentrations and reduced material volume to dissipate cyclic loading.

Table 20: Variation of shaft thickness vs shaft deflection

<b>Thickness (mm)</b>	<b>15</b>	<b>14</b>	<b>13</b>	<b>12</b>	<b>11</b>	<b>10</b>	<b>9</b>
<b>Deflection (mm)</b>	1.21693	1.13580	0.97354	0.97354	0.89242	0.81129	0.73016
<b>Thickness (mm)</b>	8	7	6	5	5	3	2
<b>Deflection(mm)</b>	0.64903	0.56790	0.48677	0.40564	0.32451	0.24339	0.16226

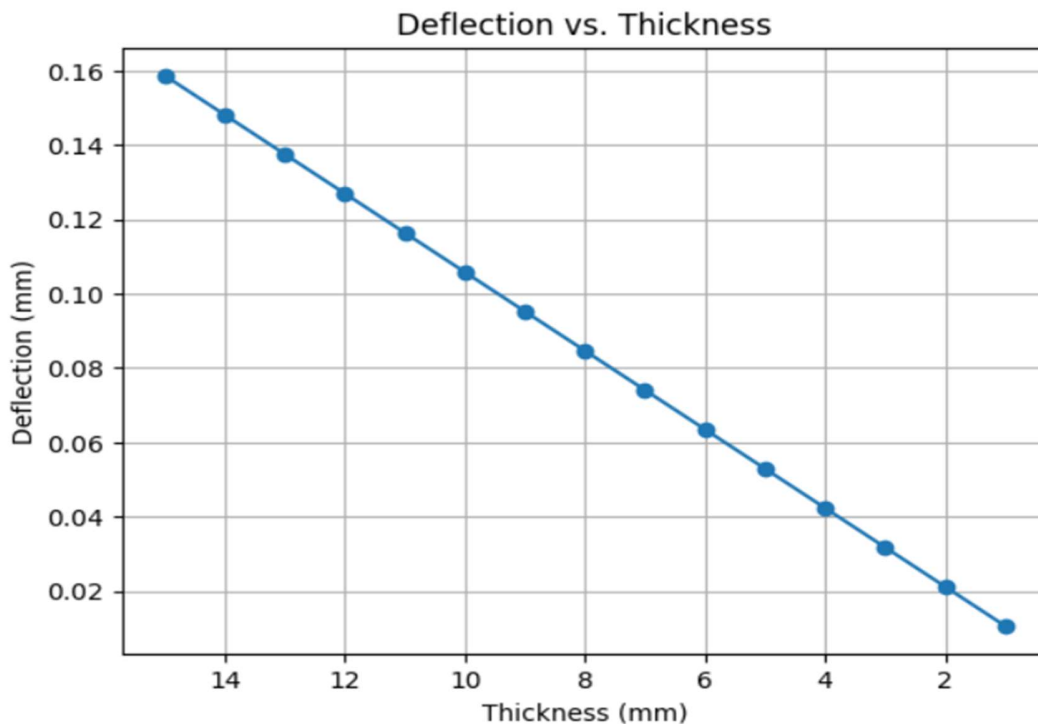


Figure 27: Deflection vs Thickness Graph

In summary, the optimization of shaft design through the incorporation of a hollow configuration has resulted in significant improvements in performance metrics such as deflection, stress distribution, and mass reduction.

## 7 Conclusion

Optimization of an idler roller can be divided into two parts: weight reduction and dust/water tightness of idler roller. This master thesis focused on the structural optimization of a standard conveyor idler, manufactured by RULMECA and installed at LKAB facility, to reduce the overall weight and propose a solution which enhance the durability, efficiency and environmentally stability of conveyor system. The optimization involves analysis of load distribution, static structural and modal analysis, geometric optimization, and material selection.

At first, load analysis of idler roller was done to determine the static and dynamic forces acting on an idler troughing set and on individual center idler, shown in Table 11 “Static and Dynamic forces”, followed by structural analysis, both numerical and analytical, to determine the stress distribution, deformation characteristics and mode shapes inherent by an idler roller system. The model analysis of idler system is done in ANSYS to determine the dynamic behavior of the system with different mode shapes. The vibration characteristics and resonance frequencies for different mode shapes are determined which shows possible vibrational behavior of idler system when external forces are applied. These modes shape, shown in Figure 24, can help to develop damping strategies and design modifications to reduce or mitigate the effect of undesirable vibrations cause by external stimuli and ensure the smooth running and operations of conveyor system.

From idler shell analysis, it can be seen the maximum stress and deformation value are very low which shows the opportunity to reduce its weight and optimize the shell by using a different material other than structural steel. As a result, three different market leading alternative materials, PVD, Resin epoxy and HDPE, are selected for replacing traditional structural steel idler shell based on their comparison with structural steel in mechanical and physical properties as shown in Table 15. Keeping the dimensions and loading same, the numerical simulations for these three alternatives are performed and the results from Table 16 shows that Resin Epoxy, PVC, and HDPE present viable alternatives with their own set of advantages as compared to steel. Particularly, PVC and HDPE provide lightweight and cost-effective options, making them attractive for applications where weight optimization and affordability are key considerations.

In case of shaft, both stress and deformation results are less than the yield strength of stainless steel and maximum allowable deflection, hence the optimization of shaft in terms of weight reduction proposes a significant opportunity to reduce the overall weight of the idler system. For solid shaft optimization, a hollow tube with three different thickness values is taken to reduce the deflection by 1/3<sup>rd</sup> of the total deflection. The results indicates that hollow shaft with same dimensions with varying thickness, improves the deflection and the stresses are still under the allowable yield strength range with 40% weight reduction as compared to solid shaft.

In conclusion, this master thesis focused on the structural optimization of conveyor idlers for significant weight reduction and provides a reference document to further research and investigation in idler technology. Through a combination of theoretical insights, advanced analytical calculations, engineers can develop idlers that are lighter, more durable, and environmentally friendly. As conveyor systems play a vital role in a wide range of industries, from mining to logistics, the continued advancement of idler optimization techniques is essential for driving progress and ensuring the long-term viability of materials handling operations.

## 8 Further Work

### 8.1 Experimental Validation

This master thesis focused on the structural optimization of conveyor idler, particularly idler shell and shaft, based on numerical simulation and analytical results. The results can be verified further by experimental validation. For static testing, the experimental step can be developed using three-

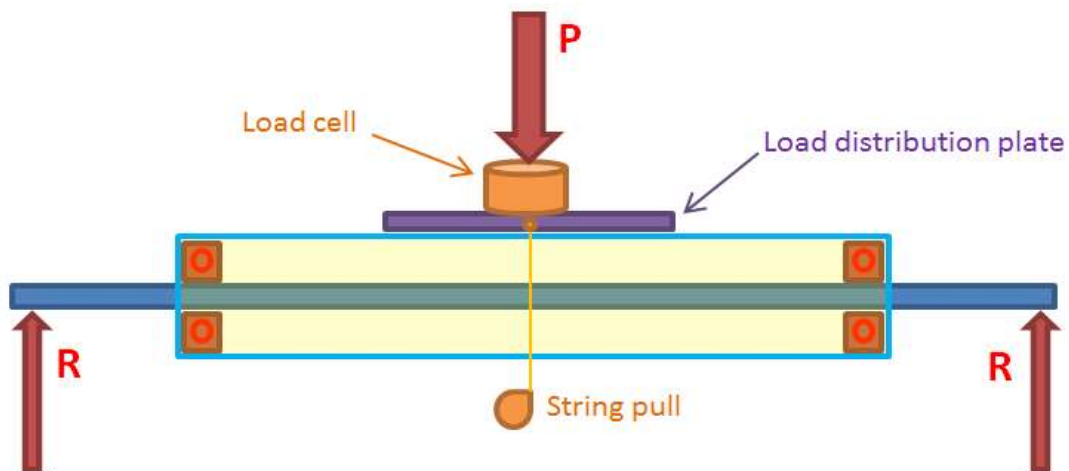


Figure 28: Three-point bending test [25]

point bending test principle, shown in Figure 28, where the idler roller is supported on both sides by slots which give vertical reaction only (a case of simply supported beam) and the load cell is used to measure the applied load on the load distribution plate which transmits the applied load uniformly to the roller. A string pull or a strain gauge can be installed to measure the deflection electronically as shown in figure below. This setup would enable precise measurement of deflection under different loading conditions, providing valuable data for comparison with numerical and analytical results. The same experiment can be repeated for three alternative materials (PVC, Resin Epoxy and HDPE) to find the maximum deflection and stresses which then can be compared with the numerical and analytical results to optimize the roller shell further.

## 8.2 Idler Components Analysis

As shown in Figure 3, an idler has different components in its assembly, each of which plays significant role for different function. The major components include bearings, labyrinth seals, internal and external seals, and stone guard. The research work can be further explored by investing those components, their role in conveyor system and how they interact with the idler conveyor when the material is transporting on it.

- **Bearings:** A significant component of an idler system is the bearing which supports the static and dynamic loads, minimized the friction between rotating components, maintain idler alignment and eccentricity. Unbalanced dynamic forces generated by the unequal material distribution or any unwanted impact load may cause local deformation in bearing components which can cause bearing failure. One way to reduce failure is to decrease the maximum dynamic load value by introducing cushioning elements between bearing and shaft. The optimized idler shell and shaft can be used to determine the dynamic forces and the results can be compared with traditional standard steel idler roller. This comparison can further highlight the significance of composites or moder materials as an alternative material to structural steel. Figure 29 shows the free body diagram of a dynamical system in which the weight of the idler and the material transported by it is represented by  $m_2$  and the bearing is represented by  $m_1$  along with elastic and damping elements. In further work on optimizing the idler, the system shown below can be solved, both numerically and analytically, for both cases using force balance equations and the results can be analyzed

to see the effect of elastic and viscous elements on the dynamic loads by varying the damping and elastic constants.

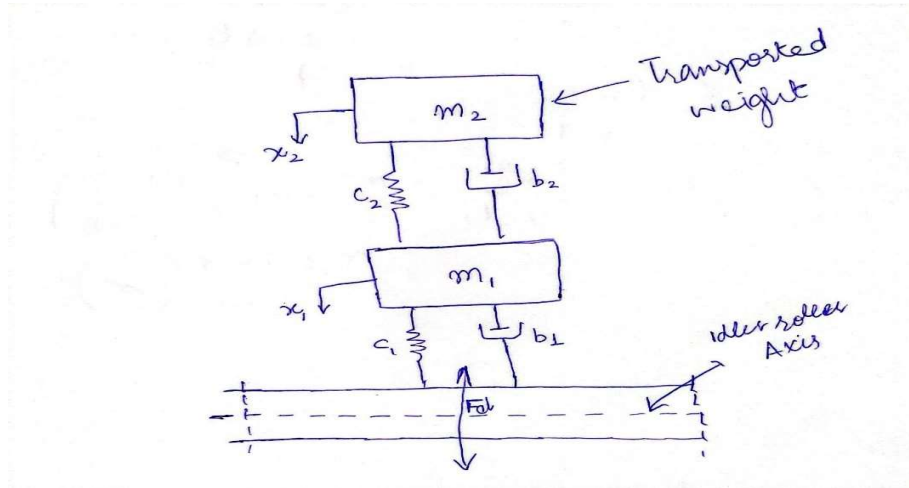


Figure 29: Free body diagram for vibrational analysis of idler roller

- **Labyrinth Seals:** Labyrinth seals prevent the ingress of contaminants, such as dust and moisture, into the bearing housing. Further research could focus on optimizing seal designs and materials to enhance sealing effectiveness and prolong bearing life, particularly in harsh operating environments.
- **Internal and External Seals:** Internal and external seals contribute to the overall sealing integrity of the idler assembly, protecting internal components from contamination and moisture ingress. Exploring advanced seal materials and configurations can improve sealing performance and extend component lifespan, reducing the risk of premature failure and downtime.
- **Stone Guard:** The stone guard serves as a protective barrier, preventing debris and foreign objects from damaging idler components. Researching innovative stone guard designs and materials can enhance impact resistance and durability, reducing maintenance requirements and enhancing conveyor reliability.

### 8.3 Dust and Water Tightness

Bearing seals play an important role to increase the durability of bearings in idler system. They prevent the ingress of dust or water and are usually made up of flame-resistant plastic material. The rolling resistance of idler and radial forces acting on the bearing while in rotation generates

heat energy in the bearing. The stationary shaft only oscillates while the idler shell and outer shell of the bearing along with rolling elements performed rotation. Due to the friction between the contact surfaces of the rotating parts, heat is generated which causes overall increase in the bearing assembly temperature. According to Andrzej (26), if the idler temperature is more than 25°C of environmental temperature, the idler is defected and needs to be replace. If it is assumed that the total work produced by friction in converting into heat energy, the heat flow will be given as [26]:

$$Q = \frac{W}{t} = Fr\omega = \frac{(R\mu)2n\pi}{60} \quad (8.1)$$

$Q$ = Total heat flow,  $W$ = Work done due to friction force  $F$ ,  $\omega$ = Rotational velocity of idler,  $R$ = Reaction at bearing, with  $\mu$ = Friction coefficient

Using this equation the total produce heat flow can be calculated and divided into three possible sections, as shown in Figure 30, by conduction  $Q_1$ = through bearing outer ring, assembly and idler shell, conduction  $Q_2$  through bearing both outer and inner ring to bearing sides and by convection to the surrounding air and conduction  $Q_3$  from bearing inner race to the shaft and then from the shaft to internal surrounding by convection.

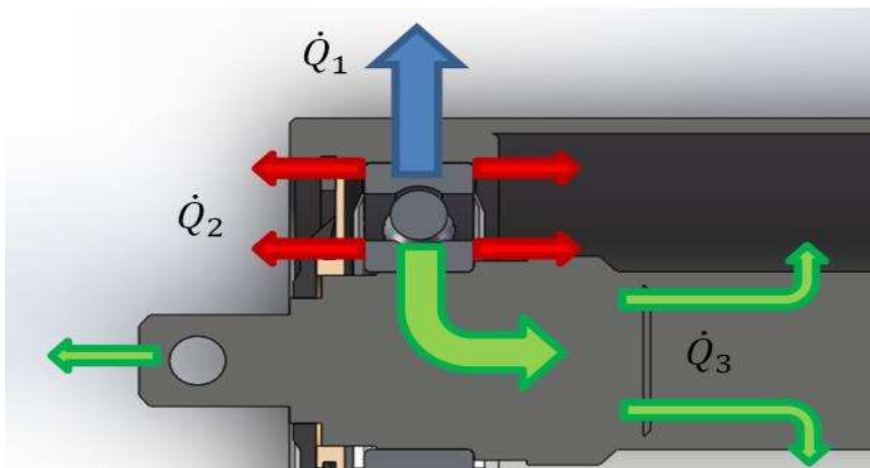


Figure 30: Heat flow directions [26]

Hence, the further work related to thermal analysis of the bearing can extend the scope of this study and help LKAB to understand the dust and water problem. The increase in bearing temperature may have a direct impact on the outer surface of sealing which if worn out could lead to moisture and dust particles to enter the bearing assembly and may cause bearing damage. Moreover, in contrast with steel, idlers shell made up of polymeric material have lower thermal

conductivity which could results in heat accumulation for a longer period inside the bearing which may increase the average bearing temperature and have direct consequences on the bearing seals and other components.

## 9 References

- [1] Bailey, S. (2023, September 22). *Who invented the conveyor belt & When?* Span Tech Conveyors. <https://spantechconveyors.com/2020/10/27/who-invented-the-conveyor-belt/>
- [2] Liu, X. (2016). Prediction of belt conveyor Idler performance. *Delft University of Technology*. <https://doi.org/10.4233/uuid:e813298e-93d8-4a76-a7ab-72b327bcde4b>
- [3] Martins, Rodrigo & Ceniz, João & Luersen, Marco & Cousseau, Tiago. (2020). Design of a conveyor belt idler roller using a hybrid topology/parametric optimization approach.
- [4] *ISO 1537:1975*. (n.d.). ISO. <https://www.iso.org/standard/6125.html>
- [5] Van Rensburg, B. J. (2013). The development of a lightweight composite conveyor belt idler roller. *University of Southern Queensland Faculty of Health, Engineering and Sciences*. <http://eprints.usq.edu.au/24621/>
- [6] Liu, X., Pang, Y., Lodewijks, G., & He, D. (2018). Experimental research on condition monitoring of belt conveyor idlers. *Measurement*, 127, 277–282. <https://doi.org/10.1016/j.measurement.2018.04.066>
- [7] Gurjar, R.S. Failure analysis of belt conveyor system by Pareto Chart. *International Journal of Engineering and Social Science*, 2(10):60–71, 2012. ISSN 2249- 9482
- [8] Vasić, M., Stojanović, B., & Blagojević, M. (2020). Failure analysis of idler roller bearings in belt conveyors. *Engineering Failure Analysis*, 117, 104898. <https://doi.org/10.1016/j.engfailanal.2020.104898>
- [9] Ricks, A. V. (2008). *Belt conveyor Idler roll behaviours*. overlandconveyor.cn. <http://www.overlandconveyor.cn/uploadfile/pdf/8-belt-idler-roll-behavior%5B1%5D.pdf>
- [10] Aditya, Amarnath, M., & Kankar, P. K. (2014). Failure analysis of a Grease-Lubricated cylindrical roller bearing. *Procedia Technology*, 14, 59–66. <https://doi.org/10.1016/j.protcy.2014.08.009>
- [11] *ISO 15243:2017*. (n.d.). ISO. <https://www.iso.org/standard/59619.html>
- [12] SKF, Railway technical handbook 1 (2011) 122–135
- [13] RKM International Roller Company. (2023, October 8). *RKM International Roller Company - For all your Roller and Idler needs*. <https://rkmrollers.com.au/>
- [14] *Material handling components for conveyor* | Rulmeca. (n.d.). <https://www.rulmeca.com/en/>



- [15] ASGCO. (2023, December 5). *Complete Conveyor Solutions* | ASGCO | *Engineered Products & Services* | ASGCO. <https://www.asgco.com/>
- [16] CONVEYOR INNOVATIONS INTERNATIONAL PTY LTD. <https://ci-int.com/products/>
- [17] CPS Conveyors, Conveyor Product and Solutions. (2023, November 10). *CPS Conveyors* | *Conveyor Product and Solutions*. CPS Conveyors | Conveyor Product and Solutions -. <https://cpsconveyors.com.au/>
- [18] Cross, N. (1989). *Engineering design methods*. <https://ci.nii.ac.jp/ncid/BA08022576>
- [19] Conveyor Equipment Manufacturers Association. (2018, August 15). *PUBLICATIONS-2 - CEMA*. <https://cemanet.org/publications-2/>
- [20] Su, J., Meng, W., & Zhao, X. (2019). Multi-objective optimization design and reliability analysis of idler with hollow step-shaft. *Journal of Advanced Mechanical Design, Systems and Manufacturing*, 13(4), JAMDSM0084. <https://doi.org/10.1299/jamdsm.2019jamdsm0084>
- [21] *Rollers and components for bulk handling*. (n.d.). RULMECA. [https://rulmecacorp.com/Conveyor\\_Idler\\_Roller\\_catalog/Complete\\_Idler\\_Roller\\_Catalog.pdf](https://rulmecacorp.com/Conveyor_Idler_Roller_catalog/Complete_Idler_Roller_Catalog.pdf)
- [22] *Dunlop Conveyor Belt Design Manual*. (n.d.). [https://www.ckit.co.za/secure/conveyor/troughed/belt\\_tension/dunlop-belting.htm](https://www.ckit.co.za/secure/conveyor/troughed/belt_tension/dunlop-belting.htm)
- [23] Barnard Janse van Rensburg (2013), “*The development of a Light Weight Composite Conveyor Belt Idler Roller*”, University of Southern Queensland Faculty of Health, Engineering and Sciences
- [24] Ooi, J. B., Wang, X., Tan, C. S., Ho, J., & Lim, Y. P. (2012). Modal and stress analysis of gear train design in portal axle using finite element modeling and simulation. *Journal of Mechanical Science and Technology*, 26(2), 575–589. <https://doi.org/10.1007/s12206-011-1040-5>
- [25] Wheatley, G., & Zaeimi, M. (2021). Composite shaftless roller design for conveyor system. *Periodica Polytechnica. Mechanical Engineering*, 65(3), 261–268. <https://doi.org/10.3311/ppme.17554>
- [26] Tasic, M., Mitrović, R., & Mišković, Z. (2022). Experimental and numerical transient thermal analysis of the idler bearing housing made of steel or polymer material. *Thermal Science/Thermal Science*, 26(6 Part A), 4831–4840. <https://doi.org/10.2298/tsci220429129t>

# Appendix A

## Idler roller technologies

### RKM Roller Company PTY LTD

The RKM standard steel roller features triple-layered sealing technology to prevent the ingress of foreign material, making it suitable for various material handling environments such as coal, grain, and iron ore. Constructed with a plain steel shell body rolled using electric resistant welding and reinforced with an optimal reinforcing disc, it offers structural support. The sealing system comprises primary, secondary, and tertiary seals, including heavy-duty nylon outer shields, dust and water-resistant lip seals, and male and female labyrinth pre-greased seals to protect the deep groove ball bearing with C3 internal clearance.

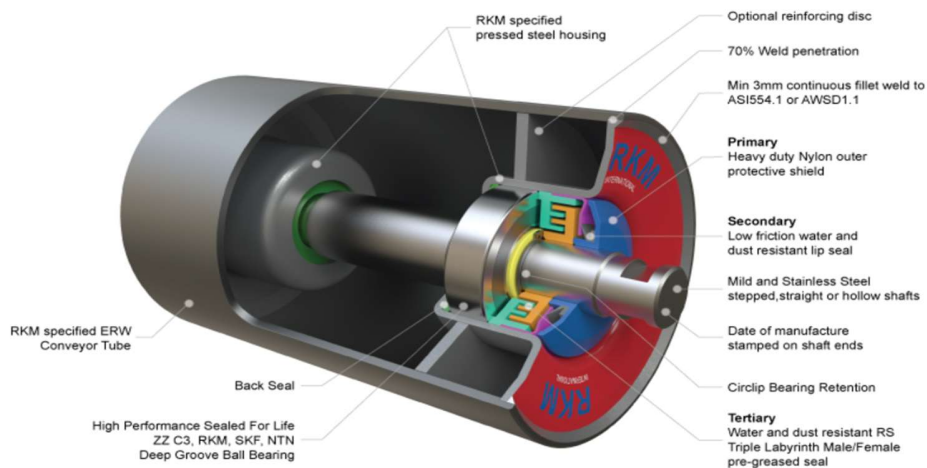


Figure 31: RKM standard steel idler[13]

RKM also offers upgraded versions like the high-performance low noise steel roller and heavy-duty low noise steel roller, incorporating features such as roller eclipses for reduced noise and rock jam protection covers for harsh environments.

Additionally, the RKM Heavy Duty Light Weight Composite Roller presents a lighter yet robust alternative to steel rollers, utilizing glass fibers bound with resin for superior flexural strength and stiffness. This composite roller offers advantages such as reduced weight, comparable strength to steel, advanced wear properties, and reduced operational noise levels, all while adhering to precision standards for minimal runout and side-load.

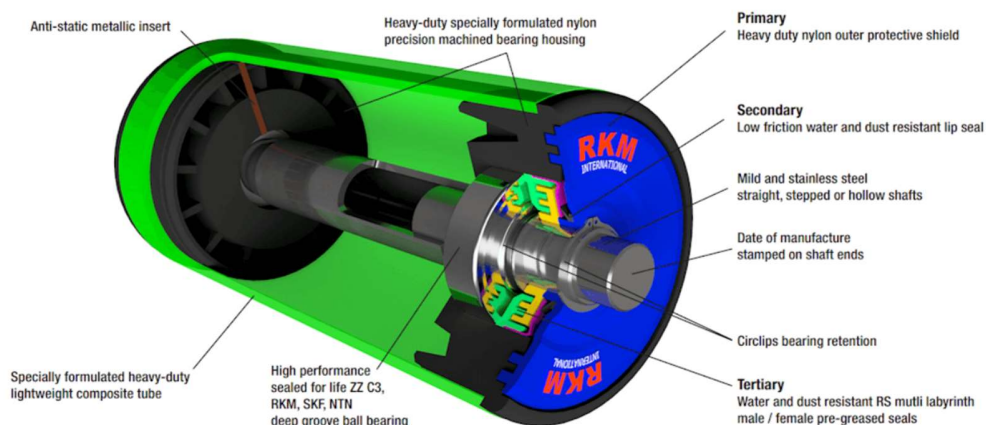


Figure 32: RKM Composite roller [13]

## Rulmecca

At LKAB, rollers from Rulmecca have been installed at most of the conveyor system. They have shared extensive open-source information regarding bulk rollers and bulk technical information on their website. Rulmecca produce almost all types of idlers (impact, carrying, return, belt tracking and cleaning rollers) and three categories of steel rollers series named as PSV, MPS, PSV-FHD and anti-corrosive aluminum idlers as well as thermoplastic idlers.

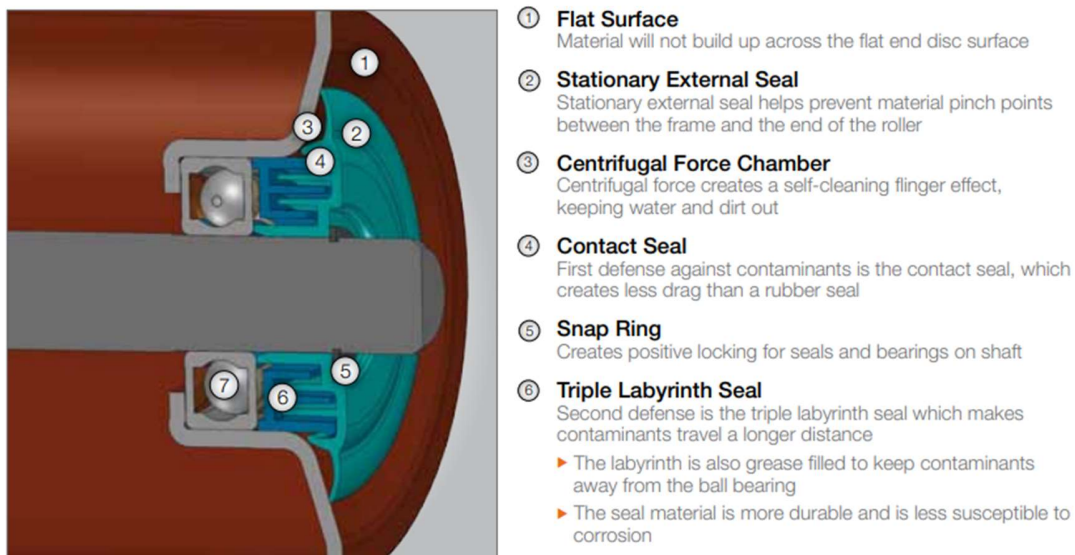
PSV series rollers are designed for higher loads, larger lump size material with applications in mines, caves, and cement work, with operating temperatures range from -20C and + 100C. A steel welded tube is cut and machined to make roller shell with a steel monolithic bearing housing, deep drawn and sized to a force tolerance ISO M7, welded to the tube body using a continuous wire feed system, "UNIBLOC". Precision ball bearings of different series 6204,6205,6305,6206 with C3 clearance tolerance are used. A hermetic sealing system with a strong external stone guard is used to protect the bearing from dirt and water. The external sealing section comprises of a soft anti abrasive rubber lip ring provide self-cleaning principally because of cover cap design and bearing housing shape which centrifugally repels water and dust naturally towards outside. The internal sealing section is a triple lip labyrinth in PA6 Nylon greased with lithium-based water repellent to further protect the bearing.

TOP series rollers, thermoplastic polymer roller, are used where weight reduction (around 50% for carrying idlers) is required with corrosive environment, higher humidity, low noise, and vibrations. Their working temperature range is -25/50 C, lower than PSV series. The outer shell is made up

of anti-corrosive HDPE (high density polyethylene) tube with a deep pressed fit bearing housing composed of Homopolymer Acetal Resin (POM), a very robust, shock resistant, light weight and flexible material. Drawn steel spindle is used with radial precise bearing of 6204 and 6205 series, available in both hermetic and contactless sealing system with lithium grease NLGI grade 2 lubrication.

## ASGCO

It is an Ireland based company founded in 1971, manufactures bulk transportation conveyor components with three main divisions that serves specific material handling industry. They produce idler rollers with reference to CEMA standards. Under ASGCO, Syntron material handling solution is providing idler rollers with CEMA B, C, D, E and F specifications. Their C2000 idler tube is made up of ASTM A513 with a zinc plated yellow colored pressed fit bearing hub for corrosive resistance. An external deflector is used to provide protection against impact and corrosion with a triple labyrinth zinc plated sealing solution. The shaft is made up of low carbon C1018 cold drawn and a deep groove ball bearing of 6304 -2RS series is used with 2RS rubber seals to enhance dust and water protection.



- ① **Flat Surface**  
Material will not build up across the flat end disc surface
- ② **Stationary External Seal**  
Stationary external seal helps prevent material pinch points between the frame and the end of the roller
- ③ **Centrifugal Force Chamber**  
Centrifugal force creates a self-cleaning flinger effect, keeping water and dirt out
- ④ **Contact Seal**  
First defense against contaminants is the contact seal, which creates less drag than a rubber seal
- ⑤ **Snap Ring**  
Creates positive locking for seals and bearings on shaft
- ⑥ **Triple Labyrinth Seal**  
Second defense is the triple labyrinth seal which makes contaminants travel a longer distance
  - ▶ The labyrinth is also grease filled to keep contaminants away from the ball bearing
  - ▶ The seal material is more durable and is less susceptible to corrosion

Figure 33: C2000 Idler with specifications [15]

In an alternative to steel roller, Syntron material handling have introduced a composite roll made up of glass reinforced polyurethane, 50% lighter than traditional steel rolls, having higher impact resistance and crack resistance because of excellent load distribution by glass fabric. The shell is

made up of fine quality glass fabric saturated with a two-part thermoset with recommended temperature range of -40/200F. Polyurethane resin resists the material build up on the surface which prevents any belt damage and because of low thermal expansion coefficient as compared to steel, it reduces the differential expansion between components of roller.

### **Conveyor Innovations International Pty Ltd**

Conveyor Innovations International (CII) is an engineering company serving the Australian mining industry with innovative products like the OneFits idler roller. This shaftless roller comes in black steel, Vitresteel, and carbon fibre variants, each suited for different applications. Vitresteel rollers, twice as strong as black steel, are used in high-demand settings, while carbon fibre rollers target ergonomic benefits for underground mining. The uniquely designed bearing housing withstands substantial moments, utilizing double row tapered roller bearings for low rolling friction. With no central shaft, OneFits relies on its body as the main structural component, resulting in a lightweight design. CII's GEN 7 roller, featuring state-of-the-art technology and modern condition monitoring features, aims to prevent conventional failure modes. The roller's bearing end cap, mass swaged under 35 tons force, eliminates traditional welding and reduces corrosion rates. CNC machined sealed end caps prevent moisture and debris ingress, contrasting with conventional rollers that have weep holes prone to seal damage.

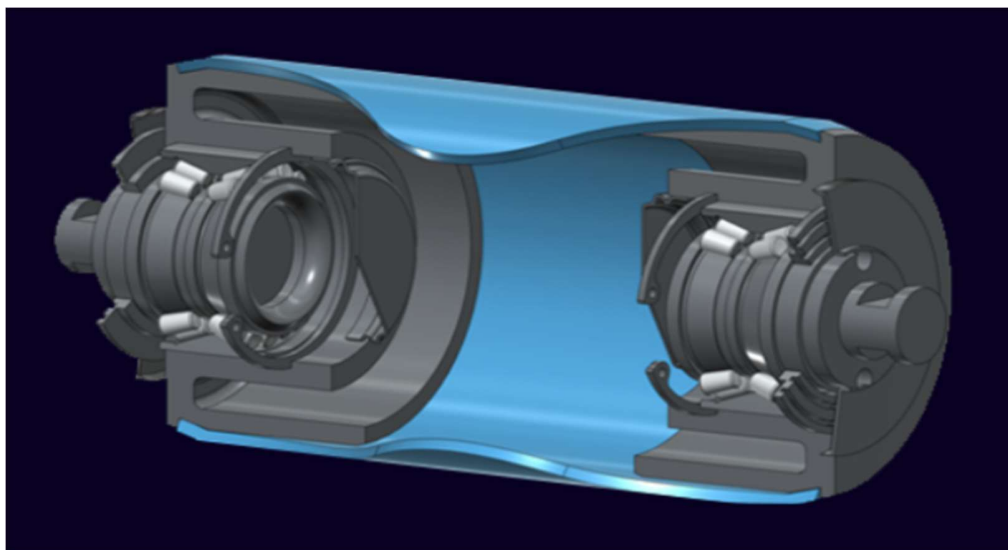


*Figure 34: Shaftless oneFits Idler CII [16]*

## Conveyor Products and Solutions-CPS

Using a composite bearing housing technology, CPS is manufacturing a variety of rollers using steel, aluminum and Yeloroll HD composite and Yeloroll conveyor rollers, providing solutions for light, medium and heavy-duty applications. Yeloroll rollers are manufactured using M-PVC (Polyvinylchloride) shell material which is 40% lightweight as compared to steel rollers. The benefit of using titanium modified plastic shell provides significant weight reduction, lower rim drag, substantial noise reduction, nonstick interface and minimum belt damage. Both the end plate and bearing housing is made by precision injection molding of nylon glass fibre composite having antistatic copper pin. The shaft is made up of mild steel or stainless steel depending upon client requirements with a C3 clearance deep groove ball bearings, protected by a reverse multi labyrinth watertight sealing.

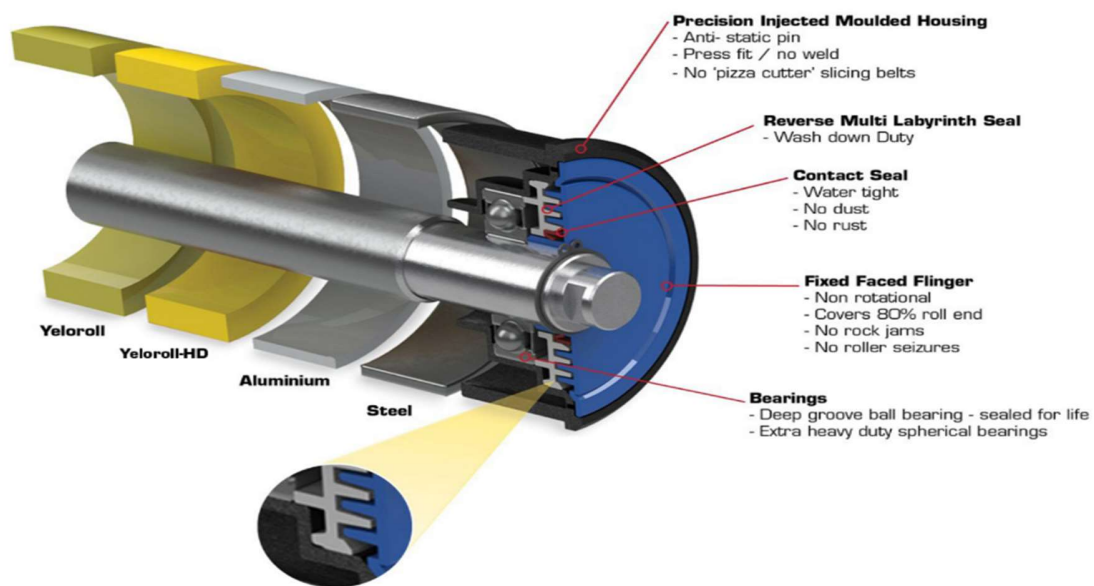
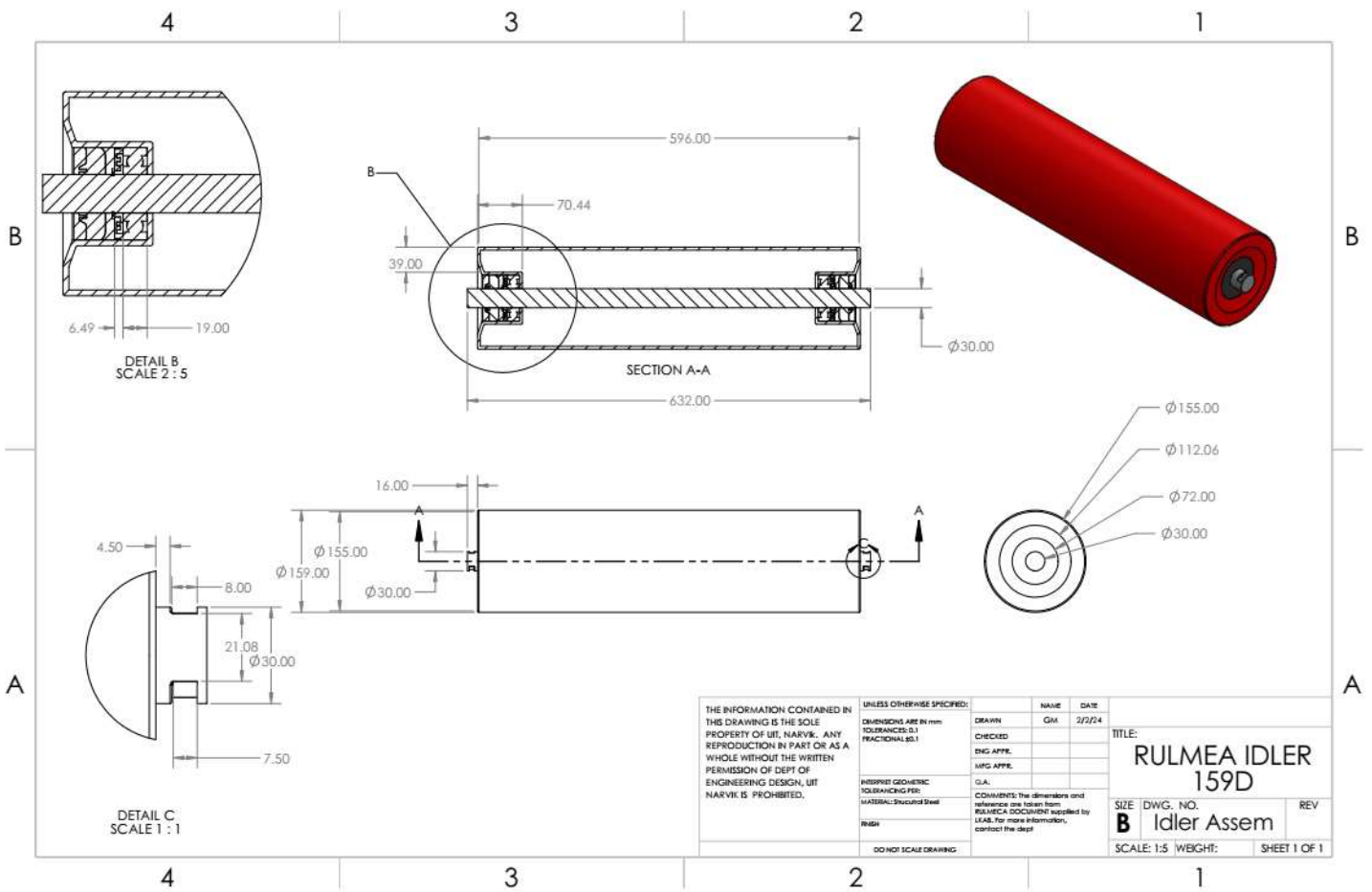


Figure 35: Yellow roller composite roller CPS [17]



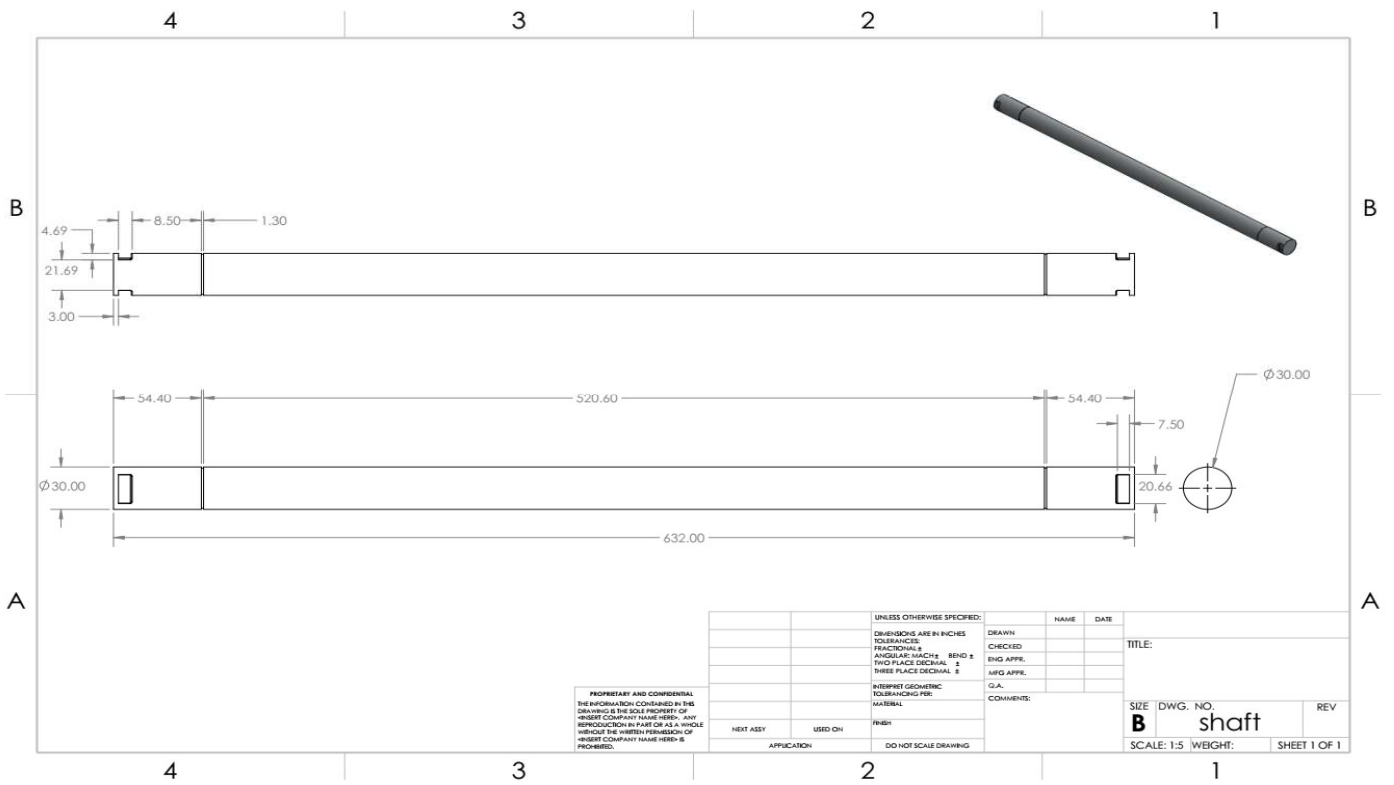
# Appendix B

## Idler 2D drawing



SOLIDWORKS Educational Product. For Instructional Use Only.

Figure 36: 2D Drawing of Rulmeca Idler with dimensions



SOLIDWORKS Educational Product. For Instructional Use Only.

Figure 37: Idler shaft



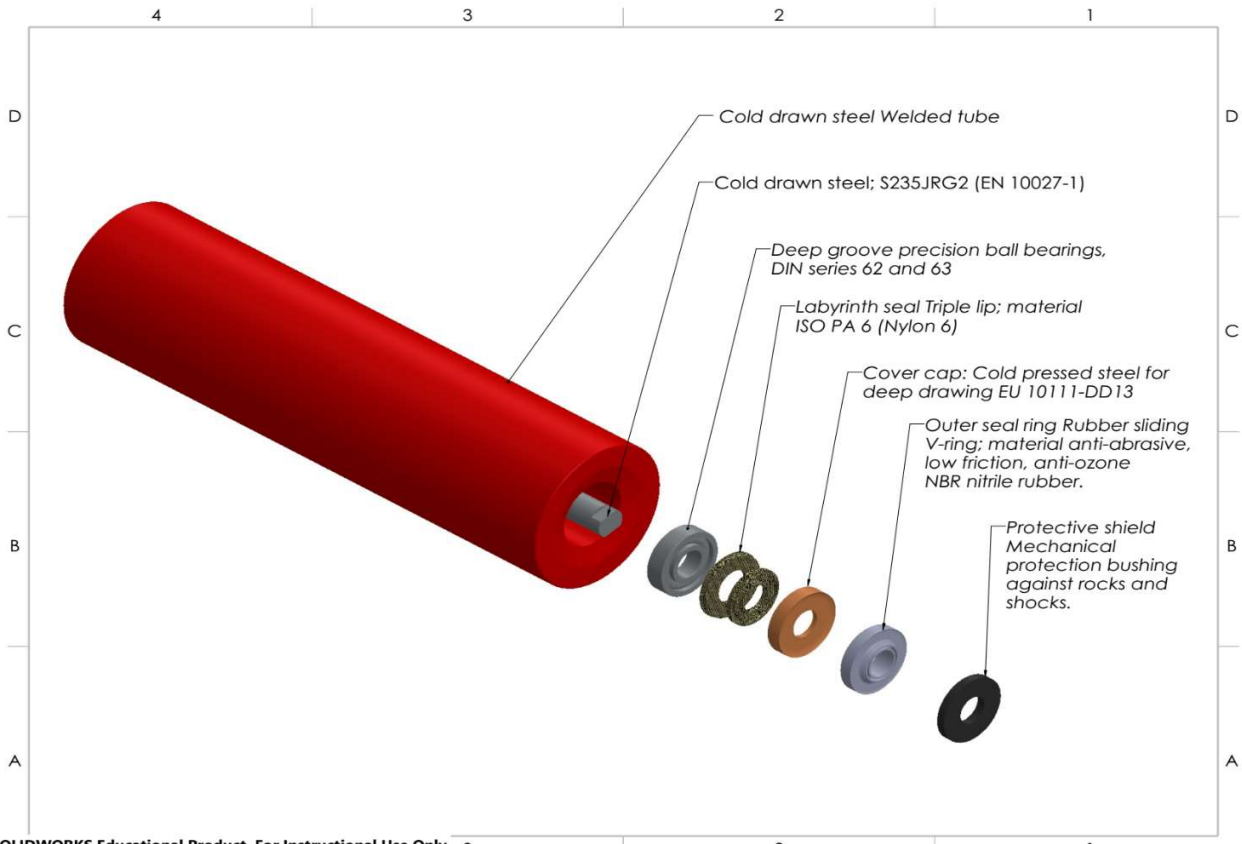


Figure 38: Idler components with specifications

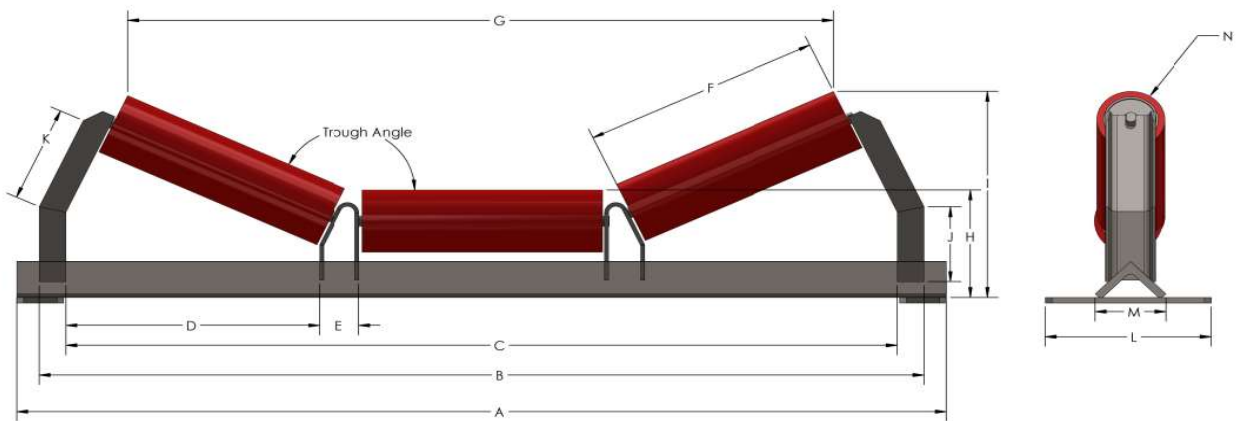


Figure 39: Typical idler troughing system

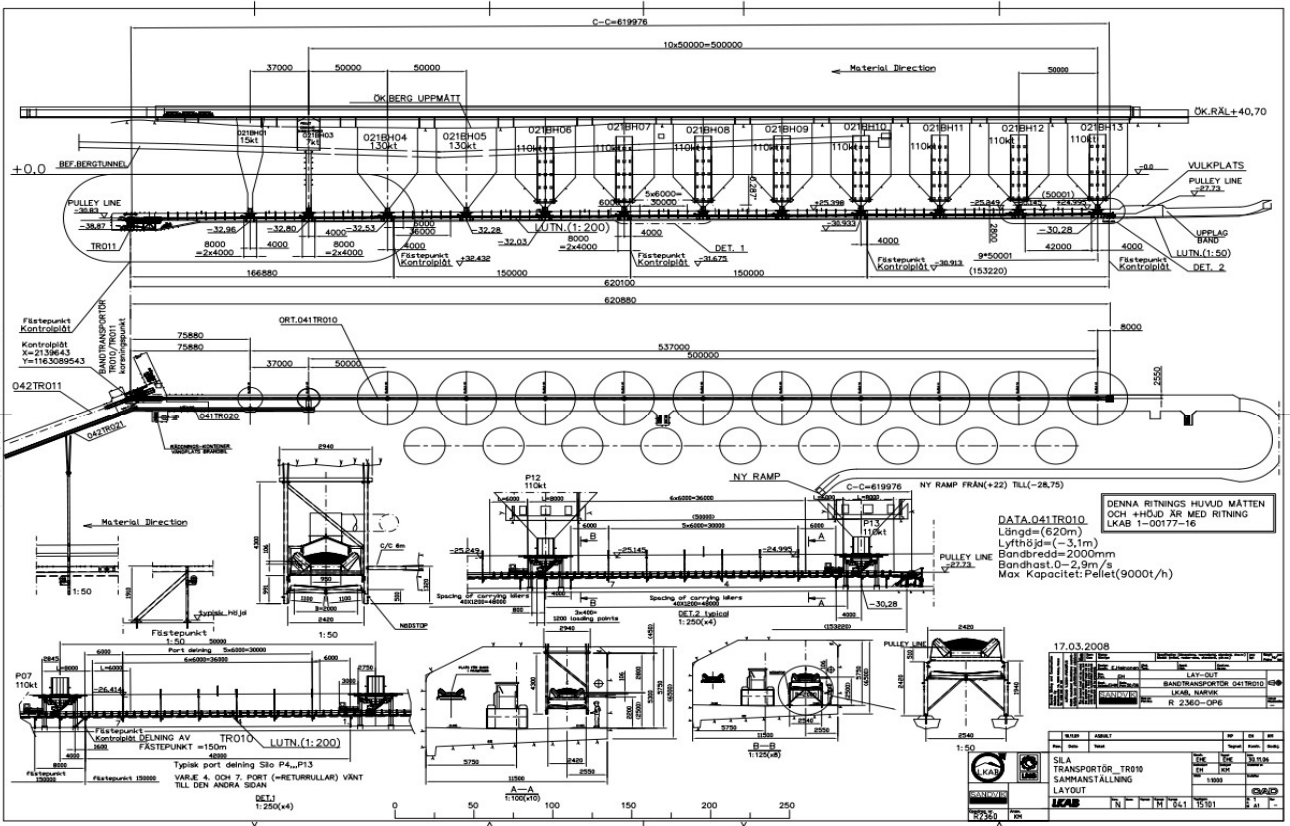


Figure 40: LKAB TR010 conveyor Assembly.

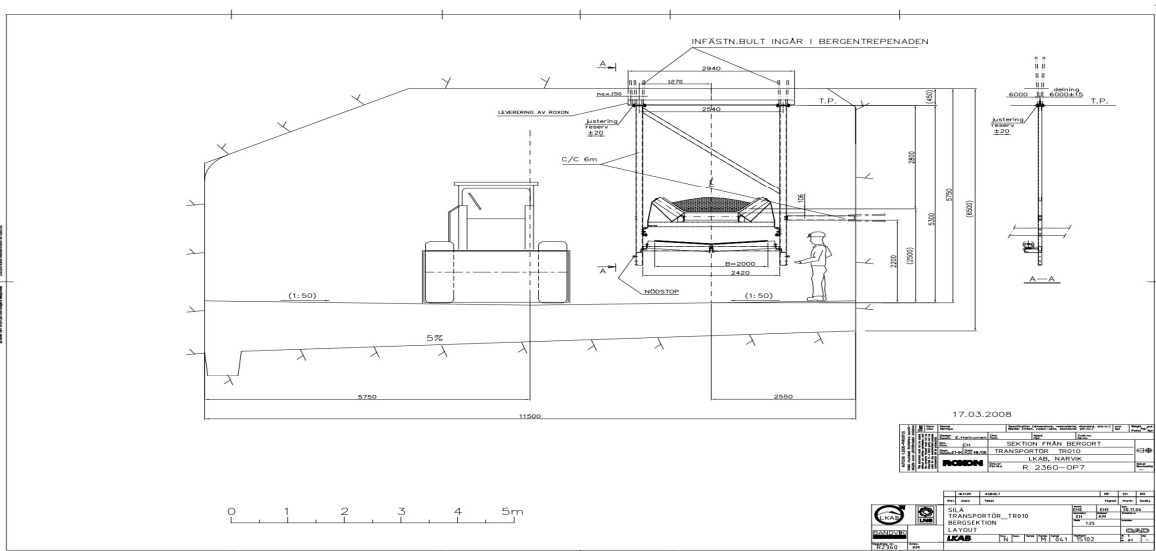


Figure 41: Front view TR010 conveyor LKAB

# Appendix C

## ANSYS Analysis Setup

Below figures shows the workflow in ANSYS for structural optimization and an example of how the analysis in setup in ANSYS for idler shell. Same procedure can be used for setting up other analysis done in this master thesis.

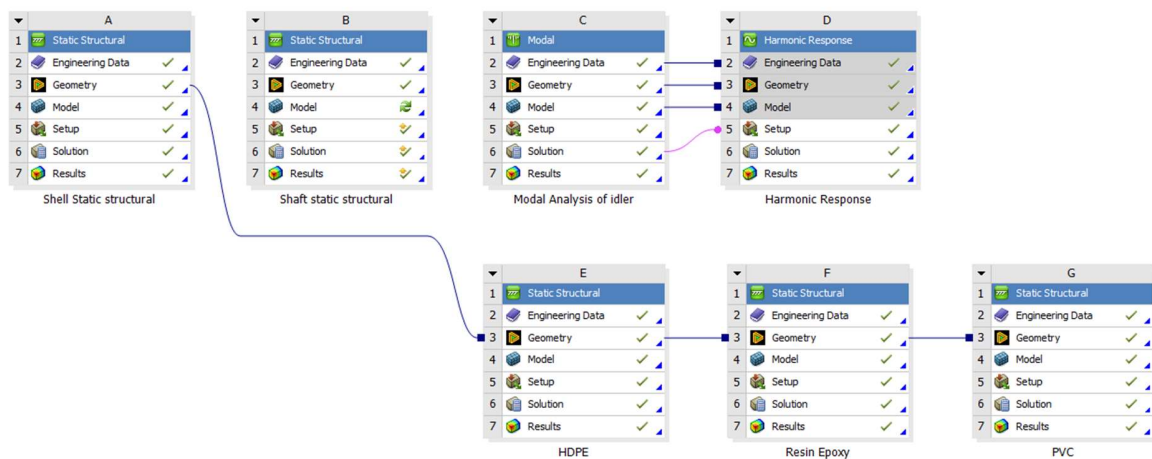


Figure 42: ANSYS workflow for structural optimization

Properties	
<input type="checkbox"/> Volume	1.3105e+006 mm <sup>3</sup>
<input type="checkbox"/> Mass	10.288 kg
Centroid X	-1.2822e-013 mm
Centroid Y	7.3649e-002 mm
Centroid Z	-1.576e-014 mm
<input type="checkbox"/> Moment of Inertia ...	60819 kg·mm <sup>2</sup>
<input type="checkbox"/> Moment of Inertia ...	3.3738e+005 kg·mm <sup>2</sup>
<input type="checkbox"/> Moment of Inertia ...	3.375e+005 kg·mm <sup>2</sup>
Statistics	
Nodes	50611
Elements	8649
Mesh Metric	None

Figure 44: properties of idler shell, nodes and elements for meshing

Defaults	
Physics Preference	Mechanical
Element Order	Program Controlled
<input type="checkbox"/> Element Size	Default
Sizing	
Use Adaptive Sizi...	Yes
Resolution	Default (2)
Mesh Defeaturing	Yes
<input type="checkbox"/> Defeature Size	Default
Transition	Fast
Span Angle Center	Coarse
Initial Size Seed	Assembly
Bounding Box Di...	640.75 mm
Average Surface ...	97679 mm <sup>2</sup>
Minimum Edge L...	471.24 mm

Figure 43: meshing properties

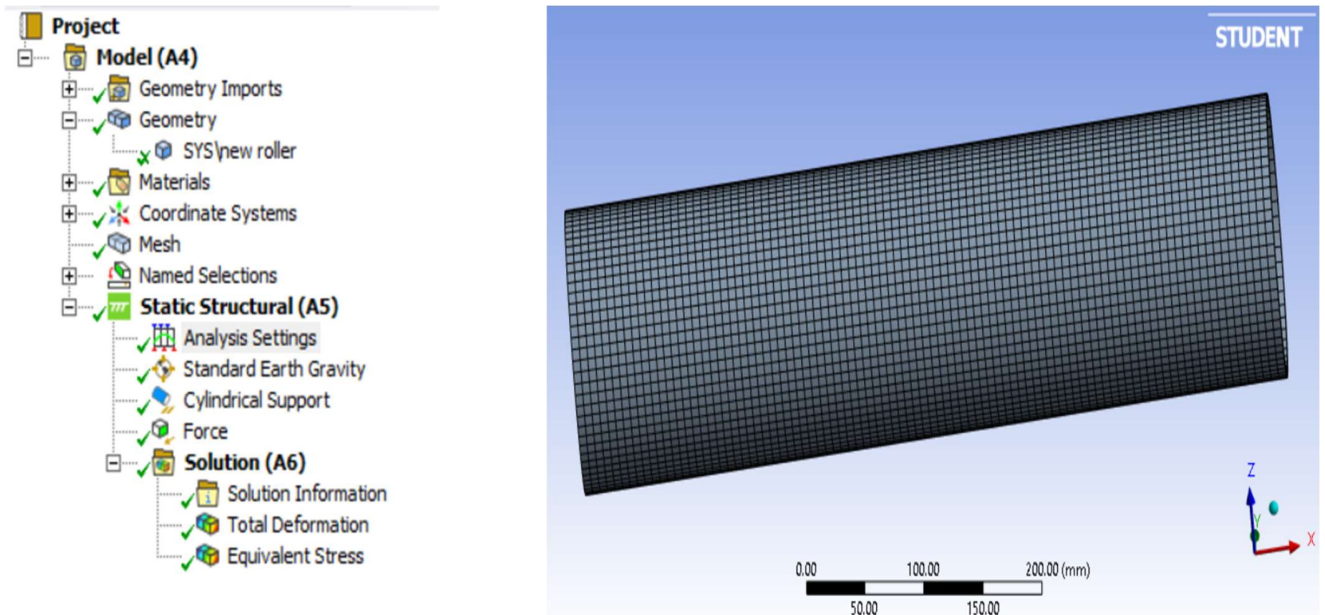


Figure 45: Shell analysis project flow and meshing configuration.

## SHELL analysis for Alternative defined materials

### HDPE

### Equivalent Stress

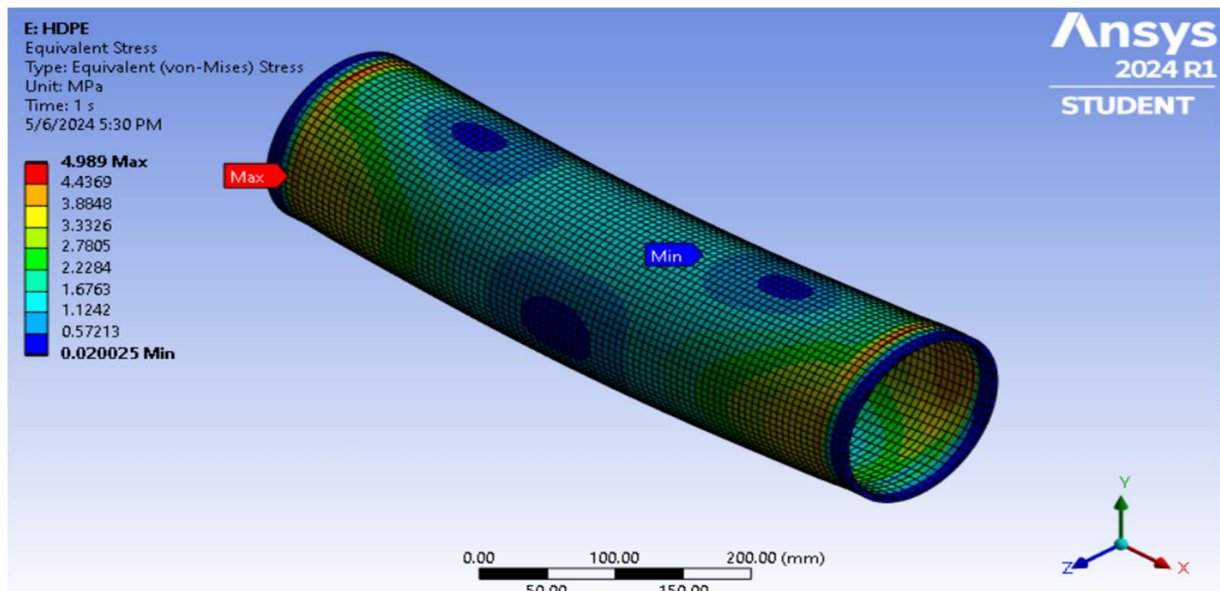


Figure 46: Equivalent Stress HDPE shell

## Total Deformation

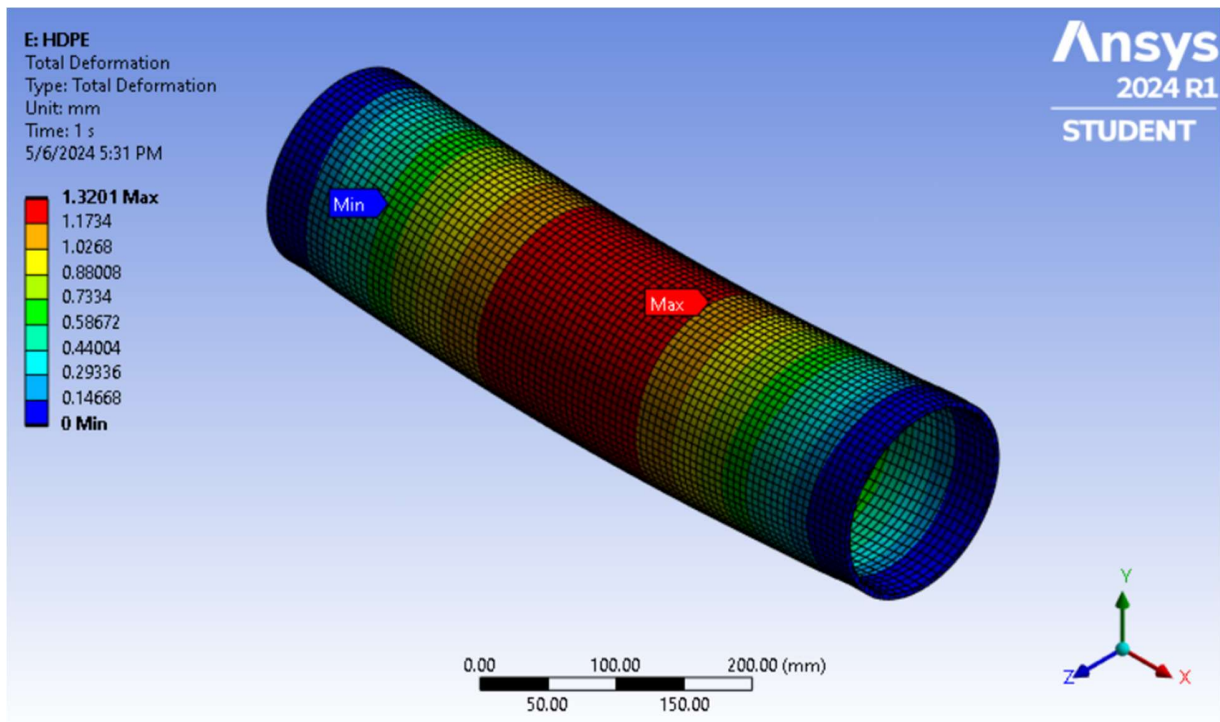


Figure 47: Total Deformation HPDE Shell

## Resin Epoxy

### Equivalent Stress

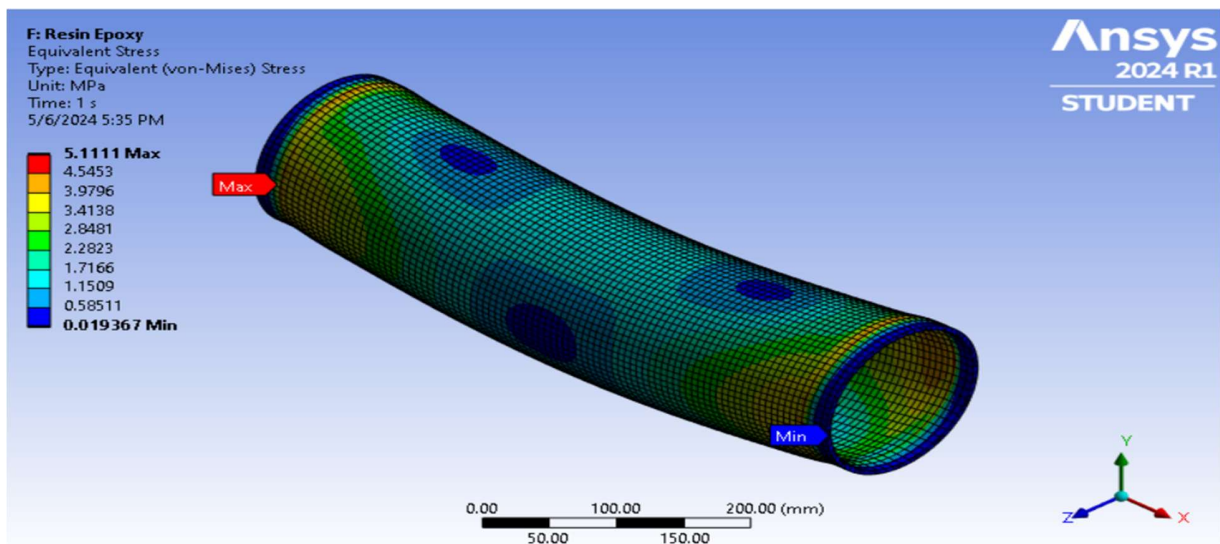


Figure 48: Equivalent Stress Resin Epoxy SHell



## Total Deformation

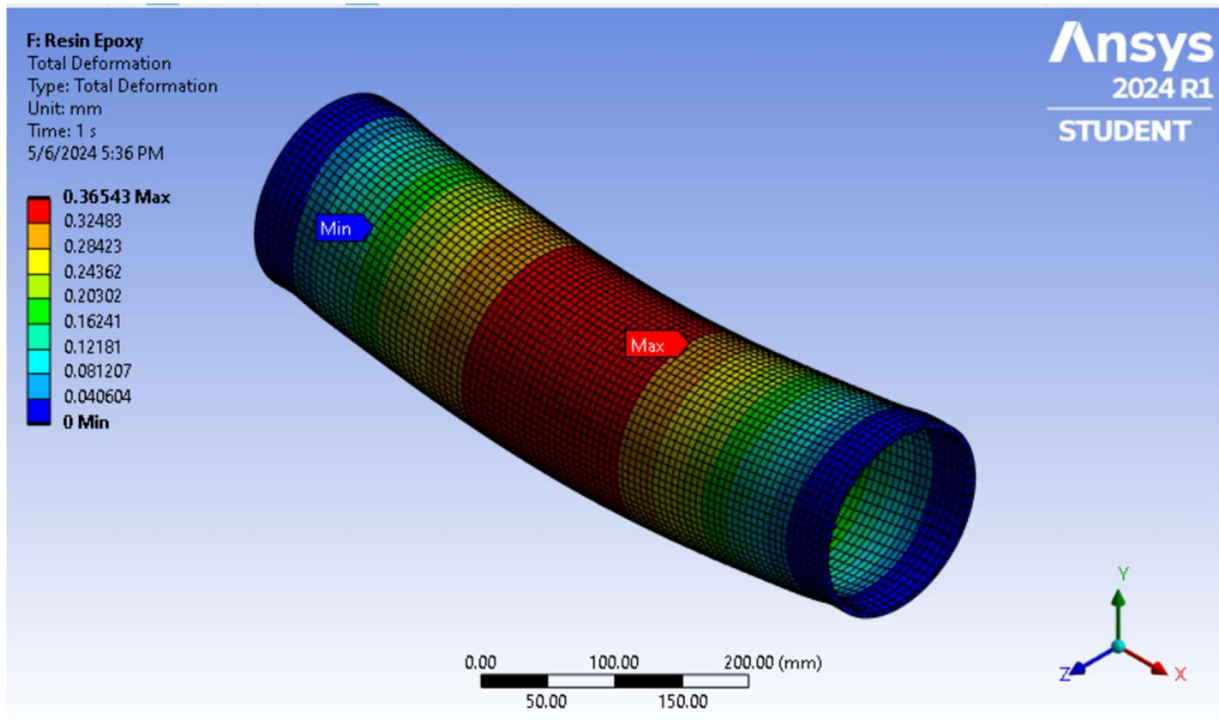


Figure 49: Total Deformation Resign Epoxy shell

## PVC

### Equivalent Stress

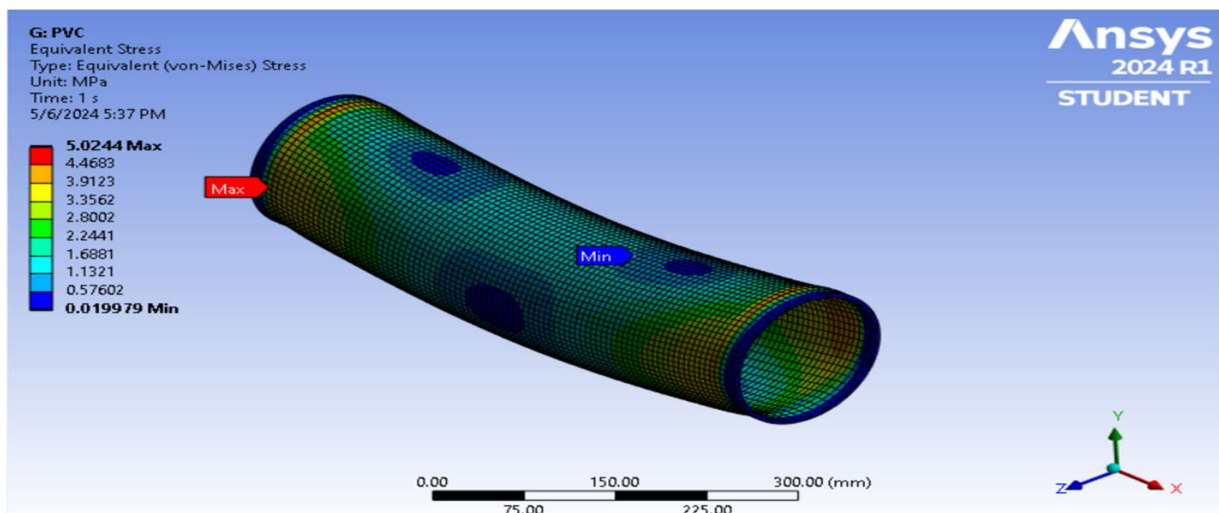


Figure 50: Equivalent stress PCV shell

## Total Deformation

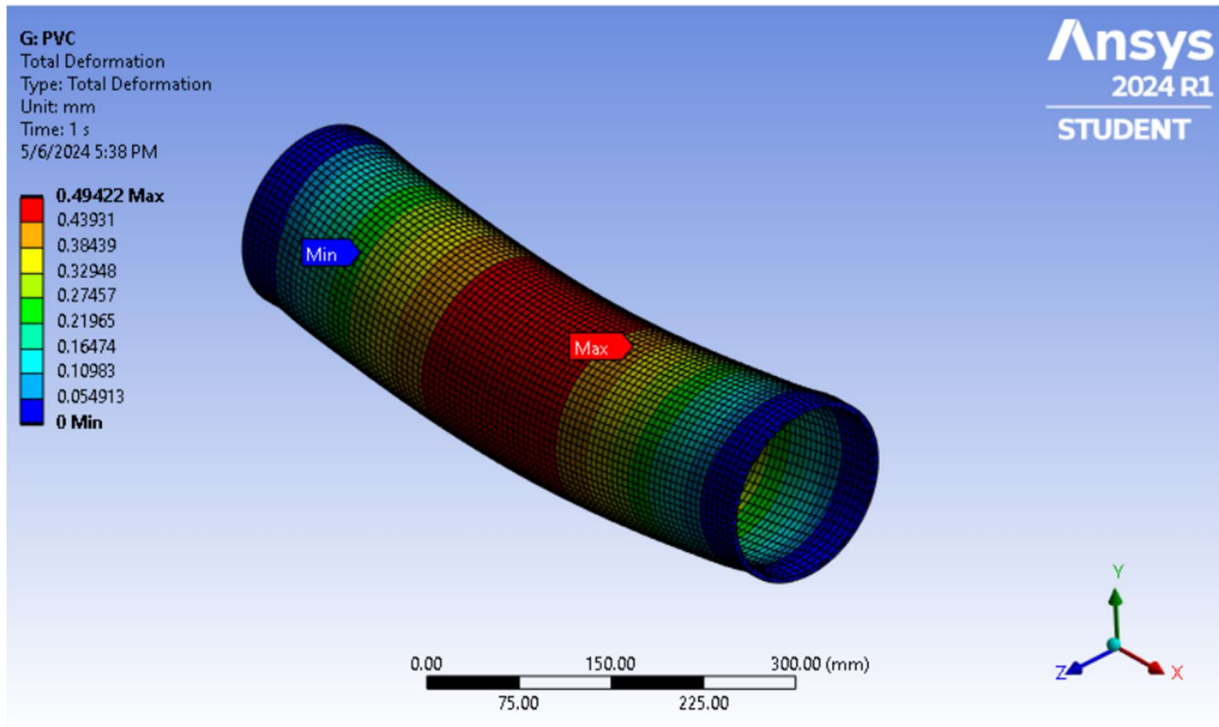


Figure 51: Total Deformation PVC shell

## Python Code for finding shaft deflections for different thickness values

---

```
import numpy as np
import matplotlib.pyplot as plt

# Given parameters
F = 6000 # N
a = 0.075 # m
E = 210 * 10**9 # Pa
r = 0.015 # m
L=0.6

deflection_values = []

# Thickness values (decrementing)
t_values = np.linspace(0.015, 0.001, num=15, endpoint=True)

# Calculate deflection for each thickness value
for t in t_values:
    deflection = (F * a**2 * (3 * L - a) ) / (6 * E * ((3/(4 * t)) * r**5))
    deflection_values.append(deflection * 1000) # Convert to mm

# Print the deflection values
print("Deflection values:")
for i, deflection in enumerate(deflection_values):
    print(f"{t_values[i]*1000:.3f}, {deflection:.5f}")

# Plotting
plt.plot(t_values * 1000, deflection_values, marker='o') # Convert thickness to mm for plotting
plt.title('Deflection vs. Thickness')
plt.xlabel('Thickness (mm)')
plt.ylabel('Deflection (mm)')
plt.grid(True)
plt.gca().invert_xaxis() # Invert x-axis
plt.show()
```



## Appendix D

### Material selection

For strength-based design of center roller shell, material selection criteria are given below:

Function: Structural support to roller assembly

Objective: To minimize the mass of Idler shell

Constraints: These include the roller shell's length, circular shape, and its ability to support bending loads without excessive deflection, while maintaining a specified bending stiffness.

Free Variables: Thickness of cross section, Choice of material

Since we know that, for minimum mass the equation is

$$m = A \times L \times \rho$$

Whereas  $m$ = mass of beam,  $A$ = cross-sectional area,  $L$ = length of beam and  $\rho$  is the density of material.

According to Euler Beam theory, bending stress on a beam is defined as

$$\sigma_{yield} > \frac{M \times y}{I_{y-shell}}$$

$$\sigma = \frac{F \times L \times y}{\left(\frac{A \times r^2}{2}\right)}$$

Solving for  $A$  and inserting it in the objective function reveals the following material index:

$$M_3 = \frac{\sigma_{yield}}{\rho}$$

For stiffness-based design, maximum deflection of the roller shell with a load on center and fixed at both ends (boundary conditions for idler shell) is given as follows:

$$\delta_{shell} = \frac{q \times L^4}{\frac{384}{5} \times E \times I_{y-she}}$$

$$I_{y-she} = \frac{\pi}{4} (r_{outer}^4 - r_{inner}^4)$$

$$\delta_{shell} = \frac{q \times L^4}{\frac{348}{5} \times E \times \left(\frac{A \times r^2}{2}\right)}$$

Solving for A and substituting in the objective function:

$$M_2 = \frac{E}{\rho}$$

Below figures are showing material selection procedure using Micheal Ashby principle in ANSYS GRANTA. Base on this process and using literature review, PVC,HDPE and Resin epoxy are selected as viable alternatives to structural steel.

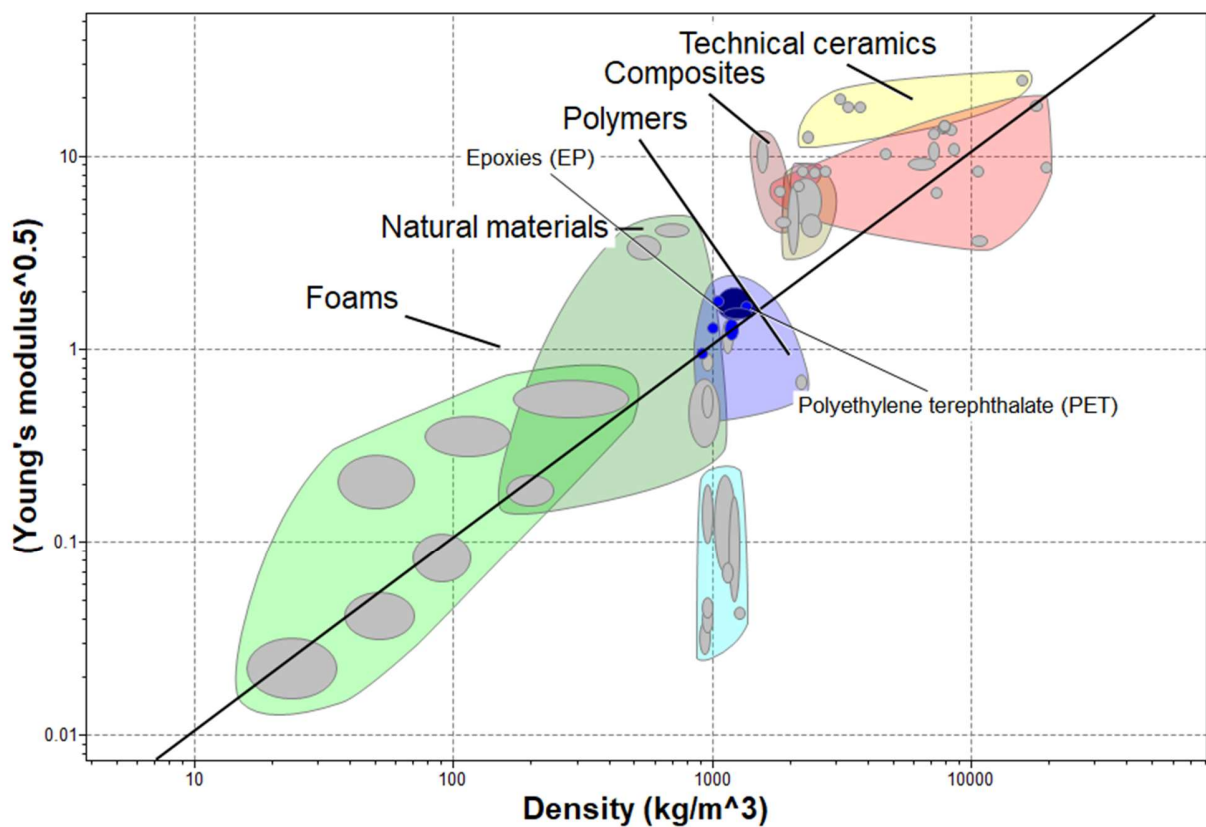


Figure 52: Material Selection Chart

**3. Results: 9 of 63 pass**

Show:

Rank by:

Name	Stage 1: Index, slope = 1
Polyvinylchloride (tpPVC)	0.00871
Cellulose polymers (CA)	0.00897
Polyester (UP)	0.00909
Polyurethane (tpPUR)	0.00974
Polypropylene (PP)	0.00977
Polystyrene (PS)	0.0101
Polyethylene terephthalate (PET)	0.0105
Epoxies (EP)	0.011
Polycarbonate (PC)	0.0131

Figure 53: Ranked Material based on material index stage 1

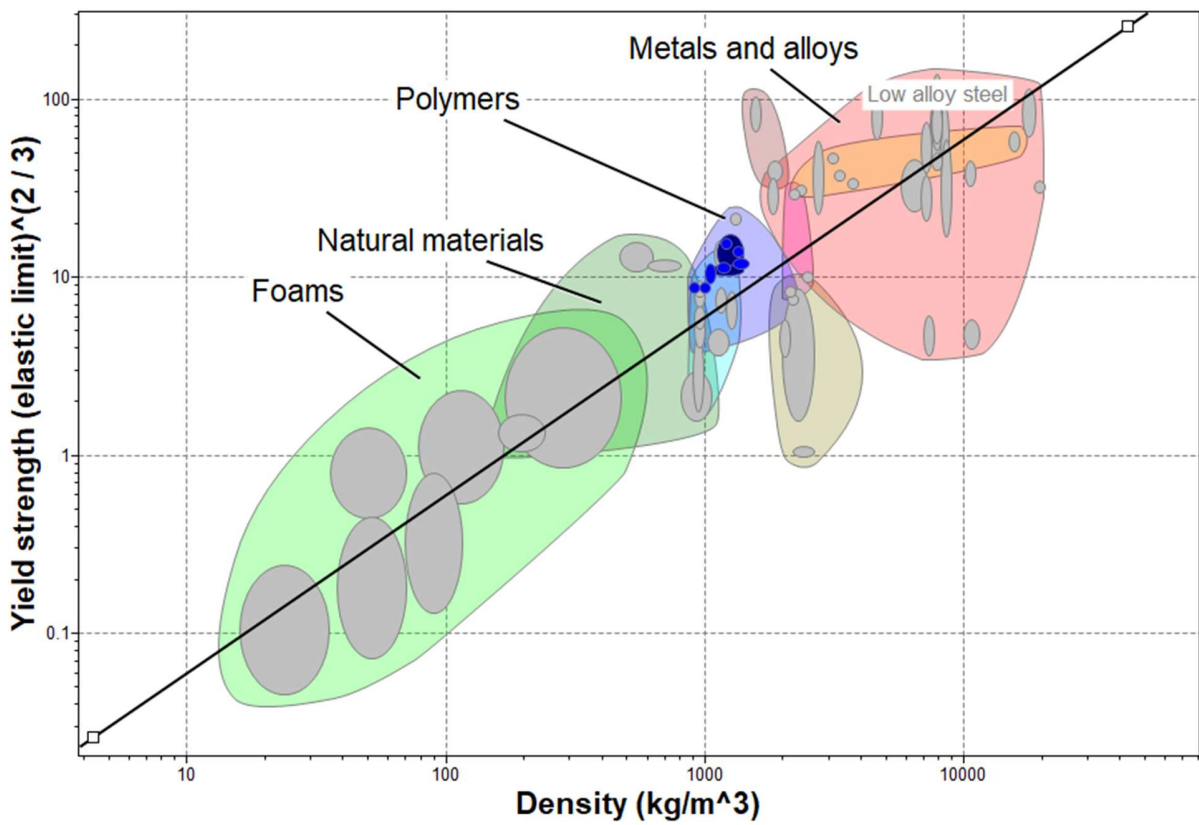


Figure 54: Strength vs Density chart

**3. Results: 9 of 63 pass**

Show:

Rank by:











 Name	Stage 2: Index, slope = 1
 Polypropylene (PP)	0.00106
 Polyurethane (tpPUR)	0.00109
 Polyvinylchloride (tpPVC)	0.00118
 Epoxies (EP)	0.00125
 Polyethylene terephthalate (PET)	0.00127
 Polycarbonate (PC)	0.00129
 Cellulose polymers (CA)	0.00132
 Polyester (UP)	0.00144
 Polystyrene (PS)	0.00172

Figure 55: Materials ranked for stage 2

